ABSTRACT

CROUCH, ANDREW DAVID. A Climatology of the Sea Breeze Front in the Coastal Carolinas and Georgia. (Under the direction of Dr. Allen Riordan).

The sea breeze circulation forms as a result of differential heating across the land-sea surface interface. The resultant pressure gradient force (PGF) induces an onshore flow at the surface and a return flow higher in the atmosphere. The sea breeze front is a reflection of this circulation, a boundary between the cool, moist, maritime air mass advancing landward and the warm, dry ambient air mass in place over inland areas. Studies have shown that the circulation forms more often in the spring and summer months when the temperature difference between land and sea surfaces is greatest.

The following study is based on the analysis of satellite imagery and standard hourly measurements of air temperature, dewpoint, wind speed, and wind direction recorded at four coastal sites: Savannah, GA, Charleston and Myrtle Beach, SC, and Wilmington, NC. One of the objects of this study is to establish specific values associated with the changes induced by passage of the sea breeze front, and to examine differences in the station-to-station incarnation of the sea breeze circulation. Variability from station to station in the nature and timing of sea breeze frontal passage was found to be a function of relative proximity to the coast. For example, sea breeze frontal passage was found to occur earliest at Myrtle Beach (the closest station to the coast), around 1300 LST on average. Savannah, the farthest of the four coastal sites from the water, was affected by the sea breeze last, with an average passage time of between 1630 and 1700 LST.

Previous studies indicate that the extent to which the circulation and associated front penetrate inland is usually on the order of about 20-60 km. GOES satellite imagery was accumulated from the North Carolina State Climate Office and analyzed with GIS (Geographic Information System) software for the purpose of determining the inland horizontal extent of the sea breeze circulation. Penetration distances of 20-40 km were common, but occasionally the sea breeze penetrated as far as 80 to 120 km.

The second part of this study attempts to develop a scheme for the prediction of the development and evolution of the sea breeze front. The factors most significant to this prediction include the synoptic wind flow regime and values for the temperature difference between land and sea surfaces. North American Regional Reanalysis data were downloaded and analyzed to gather daily geostrophic wind vectors. Water temperature data were collected and compared with air temperature measurements to determine the temperature difference, the driving mechanism for sea breeze development. Data for the Myrtle Beach site were analyzed first to provide a framework for the other stations because of relative completeness and reliability of the data sources. At Myrtle Beach, ninety percent of sea breeze development occurred with land-sea temperature differences of 2.0 degrees Celsius or higher.

A CLIMATOLOGY OF THE SEA BREEZE FRONT IN THE COASTAL CAROLINAS AND GEORGIA

By

ANDREW DAVID CROUCH

A thesis submitted to the Graduate Faculty of
North Carolina State University
in partial fulfillment of the
requirements for the Degree of
Master of Science

MARINE, EARTH, AND ATMOSPHERIC SCIENCES

Raleigh, NC
2006

APPROVED BY:

_____	_____
Gary Lackmann	Sethu Raman

_____
Allen Riordan
Chair of Advisory Committee

BIOGRAPHY

Andrew Crouch was born October 21st, 1982, in Columbia, South Carolina. He still remembers vividly the moment that first turned his attention to the weather, when Hurricane Hugo blazed a trail through the heart of the Carolinas in September of 1989 – he was six years old. Andrew attended the University of South Carolina in Columbia, taking classes and working with a great staff of climatologists in the Geography Department there. He graduated in 2004 with a Bachelor's Degree in Geography, and immediately enrolled in the Master's program at NC State University in Raleigh, NC, to study Atmospheric Science.

ACKNOWLEDGEMENTS

First and foremost I have to thank Dr. Al Riordan for guiding me through this two-year process, for helping me overcome the inevitable surprises, and for putting up with my occasional tardiness to our Friday meetings. He was instrumental in securing the contacts and resources I needed to finish this thesis, and I hope wherever retired life finds him the weather is sunny. I also want to thank Dr. Sethu Raman and Dr. Gary Lackmann for their advice and consent to be on my advisory committee.

Within the NC State Climate Office, I must thank Ryan Boyles for introducing me to the CRONOS database system and his assistance with the ArcGIS program I used for analyzing satellite data. Thanks to Robb Ellis for helping me gain access to the satellite imagery in the first place, and for building the satellite animation web page I utilized. I must also thank Michael Brennan for his help with the GEMPAK program I used to analyze geostrophic wind patterns, as well as Tom Green for helping me gain access to those data in the first place. I want to thank Pace Wilber, Stephanie Fauver, and Kirk Waters at the Coastal Services Center for their helpful advice at our meetings throughout the last couple of years, and their assistance in procuring SST data. Dr. Len Pietrefesa also had some helpful thoughts from time to time, and an enthusiasm I always appreciated. This study was conducted under the auspices of the NOAA's Climate and Weather Impacts on Society and the Environment (CWISE) project, under grant # NA03NES4400015.

Thanks also to my friends and family for their support and interest, whether real of feigned for my benefit, in this project. They poked and prodded in all the right places and at all the right times, and I couldn't have done it without them.

TABLE OF CONTENTS

LIST OF TABLES

LIST OF FIGURES

SECTION ONE: Introduction and Literature Review

1.1 The Sea Breeze Front

The sea breeze circulation develops because of atmospheric pressure differences between air above the land and sea surfaces. Figure 1.1 is a rough representation of this process. Since the specific heat of land is less than that of water, the land surface and the associated air at the lower levels of the atmosphere will heat faster than the water and the air over the water, creating temperature differentials on the order of 2 to as much as 10 ° C (Frysinger et al., 2003) in the spring and summer months. Other factors contribute to this temperature differential as well. The relative transparency of the water column allows solar insolation through the entire column, resulting in a more even distribution of heat, as opposed to the concentration of heat in the very near surface layer of soil over land. Mixing processes in the water that are absent over land also contribute to a more even distribution of heat.

From the hypsometric relationship, the warmer air over the land surface will begin to expand vertically, creating low pressure near the surface, and adjacent near-surface high pressure over the water, usually a pressure difference on the order of about 2 mb (Barry and Chorley, 1992). An onshore flow will develop along the landward-directed pressure gradient (depicted by the lower black arrow in Figure 1.1), forming a frontal boundary separating the cool, moist maritime air mass from the warmer, drier air mass it is displacing as it moves inland. Well above the surface, the vertical displacement of isobars results in the opposite configuration of pressure systems, with high pressure just onshore and low pressure just offshore.

The sea breeze circulation is typically on the order of 1 km deep, although it thins to some degree closer to the advancing edge (Barry and Chorley, 1992). The complete circulation will continue as long as the differential land/water heating is maintained. It will also expand both inland and offshore, the extent of the expansion theoretically depending on the reinforcing or prohibitive effects of the synoptic wind regime and the magnitude of the land/water temperature difference.

The sea breeze occurs more frequently in the spring months when land surfaces are warming but the associated ocean waters are still relatively cool. Typical inland penetration is on the order of 50-80 km, but has been known to extend as far as 200 km

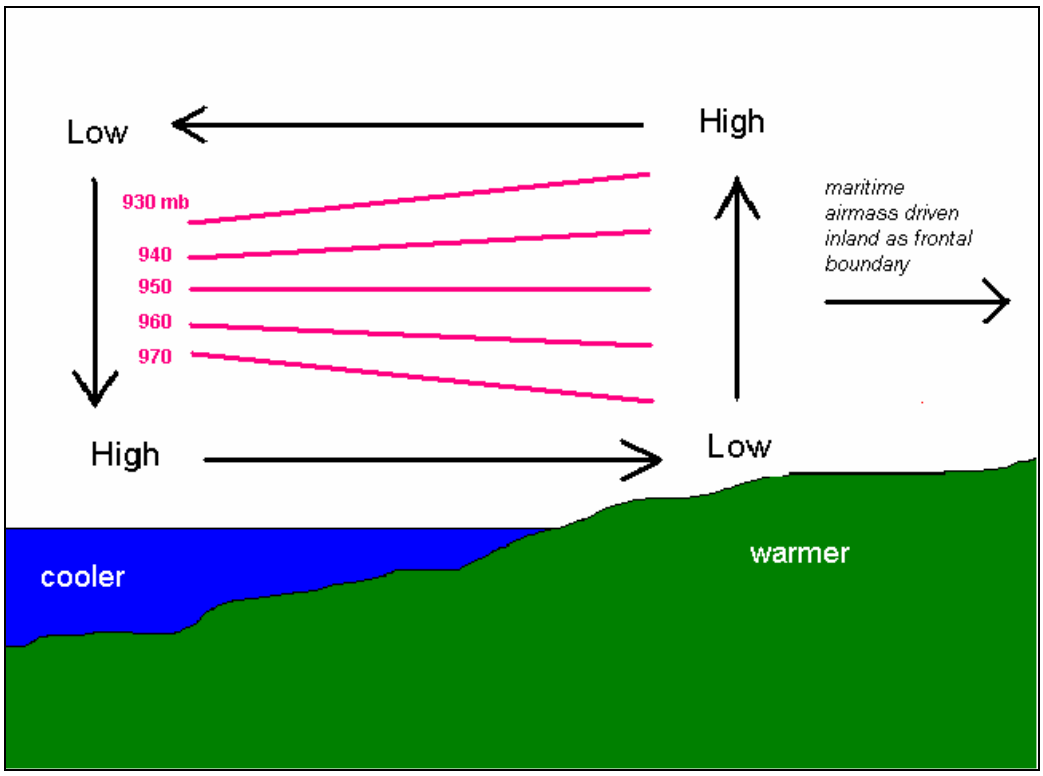

Figure 1.1 ***The sea breeze circulation – black arrows represent wind flow, while the pink lines represent constant pressure surfaces. The circulation results from the differential heating across the land-sea interface.***

inland, for example over northern Australia (Barry and Chorley, 1992). Over inland areas, passage of the sea breeze front typically results in a decrease in temperature, an increase in dewpoint or relative humidity, a shift in wind direction towards a surface onshore flow perpendicular to the coastline, and an increase in wind speed (Wakimoto and Atkins, 1994).

Many sea breeze oriented research efforts have been performed in Florida, where the sea breeze front has been identified as the main contributor to the nearly daily formation of thunderstorms on the peninsula, frequently due to the convergence of sea breezes from the Gulf and Atlantic coasts (Atkins and Wakimoto, 1997; Wakimoto and Atkins, 1994). Projects have also dealt with the sea breeze circulation in the Carolinas (Frysinger et al., 2003; Koch and Ray, 1997) and coastal New England (Miller and Keim, 2003). Some projects have explored the circulation with numerical simulations, both two- (Arritt, 1993; Nichols et al., 1991) and three-dimensionally (Baker et al. 2001, Ohashi and Kida, 2002, Dailey and Fovell, 1999).

1.2 The CaPE Project

One of the most significant and expansive projects to deal with the sea breeze circulation has been the CaPE (Convection and Precipitation/Electrification) project. From 8 July – 18 August of 1991, data were collected from aircraft, mesonet station, radar, satellite, and sounding systems (Atkins and Wakimoto, 1997). Subsequent papers based on this research focused on everything from interactions between the various mesoscale frontal boundaries in the area (Kingsmill, 1995) to the influence of synoptic-

scale wind patterns on the development of the sea breeze front (Wakimoto and Atkins, 1994).

During CaPE, as is the case with most sea-breeze related studies, the inland edge of the sea breeze circulation – the sea breeze front – was often identified by satellite as a thin line of enhanced cumulus cloudiness. At the surface, the front was characterized at surface mesonet stations by a drop in temperature and concurrent rise in dewpoint as the cooler, more moist maritime airmass was advected inland. A distinct increase in wind speed and change in wind direction to an onshore flow was usually observed in coastal stations as well. As the front propagated inland, the maritime airmass was modified by intense summertime surface heating, reducing the ability of researchers to identify the surface front the further inland it moved (Wakimoto and Atkins, 1994).

Atkins and Wakimoto (1994) analyzed data collected in the CaPE project in two papers (Wakimoto and Atkins, 1994; Atkins et al., 1995), the first one dealing with data collected by radar, satellite, and cloud photogrammetry sources, revealing a relationship between the sea breeze front propagating inland and HCRs (Horizontal Convective Rolls) developing over the convectively unstable land surface. These HCRs are a common type of boundary-layer convection consisting of clockwise and counter-clockwise pairs of helices with their major axes aligned parallel to the mean wind (in the summer, usually from west-to-east), denoted on satellite imagery by cumulus clouds aligned linearly like "pearls on a string"(Kuettner, 1959). Areas of enhanced precipitation were noted on satellite and radar images where these HCRs interacted with the sea breeze front.

Another paper by the same authors (Atkins and Wakimoto, 1997) analyzed the same data in order to establish patterns between the development of the sea breeze

circulation and synoptic-scale flow, designating the synoptic wind regimes according to three classifications, offshore, onshore, and parallel (wherein the component of the wind flow perpendicular to the coast made up 10 % or less of the total wind vector). They determined among other things that the sea breeze front was stronger and easier to detect during offshore wind regimes. Analysis of radar data revealed strong signatures (the tell-tale thin band of enhanced reflectivity or cloud cover corresponding to the sea breeze front) with offshore wind regimes due to increased convergence along the boundary. However, these fronts penetrated only a short distance inland, often forming late in the day and hugging the coast. Sea breeze fronts coinciding with onshore synoptic regimes moved further inland but were harder to detect, often with little or no signature in satellite or radar imagery.

1.3 Other Projects in Florida

Scientists at the Kennedy Space Center (KSC) in Cape Canaveral, Florida, launch site for many of NASA's space flights both manned and unmanned, have a vested interest in the weather of the region for their launch schedules, especially in light of recent incidents that have been blamed at least partially on the effects of weather conditions. Sea-breeze studies have been conducted in this area specifically for the KSC due to the importance discussed earlier of the circulation to the daily weather of the Cape Canaveral area. For example, the KABLE (KSC Atmospheric Boundary-Layer Experiment) was established in the year between November 1988 and October 1989, an observational field study that used both in situ and remote sensors. Data analysis revealed a complex relationship between the sea breeze from the Atlantic side of the peninsula and the "river"

breeze generated by the nearby Indian and Banana Rivers as well as the Mosquito Lagoon, a relationship that was highly sensitive to the synoptic wind regime (Zhong and Tackle, 1992). Numerical models have also analyzed the relationship between breezes generated by the Atlantic and Lake Okeechobee, further south on the peninsula, as well as the irregular coastline around Tampa Bay (Nichols, et al., 1991).

1.4 The Sea Breeze Index

Operational forecasters in the Charleston, SC NWS (National Weather Service) forecast office examined data for the summer of 1998, specifically records of air temperature, water temperature, and wind vector from 8 June to 1 July, to establish a simple climatology of the sea breeze and its effects on their forecast area (Frysinger, et. al., 2003). The authors utilized the Sea-Breeze Index (SBI) derived from the Ideal Gas law and Bernoulli's Equation and developed by Walsh (1974) in the form:

$$SBI = \pm U^2 / \Delta T \qquad (1.1)$$

where U is the cross-coast component of the synoptic winds (offshore = +) and ΔT the temperature difference between the land and sea surfaces (where $\Delta T = T_{land} - T_{ocean}$). . This index can be used only for those days characterized by positive ΔT ($T_{land} > T_{ocean}$) and an offshore synoptic-scale wind flow. An equilibrium level for the sea breeze system is defined by the following equation:

$$U^2 = (2gh/T)\,\Delta T \qquad (1.2)$$

where g is the gravitational constant (9.81 m/s^2) and h is the depth of the air layer exchanging heat with the surface. Rearranging (1.2) to the form of (1.1) results in the following:

$$U^2 / \Delta T = 2gh/T = SBI \qquad (1.3)$$

so that, assuming an *h* depth of 50 m and a mean *T* temperature of 30 ° C (303 K), the equilibrium SBI value = 3.23 $m^2s^{-2}K^{-1}$. This value represents the slope of a line emanating from the origin on a graph of U^2 versus ΔT. Sea breeze hours (defined by incidences of onshore flow) typically fall below and to the right of this line, while non-sea breeze hours fall above and to the left. Note that for the Frysinger study, analysis was conducted on an hourly basis, rather than daily as in the remainder of this thesis.

Several tests were run for the summer and fall months of 1998 using portable air and water temperature sensors at the Folly Beach fishing pier and the air temperature gauge for the CHS Automated Surface Observation System (ASOS) station. Another portable recording station was established at St. George, SC, as a measurement of synoptic winds (component *U*). For these data the critical value of the SBI for formation of the sea breeze front, the value which corresponded with the best ratio of sea breeze to non-sea breeze hours below and to the right of the line, was approximately 2.8 $m^2s^{-2}K^{-1}$, while an SBI value of 3.8 $m^2s^{-2}K^{-1}$ encompassed all sea breeze occurrences.

Based on these trial tests, the index was improved by degrees using progressively more complex forecast criteria, accounting for such factors as sea-breeze frontal recession and collapse (which often occur later in the day as the driving mechanism of differential heating begins to break down) and critical values for geostrophic wind. Although this method is not usable for instances of sea breeze formation during onshore synoptic flow regimes, the forecasters who developed it found that it led to a significant improvement in forecasting skill over climatology, and that it could be integrated into the forecast for the Charleston area, at least in a short-term capacity. The authors further

surmised that with some minor modification the same simple model could be utilized for other coastal regions as well (Frysinger et al., 2003), and one might assume that the modifications would not be extensive to adapt the model for a coastline as close as North Carolina. Further investigation into this possibility will be explored in other sections of this document.

1.5 Other Projects in the Carolinas

A study conducted by Gilliam, et al. (2004) dealt with four case studies in May of 1999 and 2000 in terms of the sea breeze front's signature on Doppler radar. Previous studies had discovered that, analogous to the signature left on satellite imagery by the sea-breeze front, the front on radar imagery is denoted by a linear reflectivity feature most likely due to the presence of insects and debris (Rayleigh scatterers) caught in the updraft ahead of the encroaching front. The four case studies, listed below, were chosen as representative of four different synoptic wind flow regimes:

May 31, 1999 --- Southeasterly flow
May 6, 2000 --- Westerly
May 12, 2000 --- South-Southwesterly
May 15, 2000 --- Northerly

The four cases presented in this study were characterized by wind flows in the 5 – 7 m/s range except for the 31 May 1999 example, which featured a weak pressure gradient and lighter ambient winds. These synoptic wind regimes were determined by examining the pressure gradients in 1200 UTC (0800 EDT) EDAS (Eta Data Assimilation System) analyses.

By geo-referencing the imagery against base maps provided by GIS (Geographic Information Systems) and analyzing the imagery with an Arc-GIS program, the authors were able to determine propagation distances for sea breeze fronts generated on the four days of the case study relative to the angle formed by the south- and east-facing coasts near Wilmington, NC. The results from Gilliam, et al. (2004), summarized below, indicate that the synoptic regime had a significant impact on where and how the sea-breeze front moved:

May 31, 1999 – southeasterly ambient flow

Front penetrated inland nearly to Raleigh, where it was detected on Doppler radar at 1900 LDT, nearly 120 km from the coast

May 6, 2000 - westerly

Penetration was greater relative to the south-facing coast (~ 45 km) than to the east-facing coast (~ 30 km)

May 12, 2000 – south-southwesterly

Penetration was greater relative to the south-facing coast (~ 65 km) than the east-facing coast (~30 km)

May 15, 2000 - northerly

Penetration was greater relative to the east-facing coast (~ 25 km) than the south-facing coast (~ 50 km)

Other studies such as the Land-Sea Breeze Experiment (LASBEX) in Monterey Bay, California have used Doppler lidar for analysis of the sea breeze, specifically in that case to determine the nature of the interaction between the complex topography of the Monterey Bay area (with mountainous terrain very near to the coast) and the sea breeze front. While the flat topography of the coastal plain of the Carolinas is an insignificant factor to the evolution of the sea-breeze front, Doppler lidar might represent a tempting method of analysis for future research because of its higher resolution imagery and lack of interference from ground clutter (Darby, et al., 2002).

Another local research study (Koch and Ray, 1997) analyzed the interaction of boundaries over the Piedmont and coastal plain of North Carolina during the summer of 1994 using *GOES* satellite, WSR-88D (Doppler) radar, and standard hourly data. The authors determined that the sea breeze front was the second most frequent boundary noted during their research period (behind thunderstorm outflow boundaries), and instigated convection nearly 75% of the days on which it was found on satellite and radar imagery, whether "auto-convective" (convection initiation on its own) or convective as a result of interaction with other boundaries. The researchers found that the sea breeze front typically penetrated inland to maximum distances of 50-90 km, but anomalous penetrations of 100 to 200 km occurred when movement of the sea-breeze front was aided by other boundaries such as thunderstorm outflows or the Piedmont trough, a local phenomena caused by differences in latent heating at the interface between the sandy soil of the coastal plain and the clay-dominated soil of the Piedmont. The study determined that satellite imagery was a more useful tool for analyzing the horizontal extent of the circulation than radar imagery, because of the limitations in the range of the radar system:

at distances greater than 80 km, the radar beam simply measures too high above the relatively shallow sea-breeze circulation, which extends only about one kilometer above the surface. The WSR-88D Doppler radar used in this study is also limited for sea-breeze related projects because of the infrequency of the use of the system in the more sensitive "clear-air" mode that is often necessary for detection of the sea breeze front.

SECTION TWO: Methodology

2.1 Geographic and Climatologic Setting

The geographic extent of this study includes the subtropical southeastern United States, specifically the states of South and North Carolina and Georgia (Figure 2.1). During the winter months, the region is frequently affected by polar fronts that bring cold, dry air down from Canada and lead to a wide variety of temperature and precipitation regimes, although the Appalachian mountains tend to be an obstacle to the coldest air. However, during the summer months the weather of the region is dominated by the Bermuda high, a strong, semi-permanent system of high pressure centered off the East coast that maintains a southerly to southwesterly wind flow over the Southeast, a wind flow frequently laden with warm, moist air from the Gulf of Mexico or the nearby Atlantic (Koch and Ray 1997, Gilliam et. al. 2004). This pattern contributes to the frequent occurrence of afternoon convective thunderstorm activity over the region, and is the dominant influence on the tracks of hurricanes over the Atlantic from July to November. The consistency of southerly wind direction readings from observational data tends to suggest the influence of this system, especially as one moves from the beginning of the sea breeze "season" (April) towards the end (July), as defined by this study.

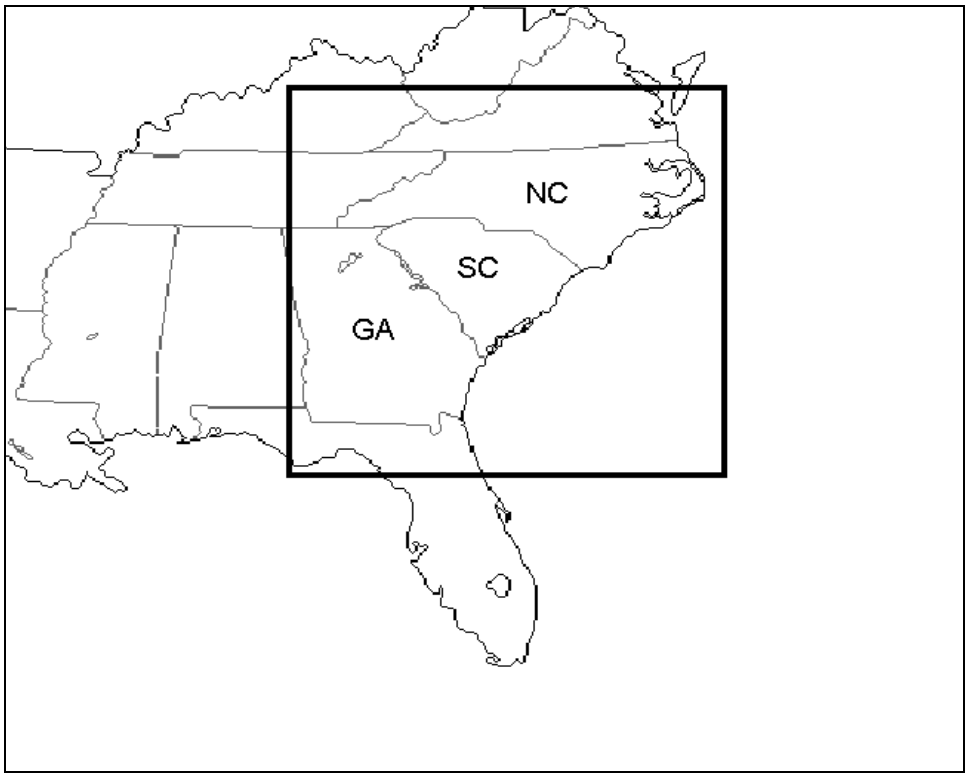

Figure 2.1 ***Geographic area of study – data from coastal sections of the Carolinas and Georgia were analyzed***

2.2 Detection

As stated previously, the sea breeze circulation develops because of differential heating between land and water surfaces. Detection of the sea breeze front at specific inland points is a function of the measurement of the changes that the front causes at those points. Typically passage of the front is associated with a slight drop in temperature and a slight increase in dewpoint (Wakimoto and Atkins, 1994) as the more moderate and moist maritime air mass takes the place of the warmer, dryer air over the inland areas during the day. The frontal passage also affects wind speed and wind direction. The sea breeze circulation initially induces a surface wind directly onshore, perpendicular to the coastline, in the case of coastal areas of the Carolinas typically southeasterly in nature. With time, turning by the Coriolis force would work to shift

winds right of this initial vector, in the case of the Carolinas a turn to southerly winds. Wind speeds typically increase to around 4-7 m/s (Barry and Chorley, 1992), although these wind speed variations have been somewhat difficult to quantify from observational data for our coastal sites. As the front penetrates further inland, intense surface heating acts to modify the maritime air mass, making detection more difficult (Wakimoto and Atkins, 1994). Also, with time and the loss of surface heating along the land-sea interface late in the afternoon towards sunset, the temperature gradient between land and sea surfaces lessens, and thus the sea breeze circulation is washed out (Frysinger, et. al. 2003). As the front washes out and the circulation dies, the circulation's signature in observational data tends to disappear as well. However, preliminary analysis of observational data for stations that record on the beaches themselves (such as the Fripp Island site near Charleston in South Carolina), proximity to the ocean means the difference in readings between maritime and inland air masses are often negligible no matter when they are taken.

Observational data for this study come from the North Carolina State Climate Office (hereafter known as the SCO). Coordination of the myriad sources of observational data around the Southeast movitated the creation of the Climate Retrieval and Observations Network Of the Southeast (CRONOS) database, a data archive from sources including automated and manned stations from Virginia to Georgia. For the purposes of this study, data were accumulated from four stations representing much of the coastal areas of North and South Carolina, specifically the ASOS sites at the municipal airports in Savannah, Georgia, Charleston and Myrtle Beach, South Carolina, and Wilmington, North Carolina. Hereafter the following three letter designations for

each site will be used in many figures and tables: SAV for Savannah, CHS for Charleston, MYR for Myrtle Beach, and ILM for Wilmington. Figures 2.2 through 2.3 show the locations of each airport site relative to the nearby coast, and Table 2.1 documents the distance from each station to the nearest coastline in kilometers, as well as the orientation of the coastline with regard to true north, expressed as the angle in degrees between the line parallel to the coast and the true north direction. The last two locations, ILM(E) and ILM(S), refer to the coasts facing east and south respectively, a distinction that will be significant later on.

Table 2.1 ***Distance of the four coastal sites from the coast (in km) and orientation of the adjacent coastlines relative to true north (in degrees)***

	SAV	CHS	MYR	ILM(S)	ILM(E)
Angle (°)	40	46	44	105	32
Distance (km)	35	27	2	36	12

For each airport station, meteorological variables from air temperature to visibility to humidity to cloud coverage at multiple atmospheric levels are recorded at one-hour intervals, but for this study, surface (2-meter) data were specifically collected for air temperature, dewpoint, relative humidity, wind speed and direction, and weather type (the designation for the observation of precipitation). This last variable was recorded for the sake of determining those days on which the lack of sea breeze detection might be explained by the presence of synoptic-scale cloud cover and/or precipitation. Data were collected for the period from 1 April 2003 to 1 August 2005, however, this study will be primarily concerned with analyzing the months of April through July of

2003, 2004, and 2005, those months in which the sea breeze is stronger and more frequent due to the frequency of sufficient land-sea surface temperature differential.

The second body of data also comes courtesy of the SCO, specifically the office's archive of satellite imagery taken from the *GOES-8* satellite through the National Climatic Data Center (NCDC). The imagery is in the visible wavelength, centered over the Southeast roughly corresponding with the same area covered by the SCO's CRONOS database. The data are archived by date, and can be accessed by a website maintained by the office as well as through the local network. For this study, data were accumulated and analyzed for the 1 April thru 1 August time period for 2003-2005. The imagery was analyzed in order to deduce the nature of the circulation over inland areas, its movement and extent as well as its interaction with other synoptic- and mesoscale features.

Horizontal mass convergence along the sea breeze frontal boundary will usually result in the linear cloud feature discussed earlier. At times (especially in July or August) static stability of the ambient air mass will be low enough to contribute to explosive convective thunderstorm development along the boundary, and some studies have shown that up to 75% of sea breeze boundaries over the Carolinas become convectively active (Koch and Ray, 1997). At other times the air mass is too stable or too dry, and little to no cloudiness is associated with the front. On satellite imagery, the sea breeze front is manifested by an often contiguous line of cumulus clouds. The area behind the front, between the front and the coast of the front's origin, is often characterized by much clearer skies due to increased stability and subsidence introduced by the change in air mass regime.

Figure 2.2 ***Savannah, GA --- courtesy Tiger Map Server. Red pin – airport site, red dot – CO-OPS water temperature data site, gold dot – SEACOOS water temperature data site***

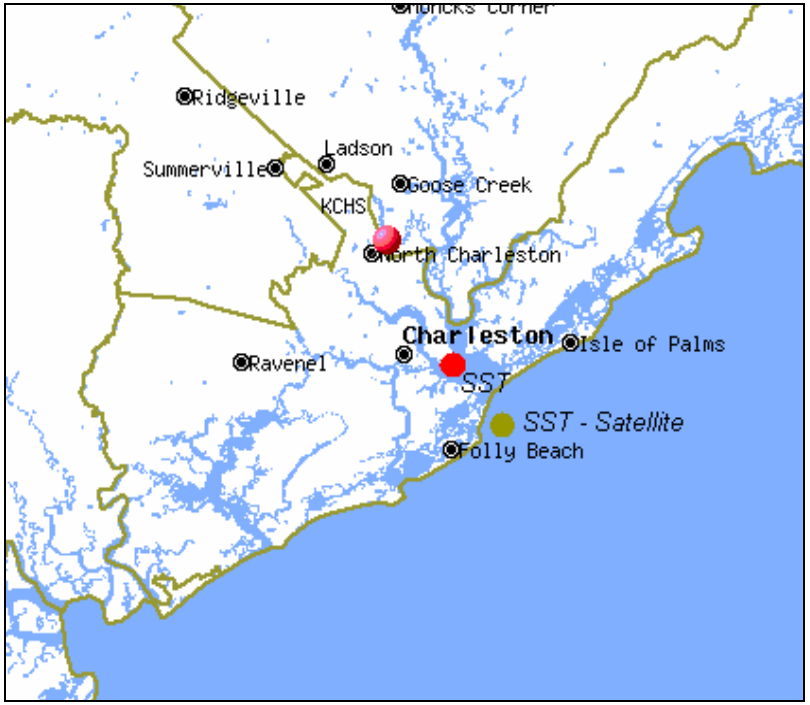

Figure 2.3 ***Charleston, SC --- courtesy Tiger Map Server. Red pin – airport site, red dot – CO-OPS water temperature data site, gold dot – SEACOOS water temperature data site***

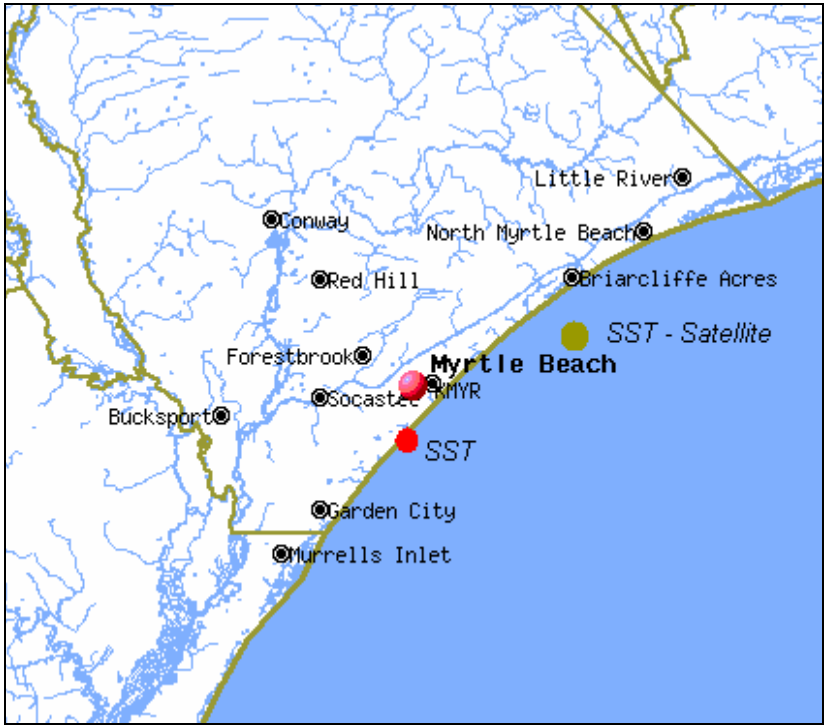

Figure 2.4 ***Myrtle Beach, SC --- courtesy Tiger Map Server. Red pin – airport site, red dot – CO-OPS water temperature data site, gold dot – SEACOOS water temperature data site***

Figure 2.5 ***Wilmington, NC --- courtesy Tiger Map Server. Red pin – airport site, red dot – CO-OPS water temperature data site, gold dot – SEACOOS water temperature data site***

Figure 2.6 shows an example of the effects of the sea breeze front on cloud formations, from June 11th, 2003. Ahead of the front, surface heating is still maintaining surface instability and the typical cumulus field of the spring and summer months. The kind of cloud formation shown in Figure 2.6 is not universally associated with the sea breeze, however. On many occasions, especially early in the season, there is evidently not enough instability or moisture over inland areas to produce the cumulus field necessary to identify the sea breeze, leading to an "invisible" sea breeze front.

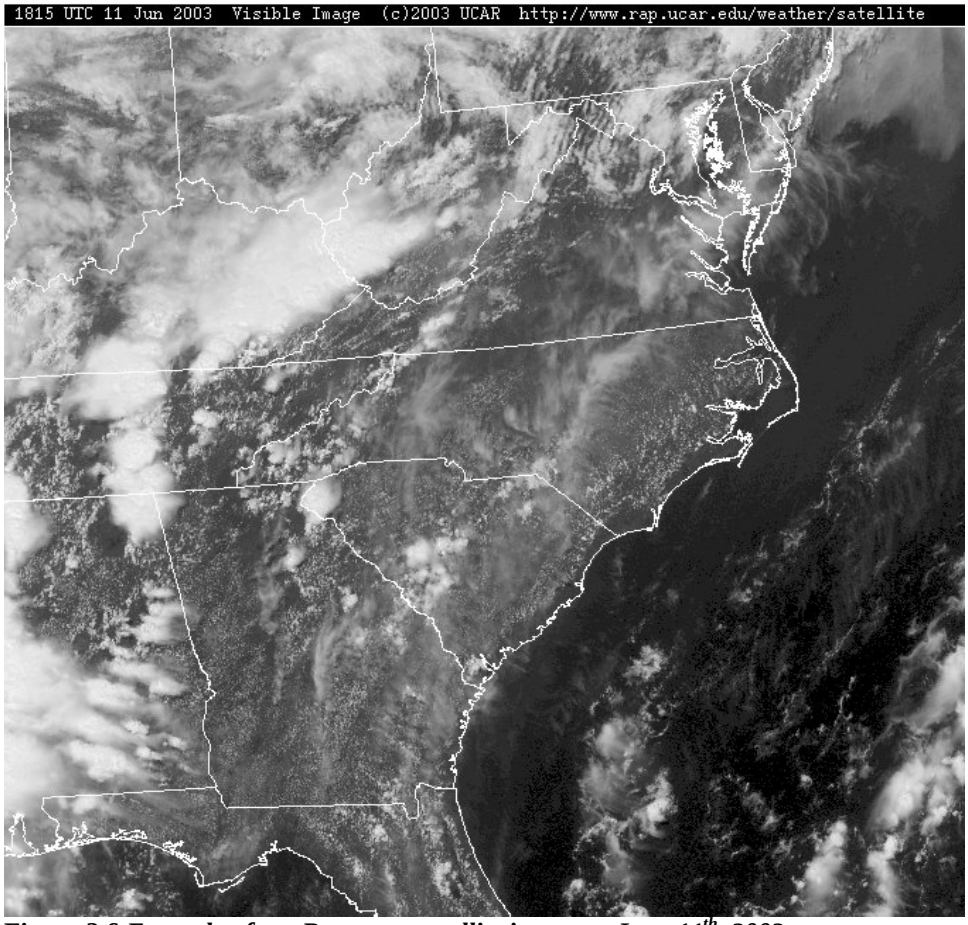

Figure 2.6 ***Example of sea Breeze on satellite image --- June 11th, 2003***
Note the line of clouds parallel to the coast about 20-30 km inland, with Cu field in front and clear air behind.

Later in the season, the cumulus field occasionally redevelops in the clear area behind the sea breeze front, creating confusion about where and when the front moves in the late afternoon and questions as to whether the maritime air mass remains dominant as the front moves further away from the coast.

To analyze the imagery, particular images chosen to represent the furthest penetration of the sea breeze front on a given day were loaded into the ArcGIS program version 9.0. The images were geo-referenced against base maps provided by the GIS

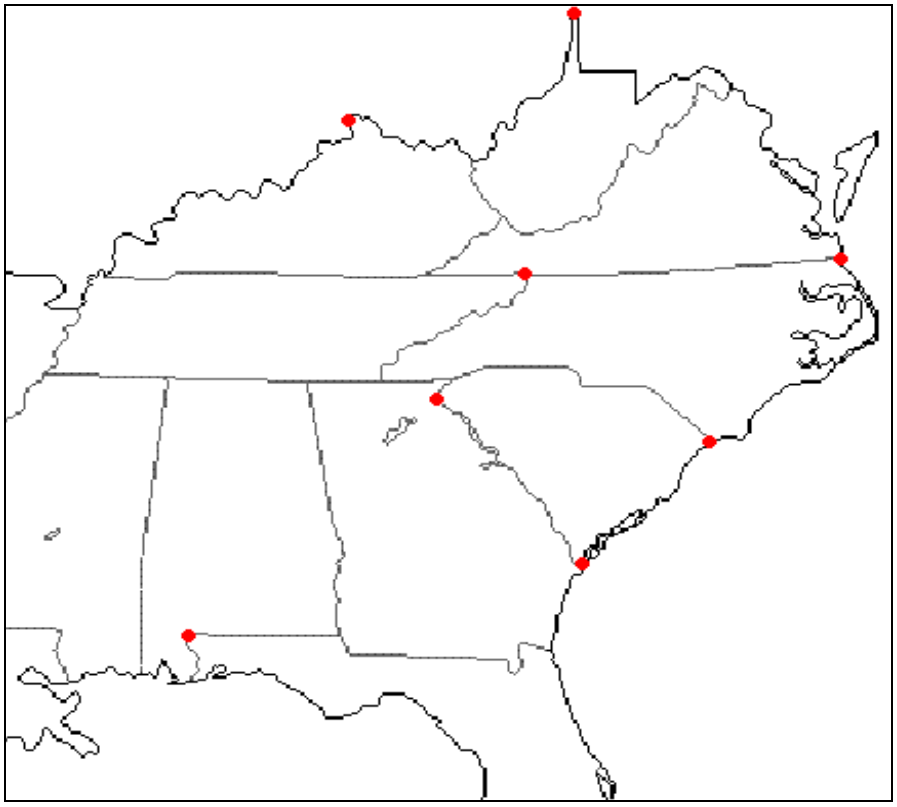

Figure 2.7 ***Control points for GIS referencing, used to analyze sea breeze penetration distances from satellite imagery.***

network using the same seven control points for every image (Fig 2.7) and adjusted using the second-order polynomial method of warping the image slightly to fit the base map. Distances were measured by the distance-measuring tool in the ArcGIS program in kilometers. Two additional sites, at Brunswick, GA and Jacksonville, NC, were added to either side of the four original coastal sites to increase the coverage of the inland penetration analysis to include much of coastal GA and coastal NC up to the just south of the Pamlico and Albemarle Sounds, as shown in Figure 2.8.

2.3 Correlation Study

Theory suggests that since the sea breeze circulation develops because of the temperature difference between land and water surfaces, sea-surface temperatures might be as important to forecasting the sea breeze as land surface temperatures, already recorded as explained above. For this project, sea-surface temperatures (SSTs) are taken from the NOAA's Center for Operational Oceanographic Products and Services (CO-OPS) data archive, which includes not only SSTs but air temperature, barometric pressure, and wind data as well data for tides and currents.

These data are taken from a network of buoys and pier sources around the nation, but for the purposes of this study data from four sites, in coastal waters corresponding to the four airport stations shown in Figure 2.8 and Figures 2.2 through 2.5, were collected for the 1 April – 1 August 2003-2005 period at four-hour intervals. As we can see from Figures 2.2 through 2.5, the sites chosen to record SST values are not as ideally located as they might be (the SST data from Wilmington in particular comes from a site some 15 to 20 km up the Cape Fear River). However some data continuity issues in the CO-OPS

data sets narrowed the options for comprehensive SST data assimilation. To increase confidence in the accuracy of water temperature measurements, SST data was also assimilated from satellite sources, archived by the Southeast Atlantic Coastal Ocean Observing System (SEACOOS), for points adjacent to the airport and CO-OPS water temperature sites (see Figures 2.2 through 2.5), and will be used for both reference and analysis purposes. These SST data represent merged products of the Advanced Very High Resolution Radiometer (AVHRR), Tropical Microwave Imager (TMI), and GOES satellite platforms, using optimal interpolation across the SEACOOS domain at a 5 km resolution. Analysis of the water temperature data from both sources will be for the most part confined to the data at 1200 LDT, the time closest to when one might expect temperature differences would represent those values associated with sea breeze development.

The second theoretical controlling factor is the effect on the circulation produced by the synoptic wind regime. During the months of April through May, the synoptic-level flow is in transition from the pattern of frequent cold frontal passage during the winter and spring months to the dominance of the so-called Bermuda High,

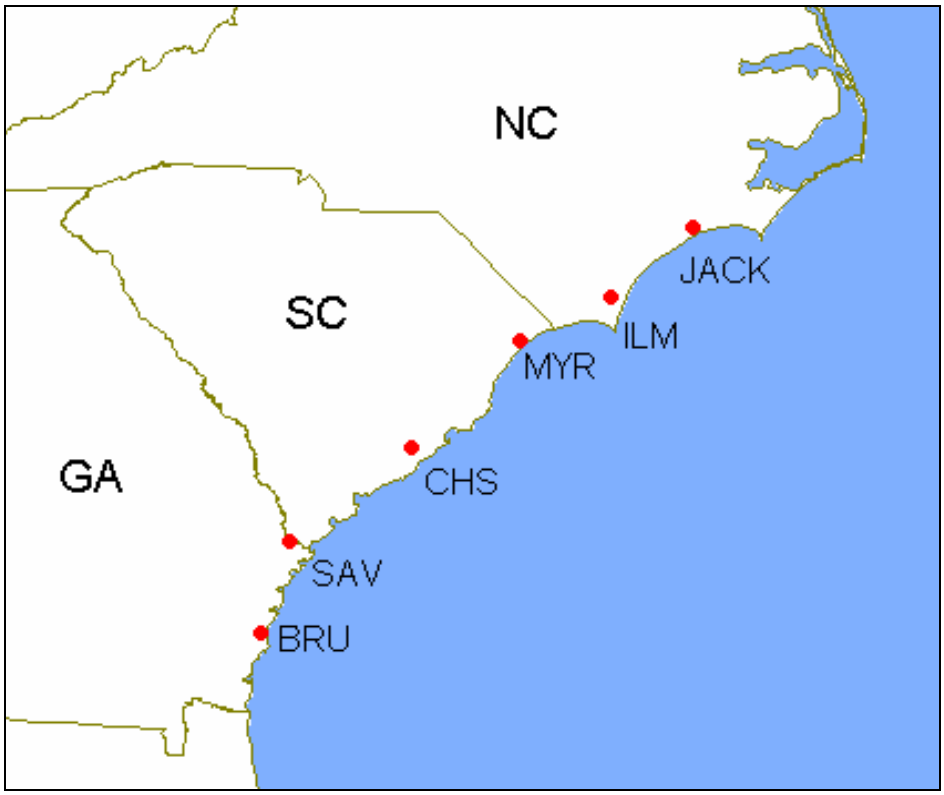

Figure 2.8 ***Reference points for distance measurement from satellite imagery.***

the semi-permanent high pressure system centered over the Western Atlantic that usually induces a general south to southwesterly flow over the southeastern states. These patterns are evident in observational data as will be shown later. Intuitively the low-level wind on a synoptic scale will have a definite impact on wind patterns on phenomena on the mesoscale, such as the sea breeze circulation. A significant offshore flow would be expected to slow down or even stop the inland progression of the sea breeze front, while onshore flow might contribute to moving it further in.

To analyze the synoptic-scale flow regime, patterns of geostrophic wind were examined. Geostrophic winds refer to those winds caused solely by the balance of pressure gradient and Coriolis forces between systems of high and low pressure. On a constant-pressure surface chart, geostrophic winds can be calculated as being in direction

parallel to the contour lines and in speed inversely proportional to the distance between the contour lines. In the case of the Southeast U.S., the presence of the nearby Bermuda High during the sea breeze season can be expected to cause a general south to southwesterly flow.

The first step in accumulating geostrophic wind data is accessing North American Regional Re-Analysis (NARR) data through the NOMADS (NOAA Operational Model Archive and Distribution System) web interface. The regional re-analysis incorporates observational data with gridded analyse, including height at several levels from the surface to the higher parts of the troposphere. For this study a dataset with a horizontal grid spacing of 32 km is sampled. The NARR data are downloaded, then converted from the NOAA's given format (grib files) into GEMPAK files using a simple FORTRAN conversion script. This conversion is necessary to examine the files using the GEMPAK (GEneral Meteorology PAcKage) program of data analysis. One of the programs within this computing package enables the user to analyze the data at specific locations corresponding to cities and accessed by their three-digit airport identifier codes, i. e. CHS for Charleston, SC or MYR for Myrtle Beach. The user is able to request geostrophic wind speed (in m/s) and direction (in degrees clockwise from the 0º or North direction). For this study, analysis indicated that the most representative and accurate measure of near-surface geostrophic wind flow came from the dataset's gridded values of height for the 1000 mb pressure level.

Data were accessed in this manner for the four coastal sites of Charleston and Myrtle Beach, SC, Savannah, GA, and Wilmington, NC for the 1 April - 1 August time period for 2003-2005, every day at 1200 LDT. This time was chosen once again to as

closely as possible examine the conditions under which the sea breeze circulation is forming, as well as to coincide with the water temperature data mentioned above.

SECTION THREE: Climatology

3.1 Classification System

The general methodology for determining whether or not the sea breeze has passed through a given surface observation station has been explained in previous sections. The methodology used by this researcher was a somewhat subjective one, especially at the beginning of research, and depended on the detection of a preponderance of the signs typically associated with the passage of the sea breeze front. The occasion of all of these signs occurring at the same time was not a necessary condition for consideration, and a designation was assigned to each day that reflected the certainty that a researcher might possess in assessing whether the sea breeze had developed and passed through the station. A certain day at a certain station would receive a classification of five if there is almost complete certainty that the sea breeze had passed through at some point, and would receive a classification of one if there was almost complete certainty that it had not. Table 3.1 reflects a summary of this assessment.

Table 3.1 ***Distribution of sea breeze observational classes among the four coastal sites, along with the relative definitions of each class.***

Class		Savannah	Charleston	Myrtle Beach	Wilmington
One	No Sea Breeze	159	160	139	143
Two	SB Unlikely	100	94	110	117
Three	SB Possible	67	54	58	62
Four	SB Likely	36	41	46	40
Five	Certain SB	4	17	13	4

Tables 3.2 through 3.5 are examples corresponding to the classes of researcher certainty regarding frontal passage. Table 3.2 is a class five day, from May 3rd, 2003. Note the tell-tale signs of the sea breeze between 1500 and 1600 LDT (Local Daylight Time), including the temperature drop, rise in dewpoint, change in wind direction (to a southerly breeze) and increase in wind speed. A rough approximation of the synoptic-scale flow can be deduced from the observed surface winds prior to sea breeze frontal passage, and indeed the geostrophic winds calculated on this particular day were quite strong and almost exactly parallel to the coastline from the southwest, as are the surface winds through 1500 LDT. Not only are the direct signs of the sea breeze circulation present but factors that typically argue against sea breeze development are absent, such as observed precipitation, stratiform in nature.

Table 3.3 is an example of a class four day, from April 5th, 2003, the frontal passage this time occurring between 1400 and 1500 LDT. Once again we note a decrease in temperature, as well as an increase in dewpoint, and the expected shift in wind direction. However on this day there is a gap in the station's record of measurement on the 1700 LDT hour, an infrequent but significant occurrence when dealing with observing stations in the CRONOS network. Since the sea breeze circulation is not typically a temporary phenomenon we must have some expectation of continuity in the changes it induces to distinguish between the effects of a sea breeze front and those induced by some other phenomena, or a glitch in the instrumentation. In fact on this particular day the wind seems to die down and become variable in direction from 1700 LDT on. In addition there is no discernible increase in wind speed, probably due to the fact that winds were already quite strong before the assumed passage of a sea breeze

front. Despite these questions, there is continuity regarding the changes in temperature and dewpoint, so this researcher is still fairly confident that sea breeze frontal passage has occurred.

Table 3.4 contains data from May 15th, 2003, from the Myrtle Beach Airport, indicating a possible sea breeze frontal passage around 1100 LT characterized by an increase in dewpoint, the typical changes in wind direction and speed, and if not a decrease in temperature then at least a plateau in the normal temperature curve atypical of a day in mid-May. However, this leveling off precedes the apparent passage of the sea breeze by an hour or two. In addition although the dewpoint does rise, it almost immediately lowers again before rising later in the afternoon. Finally the wind direction is not constant after frontal passage, although the changes are fairly minor and in general the wind stays southerly (and fairly strong). The preponderance of evidence suggests that the site was affected by the sea breeze induced maritime air mass, but detailing a specific time for

Table 3.2 ***Example of a class five day from May 2nd, 2003 --- Charleston airport. An example of a day on which the Charleston airport site was almost certainly affected a by a sea breeze front.***

	Temp. (ºC)	Dwpt. (ºC)	Wind Spd. (m/s)	Wind Dir. (º)
0800 LT	21.1	18.3	3.6	280
	23.3	18.9	3.6	290
	25.0	18.9	4.5	280
	27.2	17.8	5.4	320
	28.9	17.8	3.6	330
	29.4	17.8	5.8	280
	30.0	17.8	4.5	250
1500 LT	30.6	17.2	4.0	290
1600 LT	29.4	21.1	6.7	200
	27.8	21.1	5.8	210
	26.1	20.0	5.8	220
	25.0	20.6	5.4	210
2000 LT	23.3	20.6	4.0	210

Table 3.3 ***Example of a class four day from April 5th, 2003 --- Charleston Airport. An example of a day that was probably affected by the sea breeze front.***

	Temp (ºC)	Dwpt. (ºC)	Wind Spd. (m/s)	Wind Dir. (º)
0800 LT	20.6	16.1	4.0	220
	23.3	14.4	5.8	230
	25.6	15.0	5.8	240
	26.1	13.9	6.7	230
	27.8	13.9	8.0	230
	28.3	14.4	7.6	230
1400 LT	29.4	14.4	4.0	270
1500 LT	27.2	16.7	6.7	190
	22.8	18.3	1.8	350
	22.2	18.3	3.6	190
	21.7	17.2	3.6	180
2000 LT	20.6	17.8	3.6	240

Table 3.4 ***Example of Class Three Day from May 14th, 2003 --- Myrtle Beach Airport. An example of a day that may have been affected by the sea breeze front, but there are signals both for and against. In any case those days of class three, four, or five were considered for this study to be "sea breeze" days.***

	Temp. (ºC)	Dwpt. (ºC)	Wind Spd. (m/s)	Wind Dir. (º)
0800 LT	18.9	10.0	1.8	40
	22.2	6.1	2.2	60
	22.8	6.1	3.6	130
1100 LT	22.8	8.3	3.1	
1200 LT	22.8	10.6	5.4	170
	22.8	11.1	5.4	180
	22.8	9.4	5.4	200
	22.8	11.1	5.4	210
	22.8	12.2	4.0	210
	22.2	12.2	3.1	210
	22.2	12.8	3.6	200
	21.1	13.3	2.7	180
2000 LT	20.6	15.0	1.8	180

Table 3.5 ***Example of Class Two Day from May 16th, 2003 --- Wilmington Airport. An example of a day that was probably not affected by the sea breeze front. Those days characterized as class one and two were considered for this study "non-sea breeze" days.***

	Temp (ºC)	Dwpt. (ºC)	W. Spd. (m/s)	W. Dir. (º)
0800 LT	17.2	15.0	0.0	
	19.4	15.6	2.7	270
	21.7	14.4	3.6	270
	22.8	12.8	2.7	260
1200 LT	23.9	13.9	1.8	
1300 LT	25.0	15.6	4.0	140
	24.4	13.3	4.0	140
	24.4	12.2	4.5	140
1600 LT	23.9	12.2	4.5	170
	23.3	11.1	5.4	200
	21.7	12.8	5.4	190
	18.9	13.3	2.7	200
2000 LT	17.2	13.9	1.8	160

frontal passage or even stating conclusively that this was the sea breeze is not a certain proposition. This designation also applies to those days on which there is strong evidence of sea breeze frontal passage, but it occurs either very late or very early relative to the average frontal passage for a given area.

A case like the one presented in Table 3.5 is an example of class two. At this point and for class one days, the preponderance of evidence tends to suggest that the area was not affected by a sea breeze front. Between 1200 and 1300 LDT, there is an increase in dewpoint and a shift in the wind velocity. However there is an associated rise in temperature, and the dewpoint falls quickly after 1300 LDT. The ambiguity of these conflicting signals is enough so that this researcher cannot qualify these measurements as having been modified by the sea breeze front. Again, this does not mean for certain that

there is no sea breeze front at work in any of these cases, it simply means that for the purposes of this study class two days were categorized as being unaffected by a sea breeze front. For class one cases, there is little to no evidence of sea breeze frontal passage in the surface data. This includes days on which there is significant precipitation, frequently stratiform in nature (and thus longer in duration), or after passage of a cold front (usually early in the sea breeze season) that would preclude development of the sea breeze by diminishing the land-sea temperature difference.

For this study, days designated class three, four, or five are considered and will be referred to in further sections as "sea breeze days", or those days on which a sea breeze front formed and was detected at the airport stations. This does not necessarily mean that all of the days considered are actually days affected by the sea breeze, nor that those days not included in the study do not include any sea breeze days. However as statistics will show there is conclusive evidence that those days considered are affected by the sea breeze circulation.

3.2 Average Time of Frontal Passage

Table 3.6 is a summary of the average time of sea breeze frontal passage according to the observational data. Note that the average time of passage is much earlier in Myrtle Beach, reflecting that station's proximity to the coast, while the farthest sites from the adjacent coasts (Savannah and Charleston) have the longest times between development of the circulation and its effects on the observational data. Figure 3.1 reflects the number of instances that frontal passage was recorded at the given times. Here too we can see how distance from the coast affects the time it takes for the sea

breeze front to make it to the inland sites. The fact that the Myrtle Beach site has a much higher and sharper peak makes intuitive sense as well, as the day-to-day variability of sea breeze frontal propagation speed would produce a wider range of passage times as one moves further inland.

Table 3.6 ***Summary of the average time that sea breeze frontal passage (classes three, four, and five of the surface observation system) was noted at the coastal sites.***

	SAV	CHS	MYR	ILM
2003	4:49 PM	4:04	12:36	3:28
2004	5:09	3:24	1:07	3:26
2005	4:31	4:10	12:55	3:53

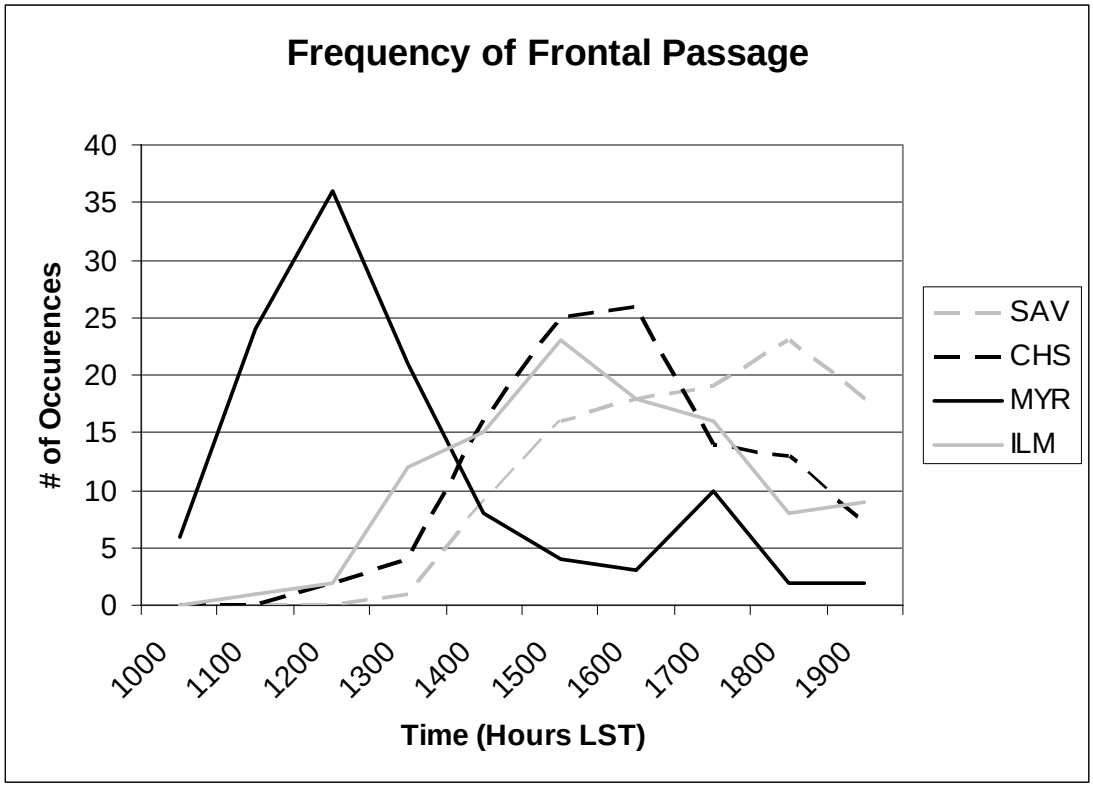

Figure 3.1 ***Frequency of sea breeze passage (classes three, four, and five of the surface observation system) at certain times for each of the four coastal sites.***

3.3 Trends in Temperature and Dewpoint

The next step in analysis of the data set was to examine trends in the meteorological variables to note changes that might be associated with the sea breeze front. Trends in temperature are the subject of Figures 3.2 through 3.7, which show the range in temperatures for the daylight hours averaged over a period of a month (Figs. 3.2 through 3.4) or the four-month sea breeze "season" (Figs. 3.5 to 3.7) for the three-year (2003 to 2005) length of the study.

The first figure (3.2) illustrates the temperature trends by month for the year 2005 from the Charleston Airport site, while Figure 3.3 covers the same period for data from the Wilmington site. As one would expect, the entire range shifts higher with each month from April to July as surface heating increases during the summer months, with the average lying almost directly between the four months. It is telling that the peak of all four graphs (the average time of day when the high temperature is reached) occurs at around 1430 or 1500 LDT in April but earlier (around 1300 LDT) in July. This regression was a common theme among the similar trends observed for the other stations as well as for the other years in the study.

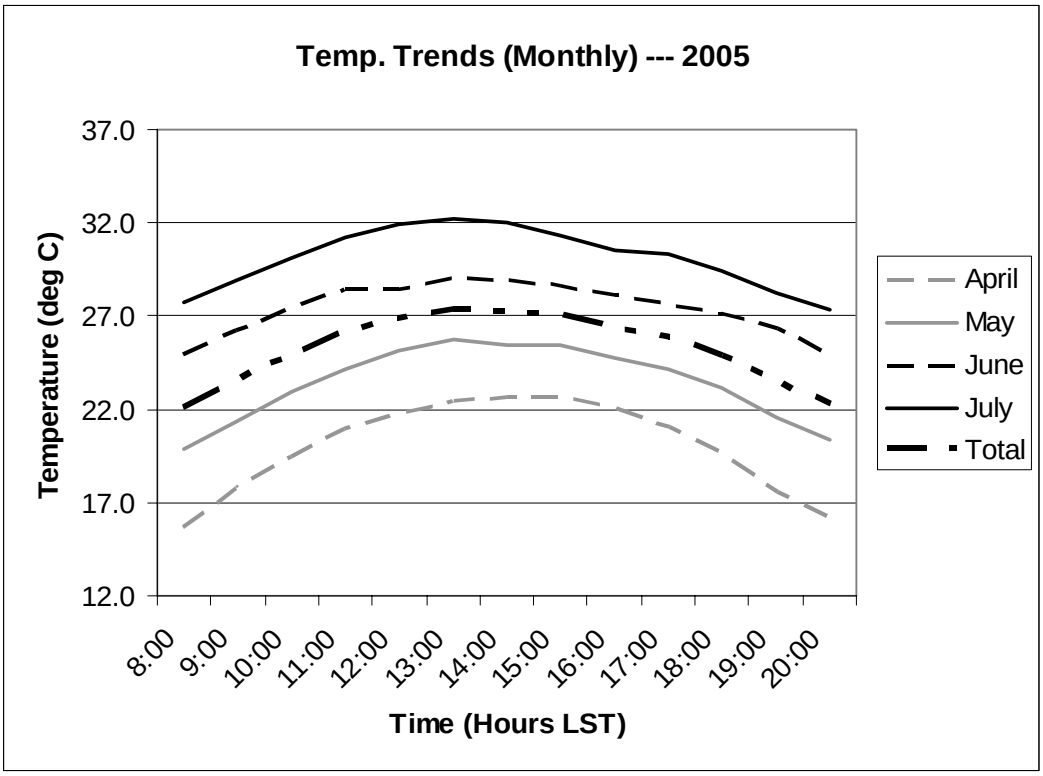

Figure 3.2 ***Temperature curve for the 0800 to 2000 LDT hours, averaged monthly for 2005 data from Charleston, SC. The center line (dashes and dots) represents the average for the entire four month period.***

Compare the trends in these two figures with that of Figure 3.4, from Myrtle Beach data. The diurnal range for Myrtle Beach is much flatter, achieving a peak much earlier in the day (around 1100 LDT) and more or less leveling off for several hours until the loss of surface heating results in the typical temperature decrease in the late afternoon

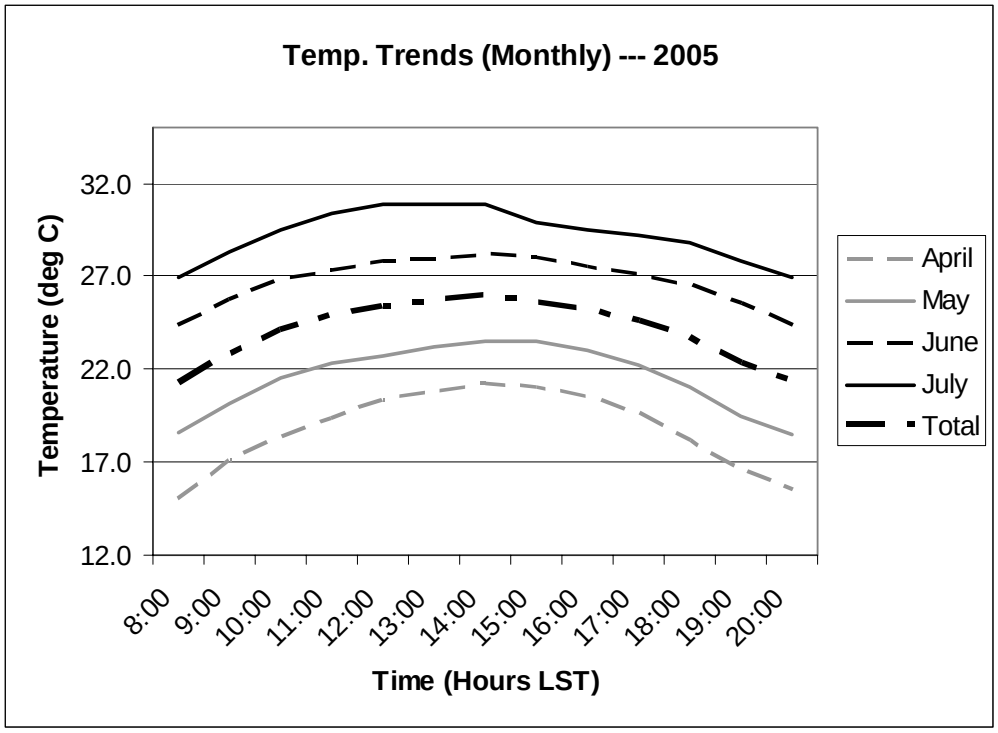

Figure 3.3 ***Temperature curve for the 0800 to 2000 LDT hours, averaged monthly for 2005 data from Wilmington, NC. The center line (dashes and dots) represents the average for the entire four month period.***

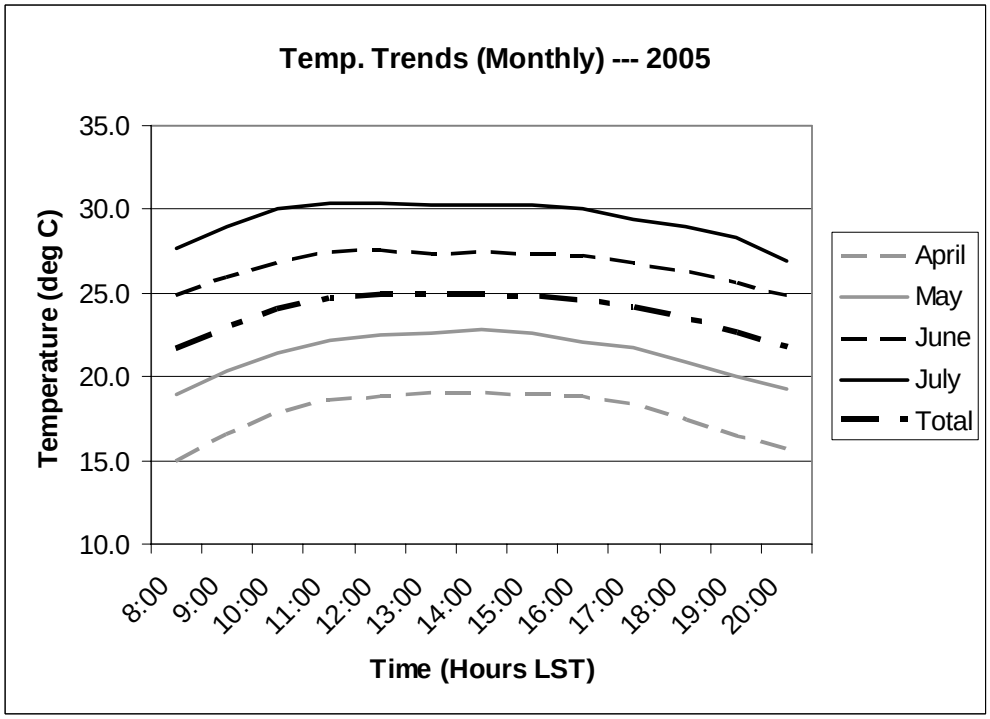

Figure 3.4 ***Temperature curve for the 0800 to 2000 LDT hours, averaged monthly for 2005 data from Myrtle Beach, SC. The center line (dashes and dots) represents the average for the entire four month period.***

hours. Obviously something is inhibiting the normal daylight range of temperatures, moderating temperatures during the optimal surface heating conditions, and this interfering phenomenon works more effectively as one gets closer to the coast.

Figures 3.5 through 3.7 broaden the scope of the analysis by examining trends averaged over the whole season for each of the coastal stations. For reference, the trend for data from Columbia, SC is also included, an inland site some 140 kilometers from the adjacent coast. The Columbia site is very rarely affected by the sea breeze front in any significant way with regard to changes in temperature, dewpoint, and wind vector, so it is useful as a reference site representing the "normal" trends in the meteorological variables on a given day sans the influence of the sea breeze front.

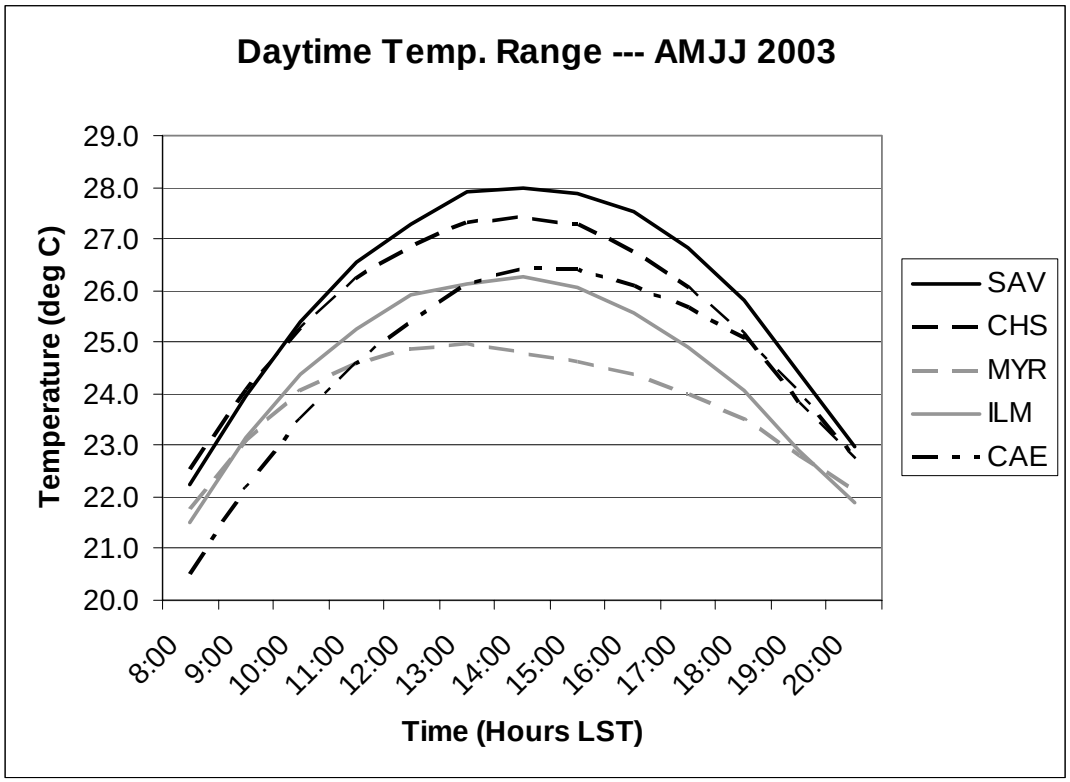

Figure 3.5 ***Temperature curves for the 0800 to 2000 LDT time period, averaged over the entire April-July "sea breeze season" of 2003, for each of the four coastal sites. The same data for the Columbia, SC airport site is included as a reference.***

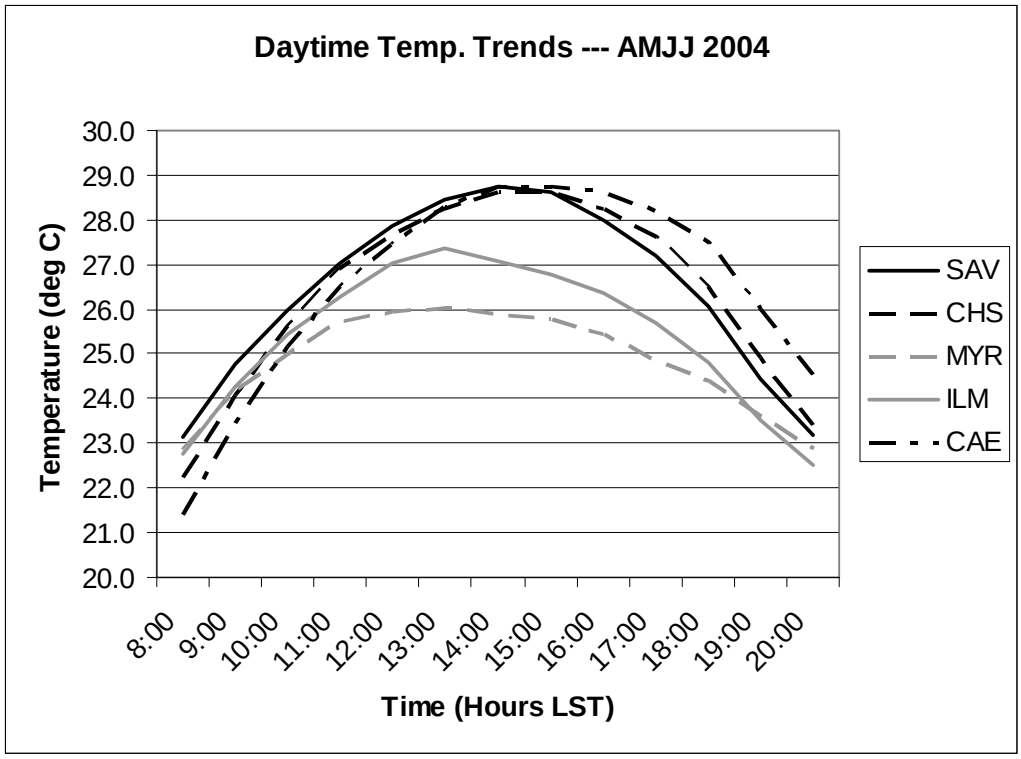

Figure 3.6 ***Temperature curves for the 0800 to 2000 LDT time period, averaged over the entire April-July "sea breeze season" of 2004, for each of the four coastal sites. The same data for the Columbia, SC airport site is included as a reference.***

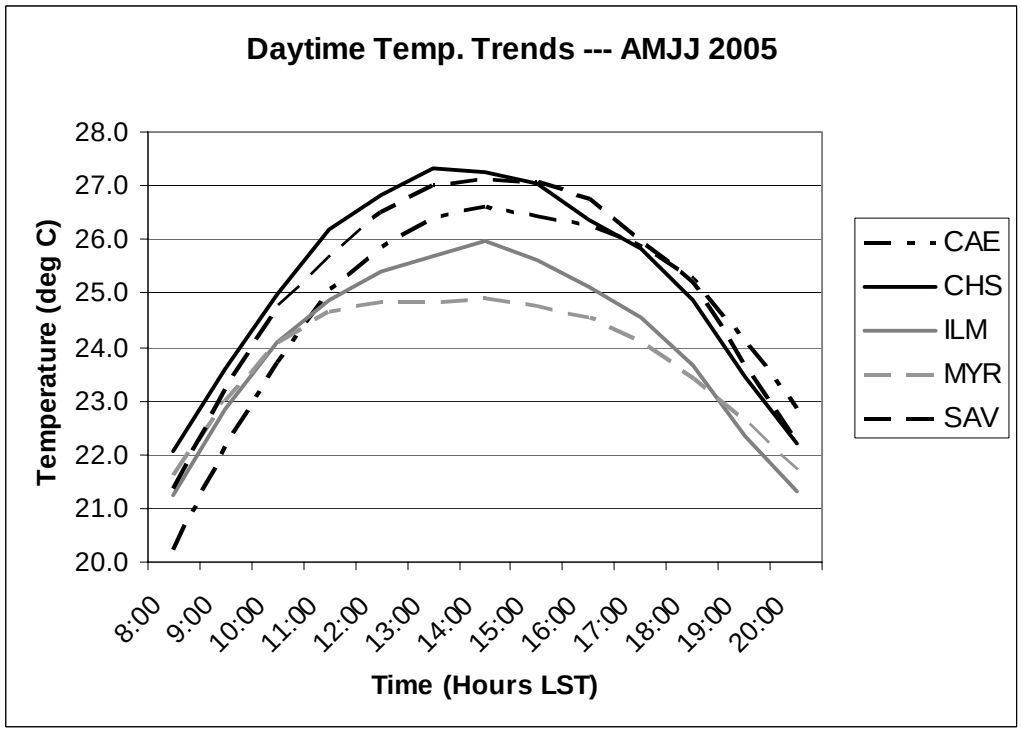

Figure 3.7 ***Temperature curves for the 0800 to 2000 LDT time period, averaged over the entire April-July "sea breeze season" of 2005, for each of the four coastal sites. The same data for the Columbia, SC airport site is included as a reference.***

Between the graphs there are idiosyncratic differences having to do with conditions specific to each year, but there are a few trends that are noticeable among all three years in the study. In each figure, the trend line with the lowest range and peak is Myrtle Beach, where the high temperature occurs around 1300 LDT and is consistently 2-3 degrees lower than the stations at Charleston and Savannah. Next comes the Wilmington station, about a degree or so higher than MYB but a degree or so lower than the other two coastal stations. The Charleston and Savannah sites record temperature trends very close to each other and higher than the other two coastal sites. Although the Columbia trend line shifts vertically in relation to the rest of the stations from the middle in 2003 up to near the top in 2004, the fundamental shape of the curve does not deviate and is significantly different from the coastal stations. While the coastal stations tend to start in the morning (from the first measurement hour at 0800 LDT) at similar temperatures, the Columbia curve starts at a lower temperature. The peak occurs later in the day, about 2-3 hours after Myrtle Beach and about an hour after Charleston and Savannah. It seems reasonable to conclude that the phenomenon inhibiting normal evolution of the temperature curve is the sea breeze circulation. We might assume that without the effects of frequent passage of the sea breeze front, the temperature curves for the four coastal stations would more closely resemble that of the Columbia site.

Passage of the sea breeze front induces changes in air moisture levels as well. Figure 3.8 is similar to Figure 3.6 but reflects trends in dewpoint temperature rather than air temperature. Note that for the dewpoint, the Myrtle Beach site records consistently higher values than the other stations. A typical diurnal curve for dewpoint resembles that of the Columbia trend line with peaks closer to sunrise and sunset and a nadir in the mid-

afternoon, as the PBL thickens and dry air is mixed down to the surface. However the introduction of the moist maritime air mass actually raises dewpoints in the late morning to early afternoon hours at the Myrtle Beach site, and keeps them relatively high through the afternoon. The other three coastal stations feature curves more similar to the Columbia data with peaks at the ends and a nadir in the middle, but the curves are gentler and seem to be offset slightly to the left from the Columbia curve, again a situation probably due to the effects of the sea breeze.

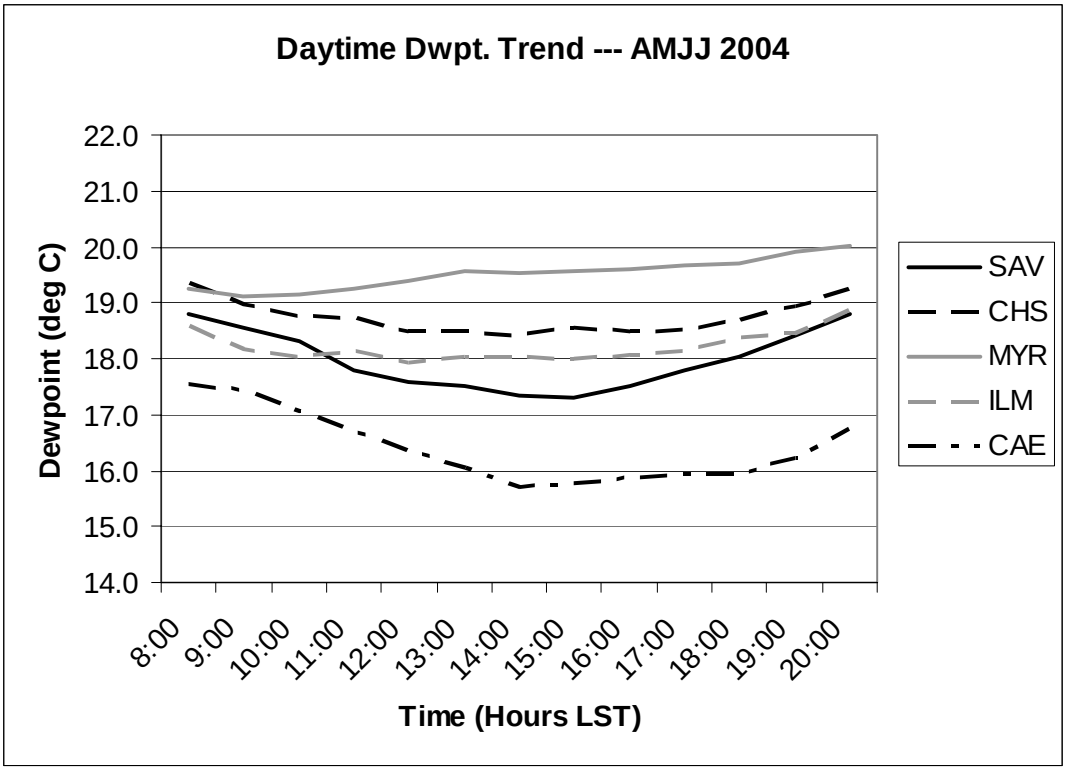

Figure 3.8 ***Dewpoint curves for the 0800 to 2000 LDT time period, averaged over the entire April-July "sea breeze season" of 2004, for each of the four coastal sites. The same data for the Columbia, SC airport site is included as a reference.***

3.4 Trends in Wind Direction

The changes induced by the sea breeze front on the wind vector are best represented by wind roses. It is useful to examine these statistics to compare values from

some time before the sea breeze frontal passage with those after passage. Figures 3.9 through 3.12 are examples of such an analysis. Figure 3.9 is a summary of the frequency of certain observed wind directions during May of the study period (2003-2005) at 1300 LDT every day, a time generally prior to sea breeze frontal passage, while Figure 3.10 represents the same data for 1700 LDT, after frontal passage. Both figures represent data from the Charleston, SC site. These figures do not necessarily represent wind directions for every day of the research period because there were occasional cases of missing data, but one can presume that the summary as listed presents an accurate picture of the sea breeze front and its effects.

The pre-frontal data (Figure 3.9) reflects the normal spread in wind directions one might expect in May over the southeast U.S. (Koch and Ray 1997, Gilliam et. al. 2004). The influence of the Bermuda High that dominates the regional weather during the season is reflected by the fact that the large majority of wind directions are noted from the southwest and south. However, by 1700 LDT (Figure 3.10), after most sea breeze frontal passages have occurred, the wind observations become almost uniformly southerly, reflecting the dominance of a wind circulation generated perpendicular or slightly south of perpendicular to the orientation of the coastline. This shift, with minor variations among the different stations possibly attributable to changes in coastal orientation or topography specific to those stations, is a common one along the coast of the Carolinas. Figures 3.11 and 3.12 show the same analysis for Myrtle Beach observational data, and again we note the dominant southerly breeze that develops after passage of the sea breeze front.

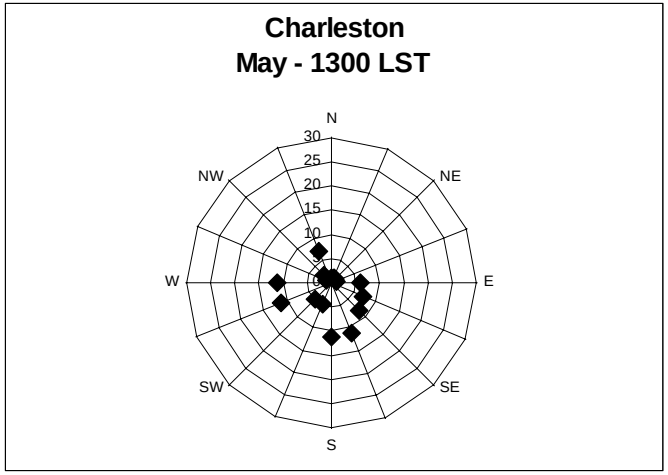

Figure 3.9 ***Frequency of wind directions noted in surface observations from Charleston, SC data at 1300 LDT***

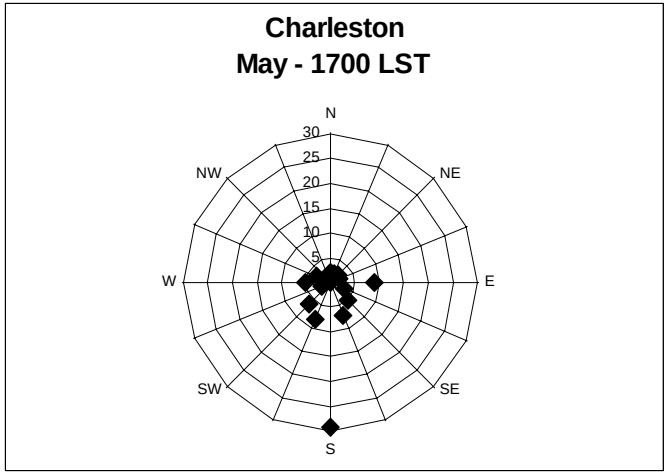

Figure 3.10 ***Frequency of wind directions noted in surface observations from Charleston, SC data at 1700 LDT***

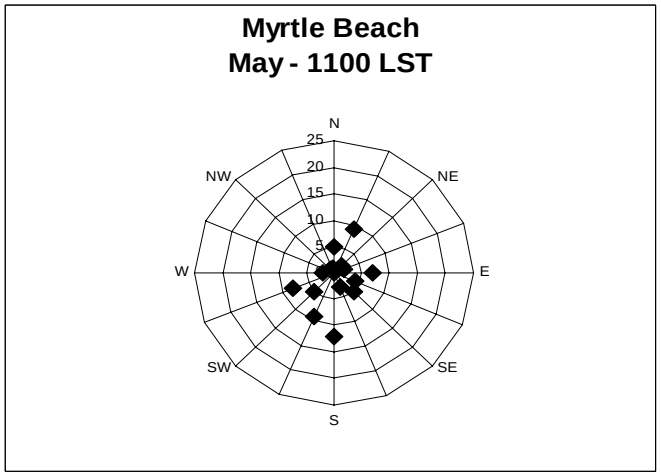

Figure 3.11 ***Frequency of wind directions noted in surface observations from Myrtle Beach, SC data at 1100 LDT***

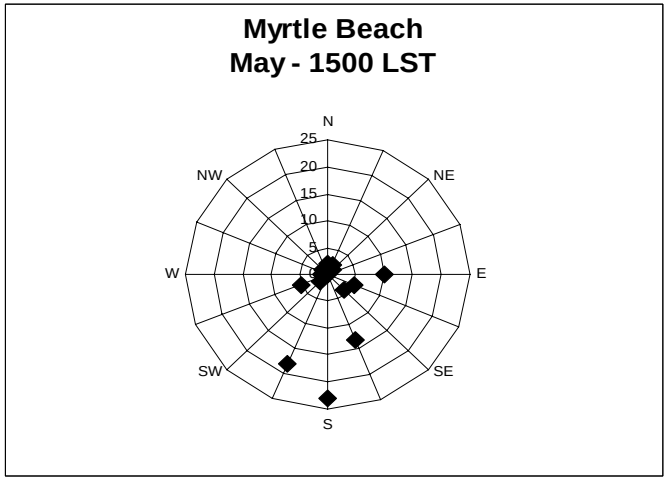

Figure 3.12 ***Frequency of wind directions noted in surface observations from Myrtle Beach, SC data at 1500 LDT***

It is important to note that the wind shifts to a direction somewhat farther south than directly perpendicular to the coastlines in question, which are all very close to or slightly steeper (less) than 45 degrees from north as shown in Figures 2.3 through 2.6. Since the coastal stations in question range up to 30 km inland, the Coriolis force might by mid to late afternoon have had enough time to significantly affect the wind vector, specifically to turn it to the right. Obviously, the overall effect on the sea breeze circulation would be a function of the angle of the adjacent coastline, and the amount of time the Coriolis force has to work on the wind flow pattern before the circulation dies with the loss of surface heating.

Figures 3.13 through 3.15 represent wind direction frequency data for Myrtle Beach for May months in the research period. Recall that the coastline adjacent to the Myrtle Beach site forms an angle of 44 degrees from North, so that we might expect the initial sea breeze circulation to lead to surface winds from around 135 degrees. Figure 3.13 reflects data for the 1300 LDT hour, very close to the average time of sea breeze frontal passage at the MYR site as analyzed previously in table 3.6. Note the dominance of the southerly wind pattern (between 180 and 200 degrees) indicative of the sea breeze circulation. As we move through the 1400 LDT hour (Figure 3.14) to the 1700 LDT hour (Figure 3.15), the dominant wind flow pattern gradually becomes more south-southwesterly, rotating a total of about 20-30 degrees between 1300 LDT and 1700 LDT. We might presume that this shift is the result of Coriolis force acting on the sea breeze circulation. However, based on calculations of the period of the half-pendulum day at the latitude of the Carolinas, the Coriolis force ought to have more of an impact, on the order of 60 degrees in four hours.

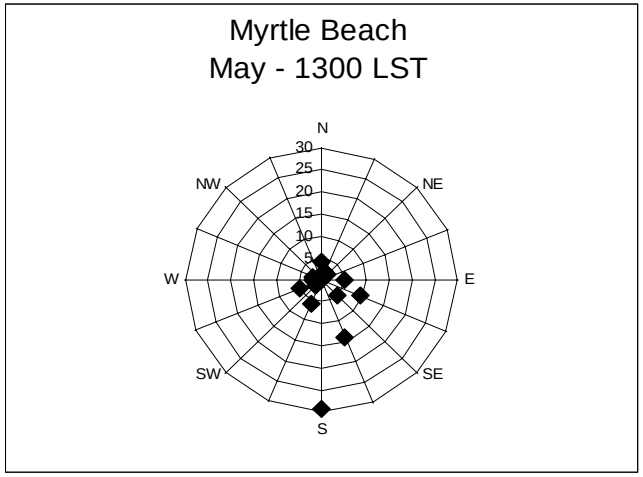

Figure 3.13 ***Frequency of wind directions noted in surface observations from Myrtle Beach data at 1300 LDT***

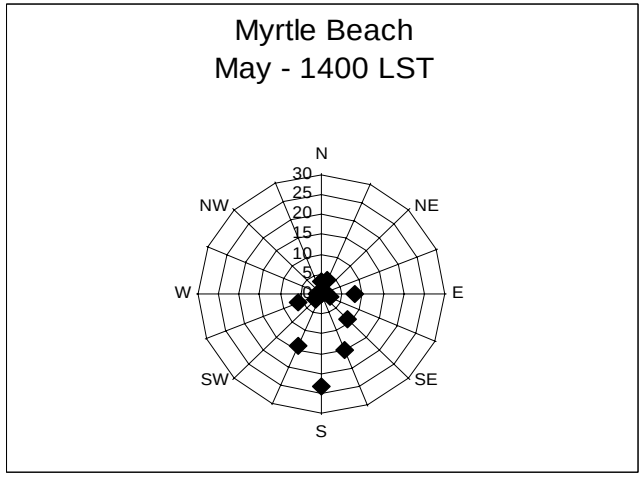

Figure 3.14 ***Frequency of wind directions noted in surface observations from Myrtle Beach data at 1400 LDT***

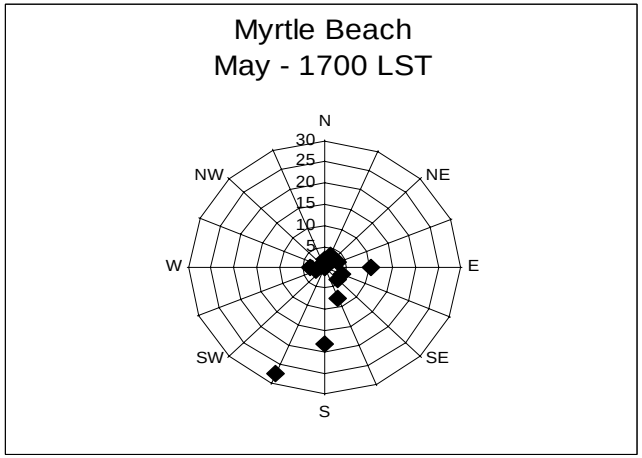

Figure 3.15 ***Frequency of wind directions noted in surface observations from Myrtle Beach data at 1700 LDT***

The same kind of discrepancy has been observed in previous studies of the sea breeze circulation. Simpson (1994) noted that wind directions during the sea breeze regime on Thorney Island near London, England did not shift at all, remaining constant throughout the duration of the event. That study found that turning by the Coriolis force was balanced by local perturbations in the pressure field, including a mesoscale low pressure system associated with the urban heat island effect over London. A similar relationship may explain the discrepancy between theoretical Coriolis turning and observed values for the locations in this study.

Another curious phenomenon takes place involving the Wilmington data. The unique shape of the coastline around the Wilmington site seems to create ambiguities for analysis and interpretation of wind vector data because of the interaction of sea breeze fronts developing along the south-facing and east-facing coasts below and beside the Wilmington site. Due to the prevailing wind patterns during the sea-breeze season, a sea breeze front forming along a shore facing south might be more apt to propagate faster and further inland, with a stronger signal in the observational data, than would a front forming along an east-facing coast. However the distance from the south coast to the Wilmington airport is about twice that from the east coast to the airport, at least partially mitigating this advantage that the southern front has over the eastern front.

Initially this study focused on direction measurements for the 1300 LDT (Figure 3.17) and 1700 LDT (Figure 3.18) hours for the Wilmington site, on either side of the average sea breeze frontal passage time (refer to table 3.6). Upon examination, however, a prominent easterly to east-southeasterly pattern is observed at 1300 LDT that is much less conspicuous in the 1700 LDT summary. Hypothetically, this might be due to the sea

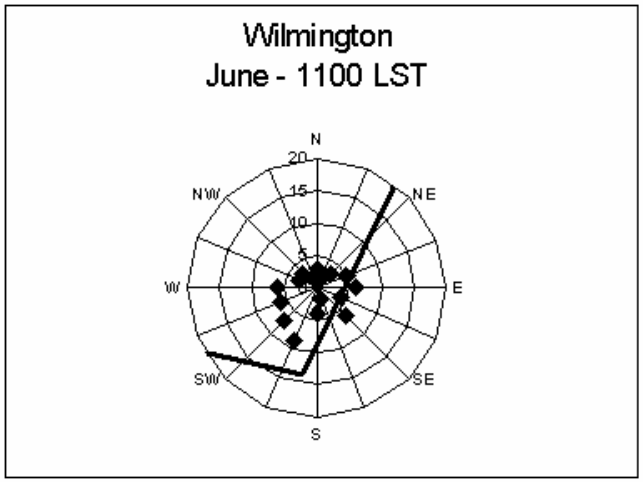

Figure 3.16 ***Frequency of wind directions noted in surface observations from Wilmington data at 1100 LDT***

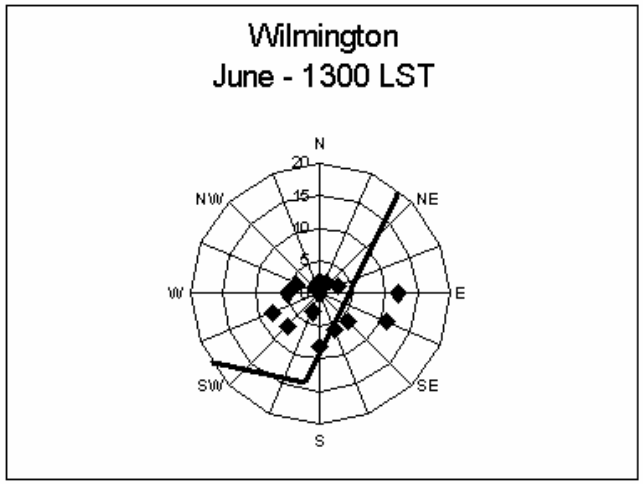

Figure 3.17 ***Frequency of wind directions noted in surface observations from Wilmington data at 1300 LDT***

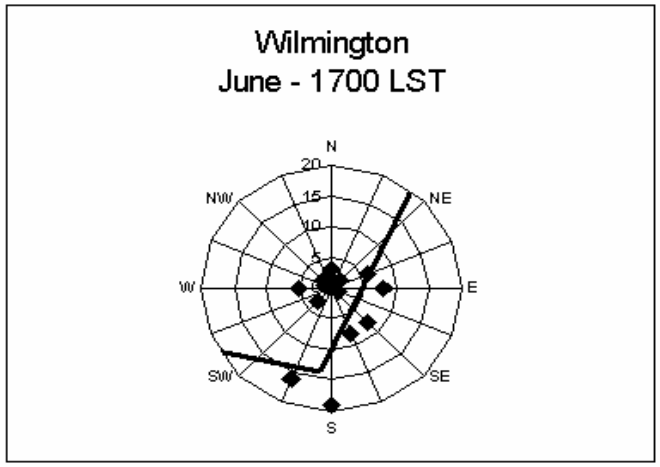

Figure 3.18 ***Frequency of wind directions noted in surface observations from Wilmington data at 1700 LDT***

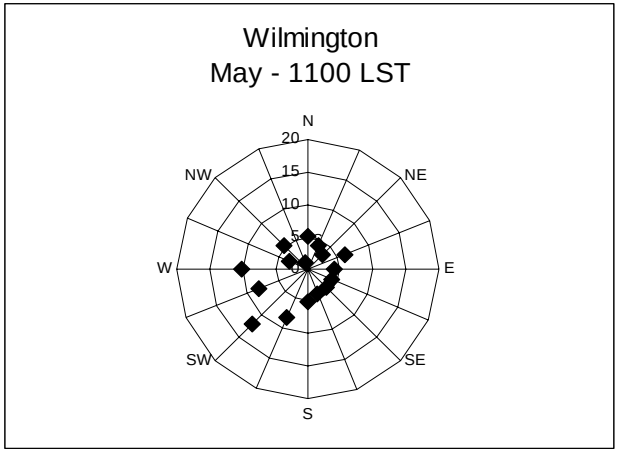

Figure 3.19 ***Frequency of wind directions noted in surface observations from Wilmington data at 1100 LDT***

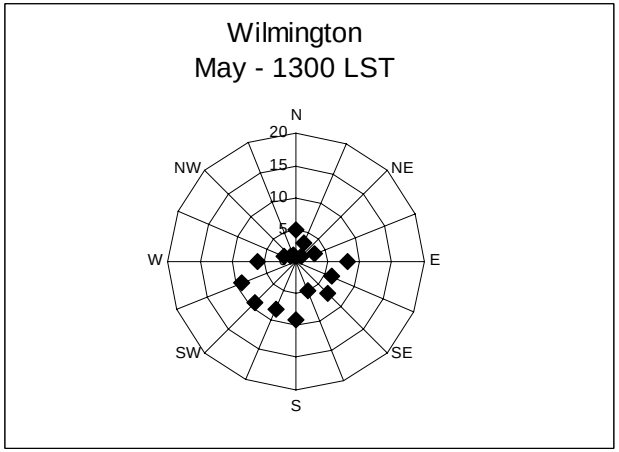

Figure 3.20 ***Frequency of wind directions noted in surface observations from Wilmington data at 1300 LDT***

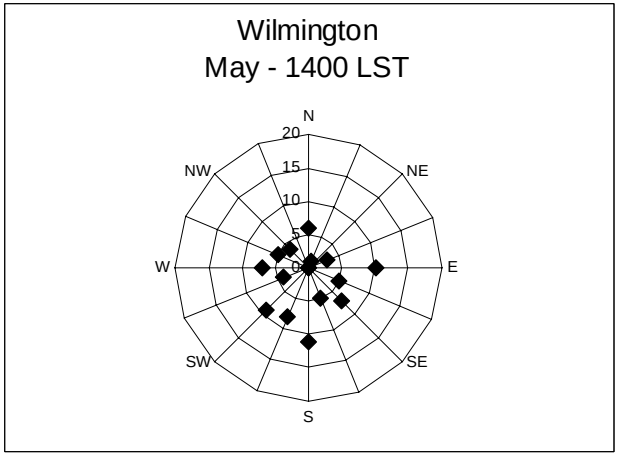

Figure 3.21 ***Frequency of wind directions noted in surface observations from Wilmington data at 1400 LDT***

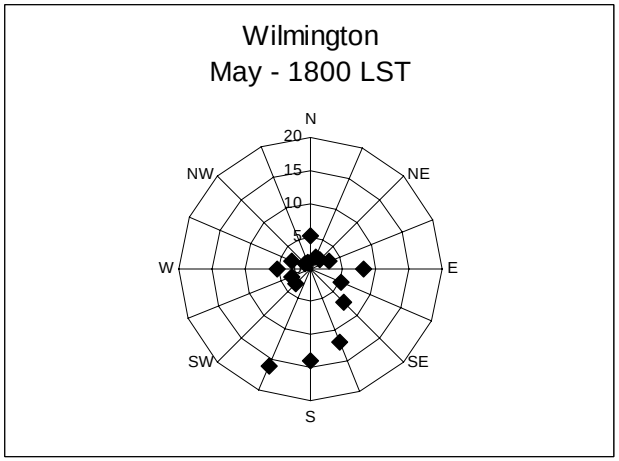

Figure 3.22 ***Frequency of wind directions noted in surface observations from Wilmington data at 1800 LDT***

breeze front generated from the east-facing coast exerting some early influence on the atmosphere before its counterpart from the south takes hold. Further analysis of data from the 1100 LDT summary of direction frequency (Figure 3.16) confirms that neither the southerly or easterly regimes are particularly prominent at this time. An approximation of the coasts forming the Cape Feare Peninsula is included for reference.

It is important to note, however, that this complex relationship is not always so well-defined. Figures 3.19 through 3.22 show a progression of hourly summaries from 1100 LDT to 1800 LDT. In the late morning (Figure 3.19) we find the typical summertime distribution with an expected peak in the southwesterly direction. By 1300 LDT (fig. 3.20) no prominent wind flow pattern remains, although there is an increase in the frequency of wind direction measurements between the easterly and southeasterly directions. Trends from the 1400 LDT hour (Figure 3.22) are similar, although by this point the peaks are from the easterly and southerly wind directions. By the 1800 LDT hour (Figure 3.22), the southerly wind regime has asserted itself, although even here the margin is not so wide with a relatively even spread from 160 degrees up to 220 degrees from north. It is certainly possible that this three-step process is simply more common in June than in other months. The complex relationship between the sea breezes from the south-facing and east-facing coasts near Wilmington also creates issues when examining satellite data, explored in later sections.

3.5 Analysis of Sea Breeze Days

Now that we have established the sea breeze as being a phenomenon significant to the observational data as a whole for our coastal sites, it might be useful to examine

separately the statistics for the days identified as being influenced by the sea breeze circulation. Recall from Table 3.1 that roughly one-third of the days within the scope of this study were identified by observational data as being influenced by the sea breeze circulation, or at least that there was a strong possibility that such an influence was occurring. Figures 3.23 and 3.24 show trends in diurnal temperature range for only those days identified as "sea breeze" days (of classes three, four, and five according to the table 3.1 classification system), encompassing the April through July period for all three years. The elimination of the class one and two days enhances the patterns established by the trends in Figures 3.2 through 3.4, with a significant drop or plateau in temperatures that

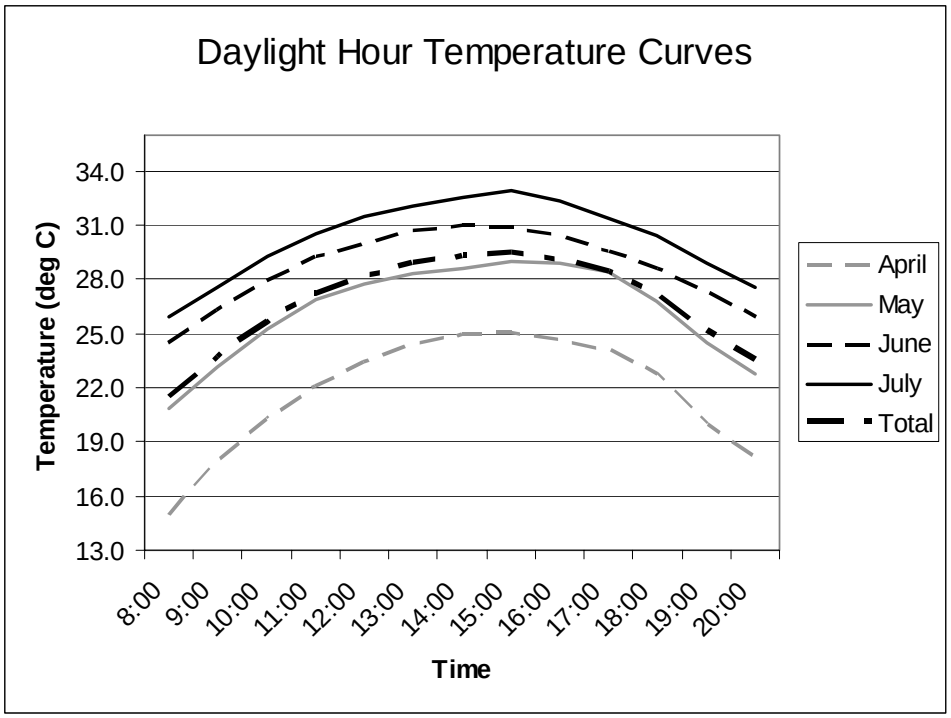

Figure 3.23 ***Temperature curves for the 0800 to 2000 LDT time period, averaged by month over only those days classified as "sea breeze days" during the entire research period for the Savannah, GA airport site.***

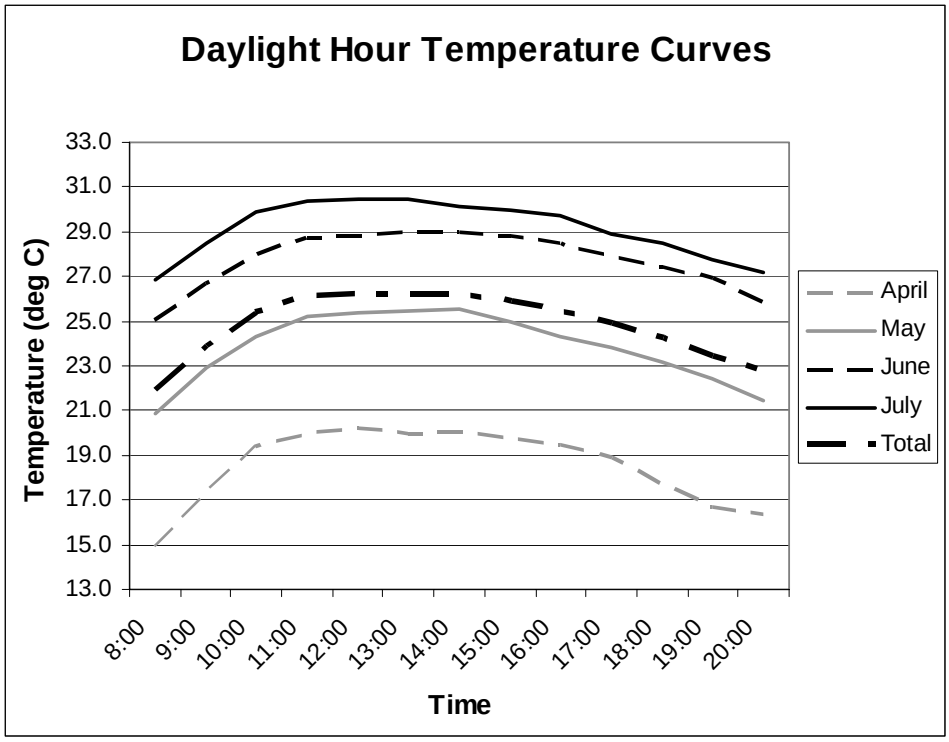

Figure 3.24 ***Temperature curves for the 0800 to 2000 LDT time period, averaged by month over only those days classified as "sea breeze days" during the entire research period for the Myrtle Beach, SC airport site.***

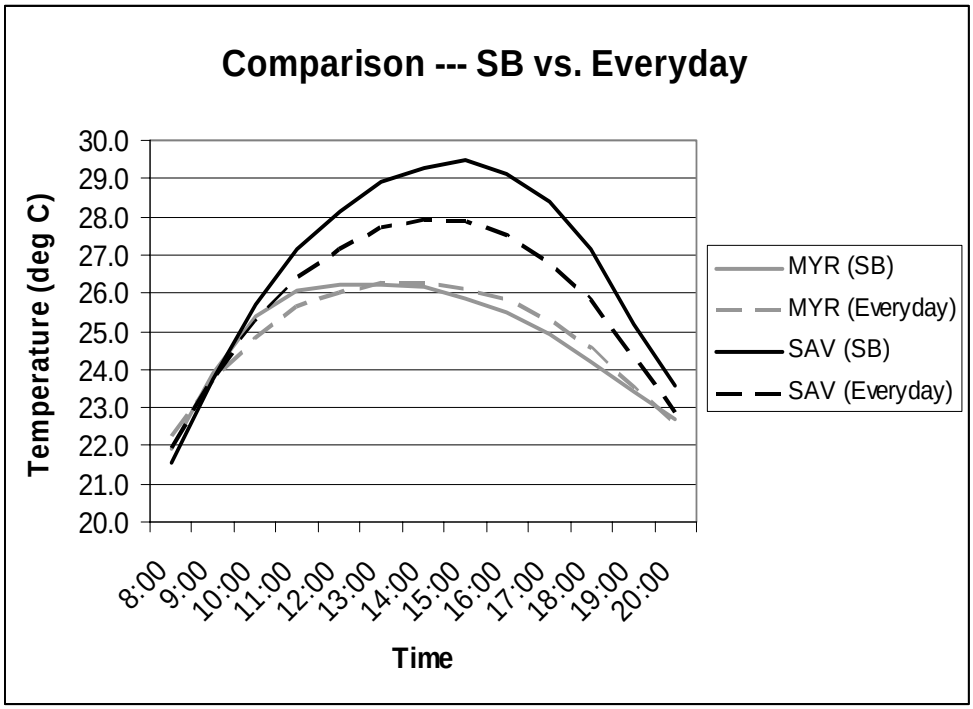

Figure 3.25 ***Comparison of temperature curves for the 0800 to 2000 LDT time period, averaged over the length of the research period for "sea breeze days" only. Gray solid and dashed lines represent analysis of Myrtle Beach, SC data, while black solid and dashed lines represent Savannah, GA data.***

occurs as the sea breeze front passes through. Again we can see that the average time of this passage is a function of the distance from the site in question to the coast.

If we compare the average temperature trends of sea breeze days versus all days (Figure 3.25), we can see immediately that the sea breeze days tend to be warmer than average, with a much steeper incline in temperatures during the morning hours. Since the difference between land and sea surface temperatures is one of the driving mechanisms for the sea breeze circulation, this fact makes intuitive sense.

Table 3.7 represents a summary of the specific hourly changes in temperature and dewpoint associated with the passage of the sea breeze front from the hour before to the hour after frontal passage. Negative values on the left refer to changes in temperature, while positive values on the right are dewpoint changes, with all values in degrees Celsius. Values on the bottom line are the standard deviations for the data. The relatively large values for these standard deviations indicate a relatively wide and even distribution of values for the temperature and dewpoint changes.

Table 3.7 ***Average changes in temperature (left, ° C) and dewpoint (right) associated with passage of the sea breeze front through the four coastal sites. Based on data from days characterized as class three, four, or five of the surface observation classification.***

	SAV		CHS		MYR		ILM	
2003	-1.41	2.51	-1.25	2.39	-0.60	2.51	-1.14	2.00
2004	-1.61	2.95	-0.91	2.40	-0.99	2.11	-1.12	1.92
2005	-1.68		-1.26	2.78	-0.84	2.39	-1.19	2.10
Mean	-1.56	2.73	-1.13	2.53	-0.82	2.34	-1.15	2.00
SD	1.00	1.58	1.14	3.28	1.27	1.84	1.25	1.34

Values for temperature change at the Myrtle Beach appear to be smaller than for the other stations, while those at Savannah are the largest. However the relatively large standard deviations tend to indicate that these site-to-site differences may not be statistically significant, that is, they may result from pure chance or coincidence. A test is needed to determine whether these differences are significant or not, and for this study the test utilized is the chi-square test. The chi-square test is a non-parametric test that seeks to reject the null hypothesis, that apparent differences in trends observed at the coastal sites are due to random chance (Connor-Linton, 2003). In this case we want to be sure that differences we see from station to station in average temperature change are actually due to some physical difference between the sites, and can be expected from all data ever recorded at the stations.

Results from the chi-square test, run for all the four coastal stations at once, indicate that the differences in mean temperature change fall just under the level required to be considered significant. However a test run for just the Myrtle Beach and Savannah sites reveals that there is a significant difference between these two stations. Obviously the differences are very close to the critical significance level for the chi-square test either way.

It makes no sense for the sea breeze to be in some way "weaker" at the Myrtle Beach site, a logical explanation for the lower temperature change, because arguably the sea breeze would be stronger at a location closer to the coast. So the question becomes, what are the circumstances that would explain such a deviation?

The best explanation might be proximity to the coast. Since the Myrtle Beach site is closer to the coast, sea breeze frontal passage occurs earlier in the day, when increasing

surface heating might serve to offset the moderation in temperature associated with frontal passage. Passage of the sea breeze front through the stations further inland like Savannah is often associated with decreasing surface heating, aiding the expected temperature moderation.

Table 3.8 ***Average changes in temperature (left, ° C) and dewpoint (right) associated with passage of the sea breeze front, for those days where such frontal passage was noted prior to 1600 LDT.***

	SAV		CHS		MYR		ILM	
2003	-0.12	2.28	-0.73	2.22	-0.35	2.21	-0.48	1.73
2004	-0.54	2.30	-0.25	1.82	-0.61	1.74	-0.73	1.65
2005	-0.06		-0.51	2.24	-0.53	1.99	-0.57	1.84
Total	-0.22	2.29	-0.45	2.04	-0.50	1.99	-0.62	1.73

Table 3.9 ***Average changes in temperature (left, ° C) and dewpoint (right) associated with passage of the sea breeze front, for those days where such frontal passage was noted at 1600 LDT or later.***

	SAV		CHS		MYR		ILM	
2003	-1.87	2.60	-1.61	2.51	-3.00	5.40	-1.76	2.25
2004	-1.88	3.11	-1.82	3.21	-2.77	3.80	-1.66	2.29
2005	-2.26		-1.63	3.04	-2.66	4.69	-1.67	2.30
Total	-2.00	2.87	-1.67	2.91	-2.76	4.49	-1.70	2.28

The statistics in tables 3.8 and 3.9, reflecting temperature and dewpoint change data summarized according to frontal passage time, further support this explanation. Table 3.8 reflects data for frontal passages that occurred before 1600 LDT, while table 3.9 reflects data for passages from 1600 LDT on. Cursory analysis reveals that for pre-1600 LDT data, the values for temperature change are much smaller than average, while those for 1600 LDT and forward are much larger – in fact the values for Myrtle Beach for 1600 LDT and later are the largest for any of the four coastal sites. The chi-square test for all of the coastal stations confirms a significant statistical difference across the 1600 LDT boundary.

Dewpoint differences also seem to increase across the 1600 LDT mark. Recall from Figure 3.8 that dewpoints tend to decrease just after sunrise and increase again late in the afternoon. Thus higher increases in the dewpoint values would be expected later in the afternoon because the effects of the advancing maritime air mass would be aided by the normal evolution of dewpoint readings. By the same token, lower values before 1600 LDT might correspond with midday mixing processes that tend to offset the increased moisture of the sea breeze air mass. However the chi-square test for dewpoint data indicates that the differences in dewpoint across the 1600 LDT boundary fall just below the level of statistical significance, thus it would not be prudent to rely on these perceived trends.

An examination of the changes in temperature and dewpoint averaged by month (as in table 3.10) also indicates that these changes are subject to variation from season to season. Decreases in the changes in dewpoint may be due to variations in air moisture content, with the highest ambient dewpoint readings found in the latter part of the sea

Table 3.10 ***Changes in temperature (left, ° C) and dewpoint (right) associated with passage of the sea breeze front averaged by month.***

	SAV		CHS		MYR		ILM	
April	-1.66	3.76	-0.80	3.18	-1.32	3.77	-0.84	2.35
May	-1.85	2.93	-1.76	2.94	-1.03	2.46	-1.26	1.81
June	-1.41	2.27	-1.14	2.13	-0.70	1.96	-1.36	1.96
July	-1.40	2.19	-0.85	1.90	-0.34	1.47	-1.19	1.87

breeze "season", thus reducing the difference in dewpoint between the ambient and maritime air masses. Based on the available information, it is difficult to determine a consensus relationship between the time of season and average temperature changes.

Figures 3.26 through 3.29 reflect changes in wind direction frequency between the hours before the sea breeze frontal passage and after, specifically wind direction measurements two hours prior to frontal passage ("Pre-Front" Figures 3.26 and 3.27) and two hours after ("Post-Front" Figures 3.28 and 3.29). As with the analogous figures in section 3.4, the trend towards the dominant southerly wind flow is obvious, although it is even more evident in these cases, almost to the exclusion of other wind direction readings. It is also evident that the predominant wind flow in the pre-front period is a southwesterly regime. This is typical of the Southeast U.S. with the Bermuda High in

control during the sea breeze season, but this statistical trend is also in part a function of the fact that the wind direction shift is easier to detect with ambient wind directions from the southwest. Wind speed also increases due to the frontal passage, as shown in table 3.11. Chi-square tests run for the wind speed data summarized below do indicate that these changes are statistically significant.

Table 3.11 ***Average wind speeds (m/s) prior to and after sea breeze frontal passage recorded from the Charleston and Myrtle Beach airport sites.***

	CHS	MYR
Pre-Front	3.7	3.3
Post-Front	5.4	5.5

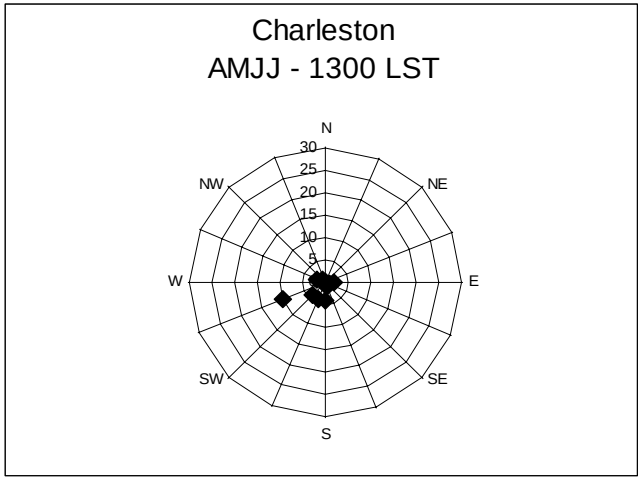

Figure 3.26 ***Frequency of wind directions noted in surface observations at the Charleston site at 1300 LDT, on "sea breeze days" only (classes 3-5).***

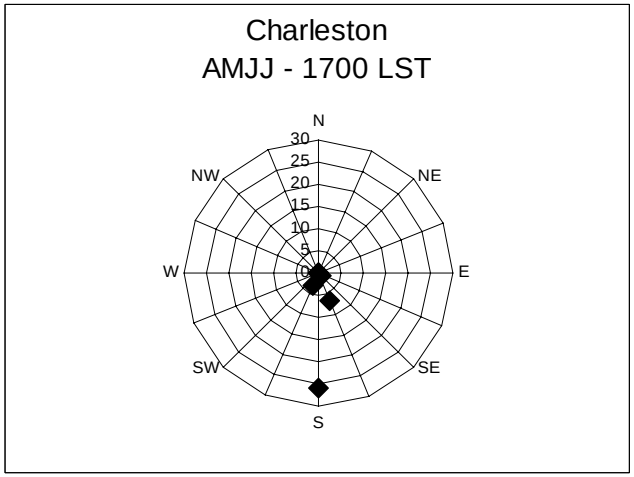

Figure 3.27 ***Frequency of wind directions noted in surface observations at the Charleston site at 1700 LDT, on "sea breeze days" only (classes 3-5).***

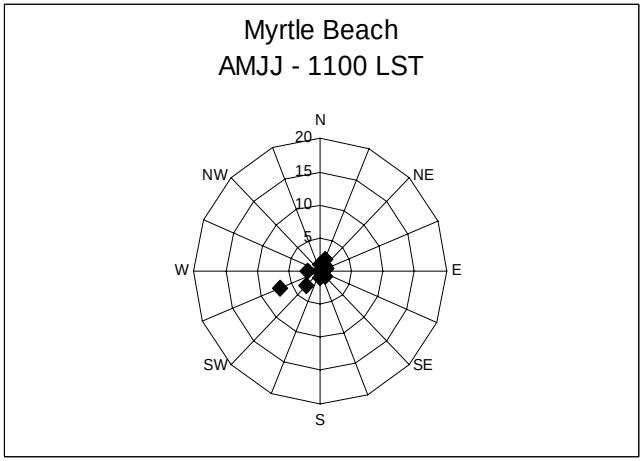

Figure 3.28 ***Frequency of wind directions noted at Myrtle Beach at 1100 LDT, on "sea breeze days" only.***

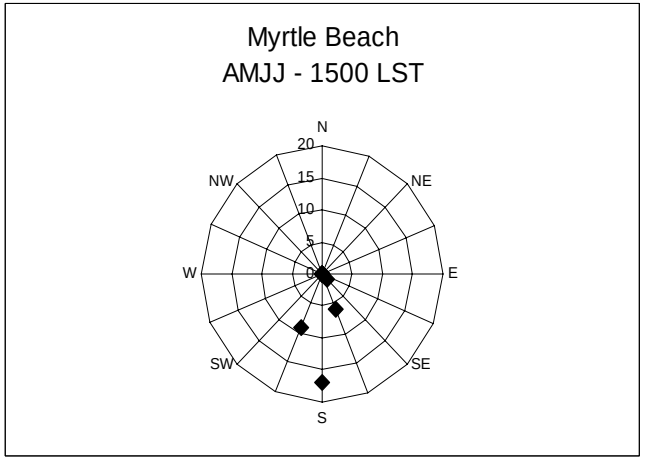

Figure 3.29 ***Frequency of wind directions noted at Myrtle Beach at 1500 LDT, on "sea breeze days" only.***

3.6 Satellite Imagery Analysis

Examination of observational data for the four coastal stations has revealed the signature of the sea breeze front among the significant meteorological variables, but to determine the typical extent of this front into inland areas, we turn to satellite imagery. The NC SCO has archived GOES satellite imagery (taken from the NCDC) and built a website based on an animation of this imagery. The process for obtaining this imagery and analyzing it using an ArcGIS program is explained in the *Methodology* section.

Initially this study focused on the four coastal stations by examining the distances the sea breeze front was able to penetrate along a line perpendicular to the nearest coastline. However it became clear quickly that this arrangement was not sufficient for the situation in and around the Wilmington site. Recall that the peculiar arrangement of the coasts around Wilmington created some ambiguity in the observational data for that area, possibly due to the interaction of sea breeze fronts that develop both south and east of the Wilmington site. Analysis reveals that there is a similar ambiguity with the satellite imagery. The Wilmington area is affected by the sea breeze front generated to the south more often than the one from the east, creating a sort of pocket over the southeastern part of NC – see Figure 3.30 for an example from May 27, 2005. Thus it seems appropriate to divide the Wilmington analysis between distances from both the south- and east-facing coasts.

Table 3.12 and Figure 3.31 represent a summary of this analysis. The values shown reflect the percentage of time that the sea breeze fronts recorded at each site from the satellite imagery made it to certain distances inland. For example, in 80 % of the recorded instances of a sea breeze being detected, the front penetrated to a distance of

about 23 km inland at the Charleston site, or to the green line in Figure 3.31. The broken yellow lines represent the lines along which the penetration distances are measured, perpendicular to the coast closest to the reference sites. We can see that frontal penetration to inland areas like Columbia, SC, and Raleigh, NC is very rare indeed, confirming that the assumption that these sites are useful as reference sources for "typical" observational weather is a sound one.

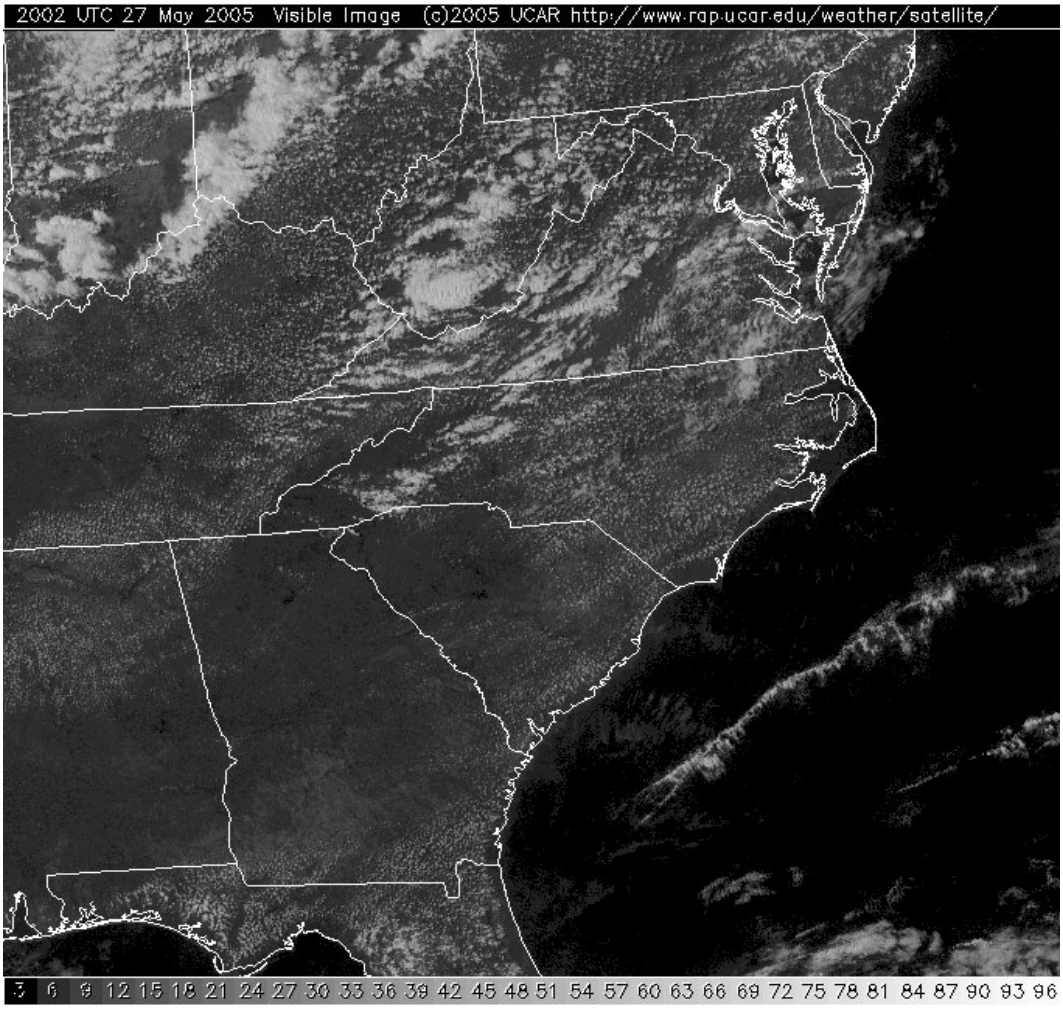

Figure 3.30 ***Example of the Southeastern NC "pocket" --- May 27, 2005***

Table 3.12 ***Percentage likelihood that the sea breeze front, recorded on satellite imagery, will penetrate to certain distances inland (in km) from points along the coast adjacent to the coastal airports.***

%	SAV	CHS	MYR	ILM(S)	ILM(E)
95	0	16	0	0	0
90	9	18	0	18	0
80	16	23	14	27	14
60	26	31	23	36	23
40	39	45	33	50	35
20	53	65	49	66	49
10	66	76	61	77	60

Table 3.13 shows the relative percentage of sea breeze events observed from surface observations and satellite imagery, as well as the percentage of days on which sea breeze events were noted from both detection methods. Detection from surface observations was more frequent than detection from satellite imagery, a logical development if we consider the presence of "invisible" sea breeze fronts undetectable on satellite imagery (consider also that the total size of the satellite imagery dataset, about 330 days, is less than that of the surface observation dataset, about 365 days). About half of the satellite-detected sea breeze events coincided with surface detection of the sea breeze.

Table 3.13 ***Summary of the number of sea breeze events noted in surface observations, satellite imagery, and those events detected from both***

	SAV	CHS	MYR	ILM
Surface	107	112	117	106
Satellite	89	94	92	86
Both	41	49	43	28

The so-called “pocket” in the southeastern NC area appears in the analysis here as well, with the furthest penetrations of any of the coastal sites coinciding with the Wilmington south-facing sea breeze. The sea breeze front penetrates further inland at Charleston and Brunswick as well, while Myrtle Beach and the east-facing Wilmington site record the sea breeze fronts that penetrate the least distance inland. In general it seems that the dominant summer-time synoptic flow from the south and southwest plays a large part in determining how far the sea breeze front penetrates inland. The specifics of this relationship will be investigated in the next section.

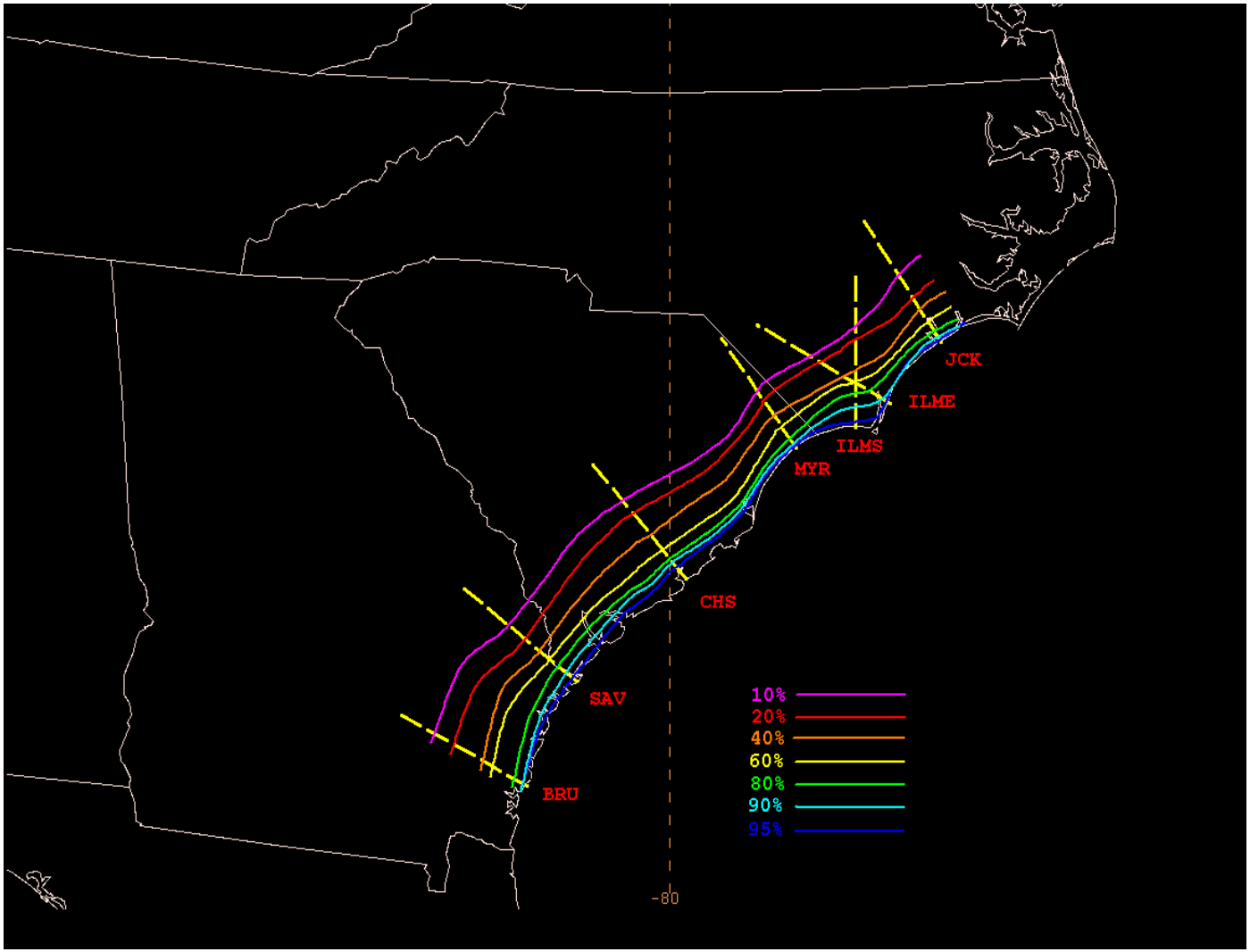

Figure 3.31 ***Percentage likelihood that the sea breeze front recorded on satellite imagery will penetrate to certain distances inland (in km) from points along the coast. The dashed yellow lines represent the lines along which distances were measured, roughly normal to the coast.***

One of the problems with the examination of these data is the fact that the sea breeze front, or at least its signature on the satellite imagery, is often distorted by phenomena over the inland areas. The question in these situations becomes to what extent these features are affecting the sea breeze front, or even whether the modified boundary even qualifies as a sea breeze front at all.

The most common distortion occurs when the sea breeze front interacts with thunderstorm outflow boundaries from complexes over inland areas, the most common type of boundary over the Carolinas during the sea breeze season (Koch and Ray, 1997). The enhanced lift that occurs with the interaction of the two low-level boundaries often creates deep convection, leading to further outflow boundaries and distortion. The outflow boundary often resembles and propagates in the same direction as the sea breeze front. Figures 3.32 through 3.35 are an example of such an event. In Figure 3.32 we see a classic sea breeze signature, the line of clouds parallel to the coast, particularly noticeable to the south from Georgia into southern South Carolina. An hour later (Figure 3.33) the front has moved further inland but has started to bend with convective activity: it appears to be further inland around Savannah than it is around Charleston or further south towards Jacksonville, Florida. An hour after that (Figure 3.34) the front has definitely begun to break apart, with convection moving quickly inland trailed by the high clouds of the thunderhead anvil cloud. By 1845 UTC (Figure 3.35) the sea breeze is still easily detectable from Myrtle Beach northward, but south of there convection has made detection nearly impossible. While there are lines of cloudiness and areas of associated clear air typical of a sea breeze circulation, they are so disorganized and

discontiguous that they are more likely attributable to the thunderstorm outflow boundaries.

Analysis indicates that 31.5 % of the sea breeze fronts detected by satellite imagery in the research period became distorted later in the day. While a measurement for sea breeze penetration was recorded for most of these days, the measurement would not necessarily represent the full penetration one might presume the front would achieve without interference from deep convection. Sixty-six percent of these "distorted" measurements occurred in the month of July.

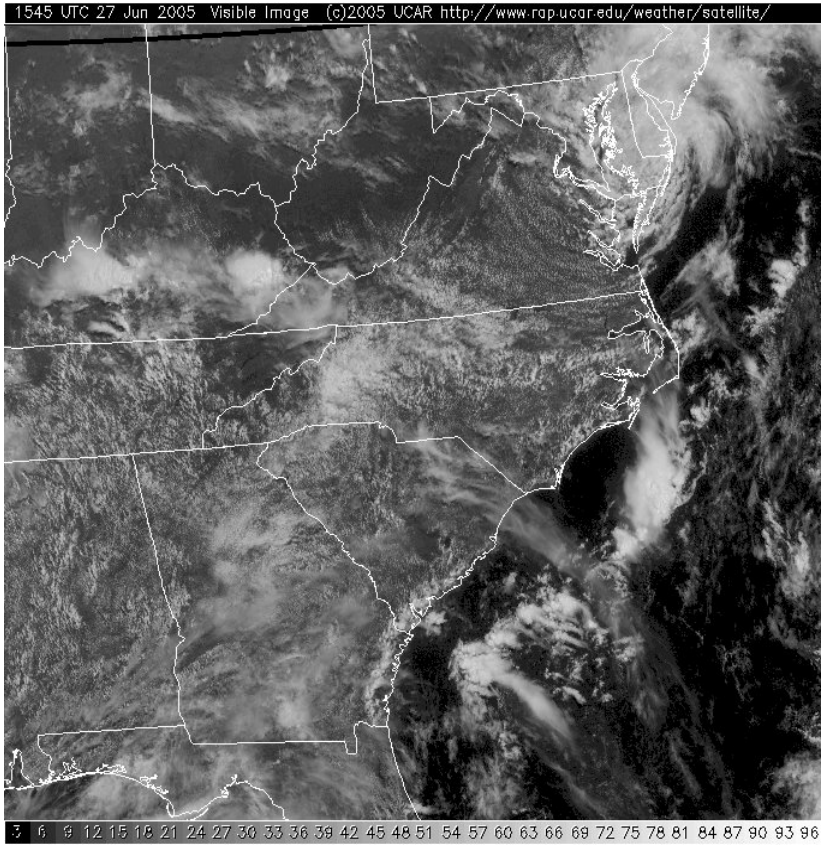

Figure 3.32 ***Example of interference with sea breeze front due to deep convection – June 27, 2005 at 1545 UTC***

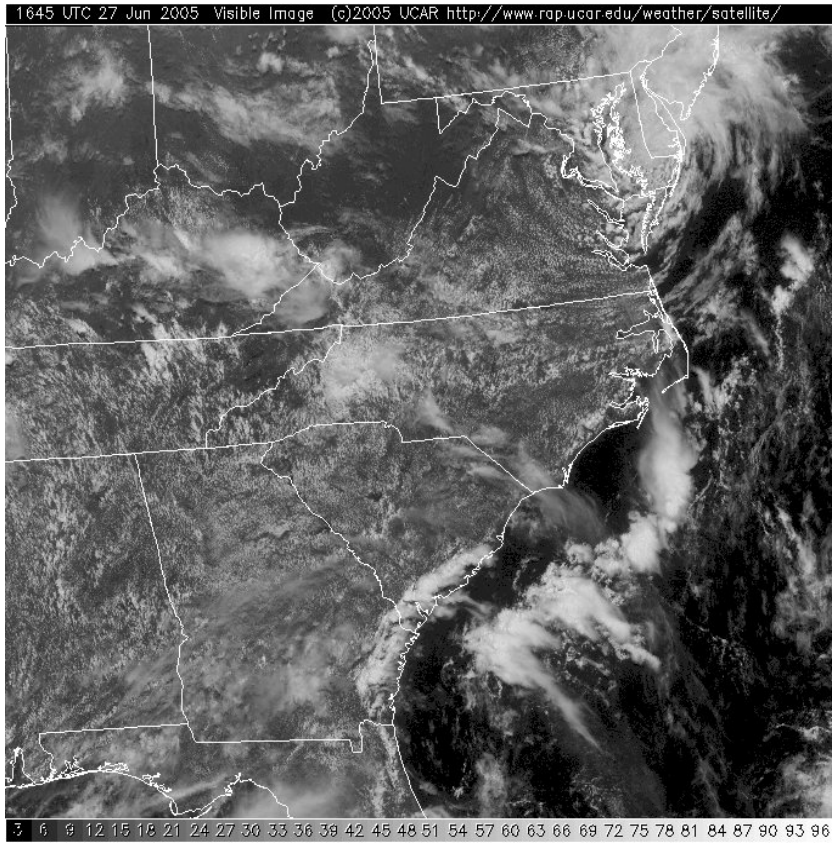

Figure 3.33 ***Example of convective interference (cont.) June 27, 2005 at 1645 UTC***

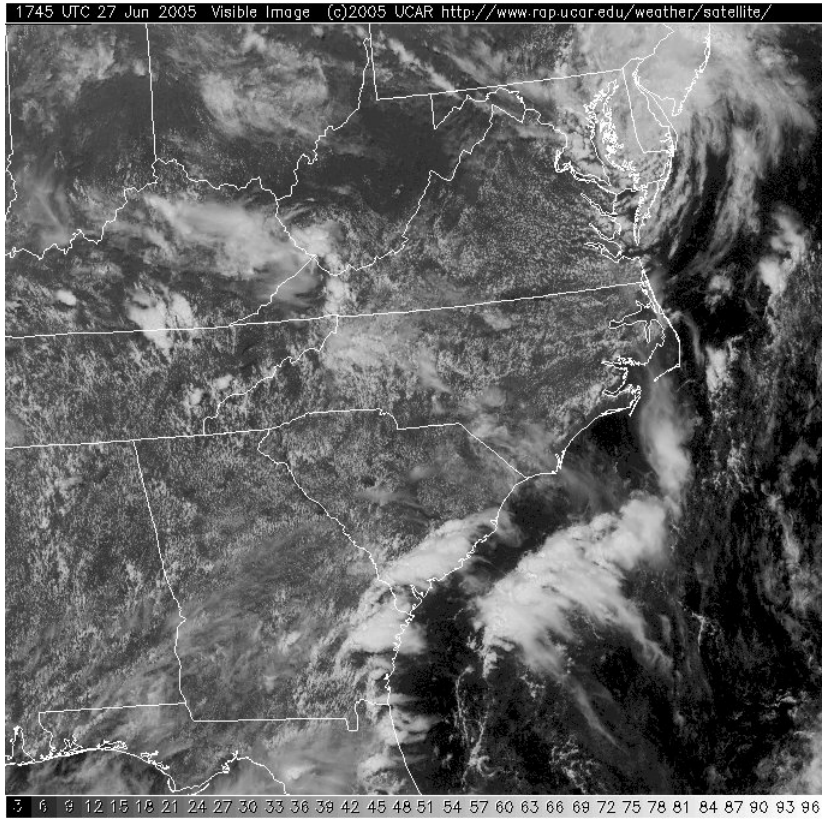

Figure 3.34 ***Example of interference with sea breeze front due to deep convection – June 27, 2005 at 1745 UTC***

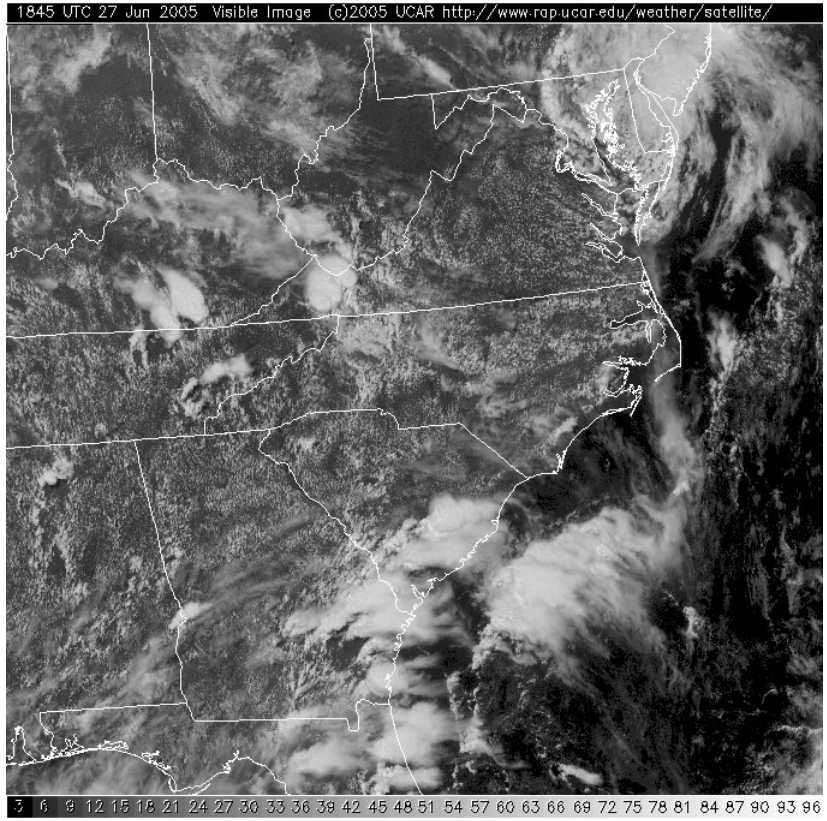

Figure 3.35 ***Example of convective interference (cont.) June 27, 2005 at 1845 UTC***

SECTION FOUR: Correlation Study

4.1 Factors Affecting Sea Breeze Development

The second portion of this study will focus on those factors that affect the evolution of the sea breeze circulation, including its development and movement after initiation. Analysis of these factors might lead to an increased understanding of how to forecast for these events.

From the theoretical description of the sea breeze circulation one would deduce that surface or near-surface temperatures for the water bodies associated with the coastal sites in question, as well as the synoptic level flow, would be the most significant factors involved in shaping the circulation.

As one would expect, there is a strong relationship between the daily maximum air temperatures recorded for the four coastal sites and 1200 LDT water temperature data for the associated water bodies. Figures 4.1 through 4.4 represent graphs of these two variables. In all four cases there is an almost direct relationship between the two temperatures, in the general sense of an increase from April to July but in specific perturbations as well, such as the sharp dip in high temperatures in April that either coincides with or is followed shortly by a dip in water temperatures, especially in the Charleston and Wilmington data. It is important to note however that the changes in air temperature show a much wider range than the changes in water temperature, reflecting the lower specific heat values of the latter versus the former. This fact of course is vital to the development of the circulation.

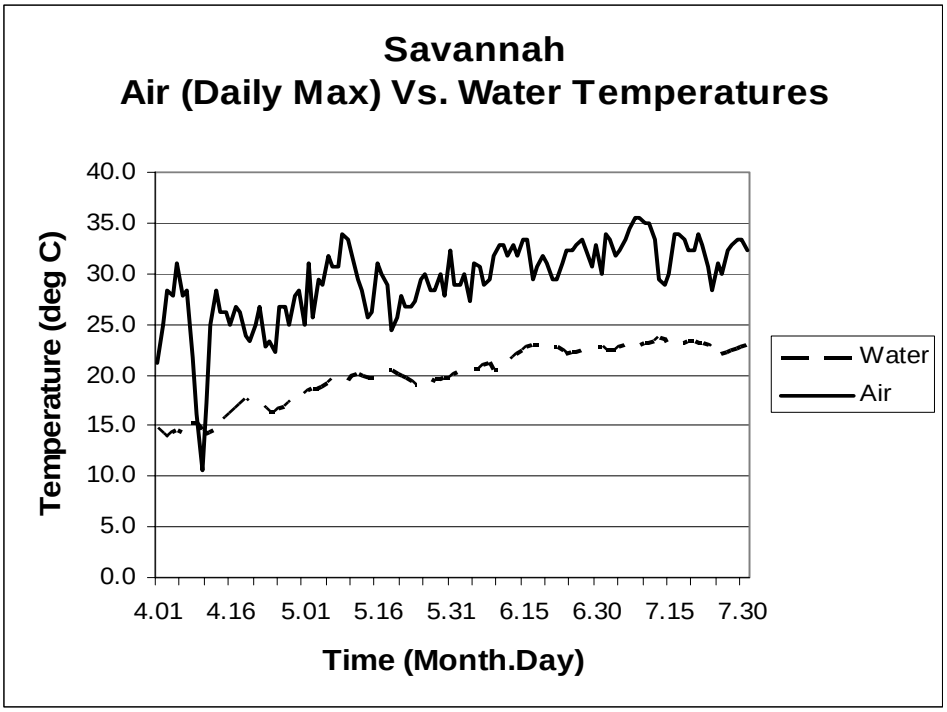

Figure 4.1 ***Daily Maximum Temperatures and CO-OPS Network Water Temperatures (measured at 1200 LDT) at Savannah***

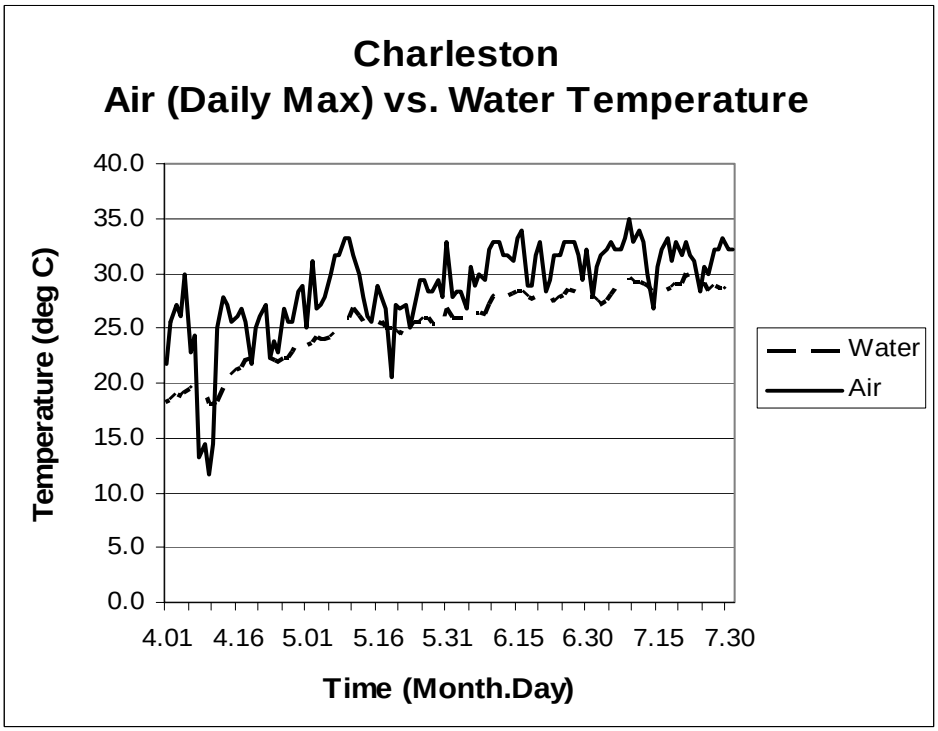

Figure 4.2 ***Daily Maximum Temperatures and CO-OPS Network Water Temperatures (measured at 1200 LDT) at Charleston***

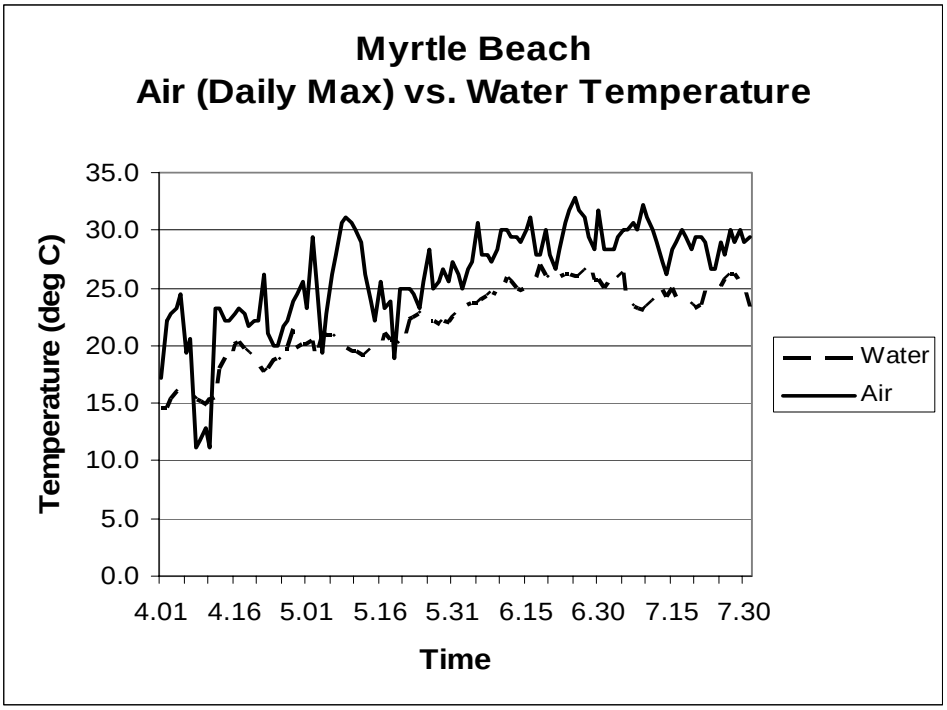

Figure 4.3 ***Daily Maximum Temperatures and CO-OPS Network Water Temperatures (measured at 1200 LDT) at Myrtle Beach***

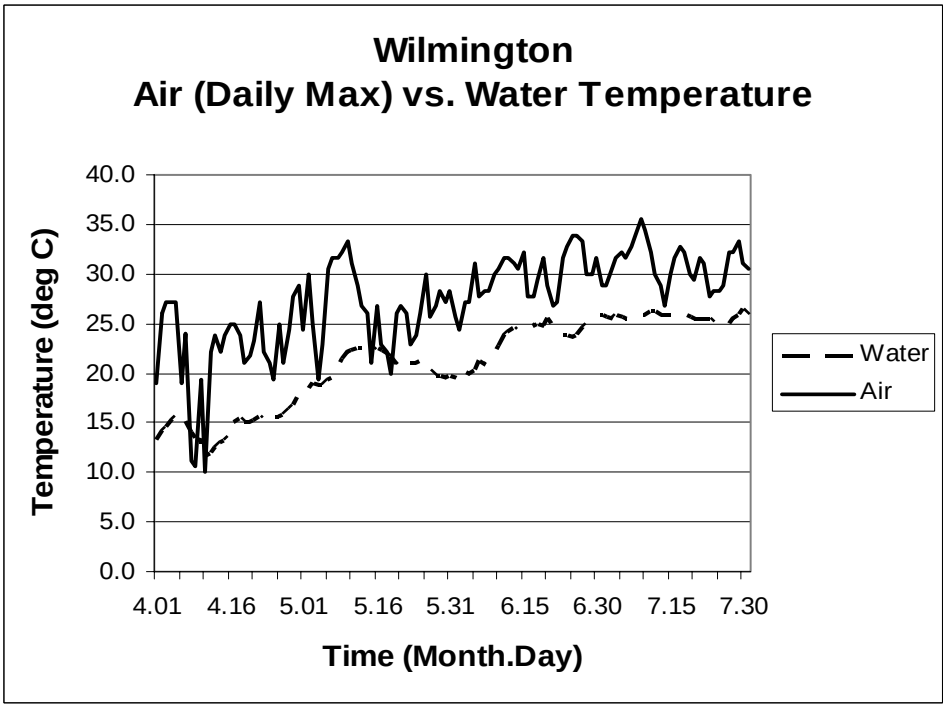

Figure 4.4 ***Daily Maximum Temperatures and CO-OPS Network Water Temperatures (measured at 1200 LDT) at Wilmington***

Figures 4.5 through 4.7 are included to show the relationship between water temperatures taken from the CO-OPS observation network and satellite-derived water temperatures taken from the SEACOOS system for the 2004 data. Savannah data is not included in this analysis due to the absence of CO-OPS water temperature data for the year 2004, although satellite-derived SST data was assimilated and was similar to water temperature data from the Charleston site. Recall from Figures 2.3 and 2.5 that the CO-OPS sites at Charleston and Wilmington are located somewhat inland from the coast, in positions that are influenced by nearby rivers (the Ashley-Cooper and Cape Feare Rivers, respectively), while satellite-derived water temperatures were taken from positions just off the coast. The water temperatures from the CO-OPS network seem to be in general slightly warmer than those obtained via satellite especially later in the sea breeze "season", reflecting the relative depth and level of vertical mixing of river waters versus ocean water. Interestingly the satellite-derived water temperatures for the Myrtle Beach area actually seemed to be warmer than the water temperatures taken from the adjacent CO-OPS site, located in the surf zone at the Springmaid Pier. In fact there seemed to be a stretch of the near-coastal waters between Myrtle Beach and the south-facing coast of the Cape Feare peninsula south of Wilmington that were consistently warmer than the other sites along the coast of the Southeast, especially early in the season. The CO-OPS water temperatures do seem to be greater than the satellite-derived temperatures starting in early June at the Myrtle Beach site, until an anomalous cool spell reduces CO-OPS temperatures in July.

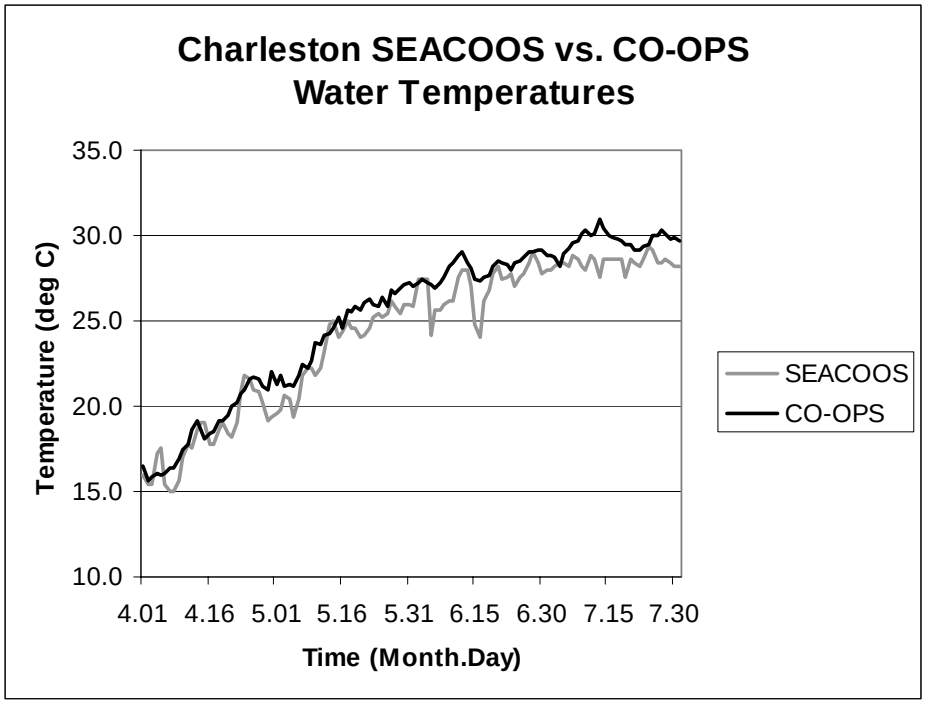

Figure 4.5 ***Water temperatures recorded from surface observation (CO-OPS network) and satellite-derived (SEACOOS) sources for 2004 adjacent to the Charleston area***

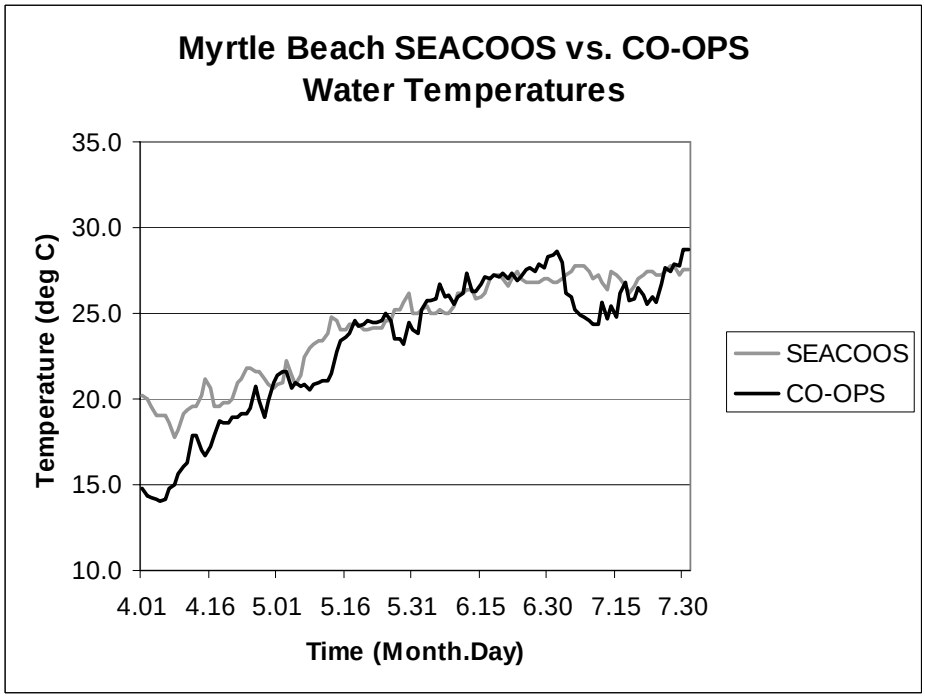

Figure 4.6 ***Water Temperatures recorded from surface observations (CO-OPS network) and satellite-derived (SEACOOS) sources for 2004 adjacent to the Myrtle Beach area***

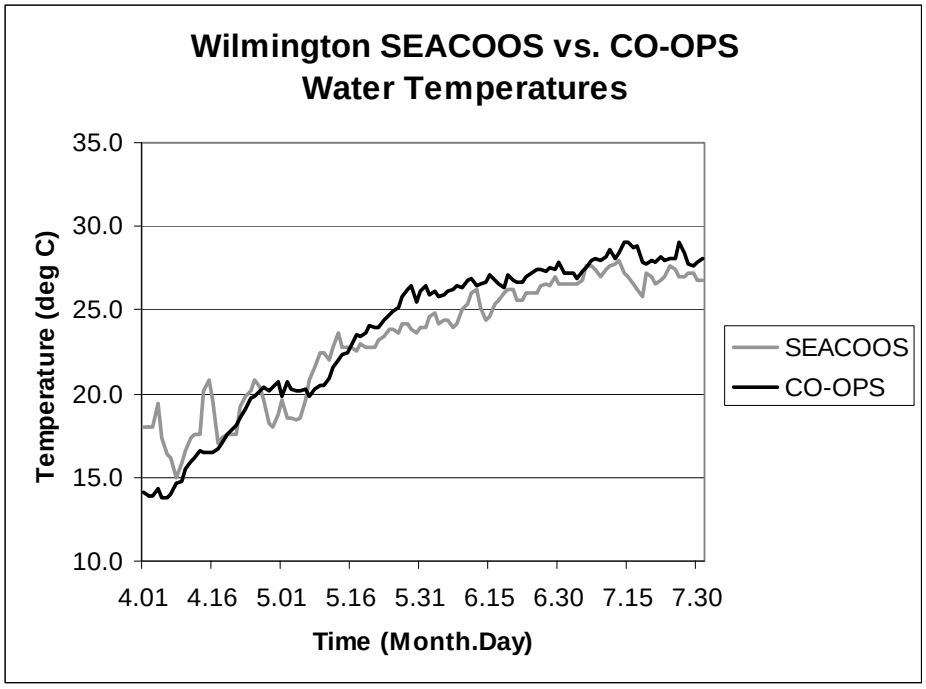

Figure 4.7 ***Water temperatures recorded from surface observations (CO-OPS network) and satellite-derived (SEACOOS) sources for 2004 adjacent to the Wilmington area***

As explained previously in the *Methodology* section, values of the geostrophic wind are calculated for the four coastal sites of the research area to represent the synoptic-scale wind pattern. Figure 4.8 represents the distribution frequency of these winds for the Myrtle Beach site. As we expect there is a predominant pattern of southwesterly winds, presumably the result of the influence of the Bermuda High just offshore. Further analysis will be carried out using the component of the geostrophic wind vector perpendicular to the coastline, known hereafter as the geostrophic wind component (G.W.C.).

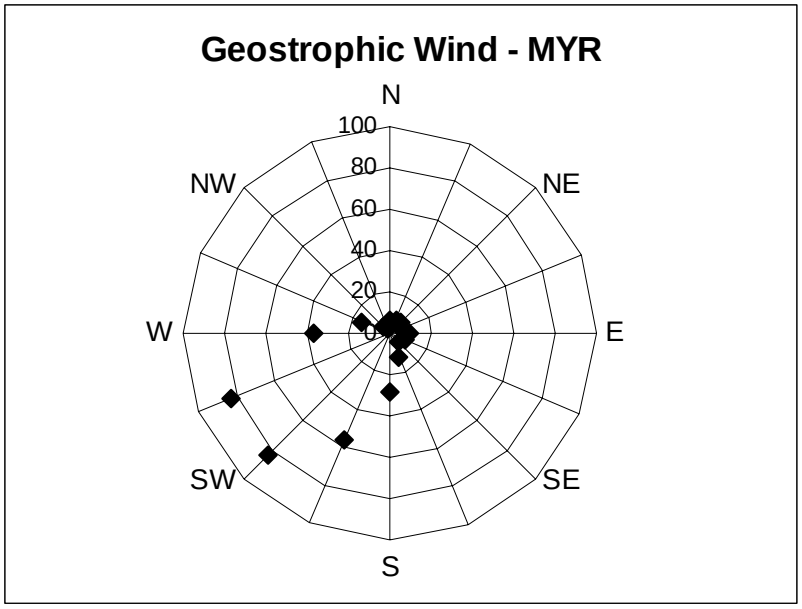

Figure 4.8 ***Frequency of wind directions noted from analysis of geostrophic wind calculated from NARR data for Myrtle Beach***

Unfortunately, due to gaps in the CO-OPS network's water temperature records, one year of data are missing from the Charleston (CHS) and Savannah (SAV) sites, specifically 2005 data and 2004 data, respectively. For more complete data (without the eccentricities involved in the Wilmington (ILM) data, discussed previously in this document), this section of the thesis examines data for Myrtle Beach (MYR) first.

4.2 Myrtle Beach

Figures 4.9 and 4.10 illustrate how the values for the geostrophic wind component (G.W.C.) and del-T values vary the sea breeze categories established in the *Climatology* section. The trendline, associated equation, and R^2 values are presented for reference. Recall the scale of that classification system, from one to five, where category one days almost certainly were not affected by the sea breeze and category five days almost certainly were affected by the sea breeze.

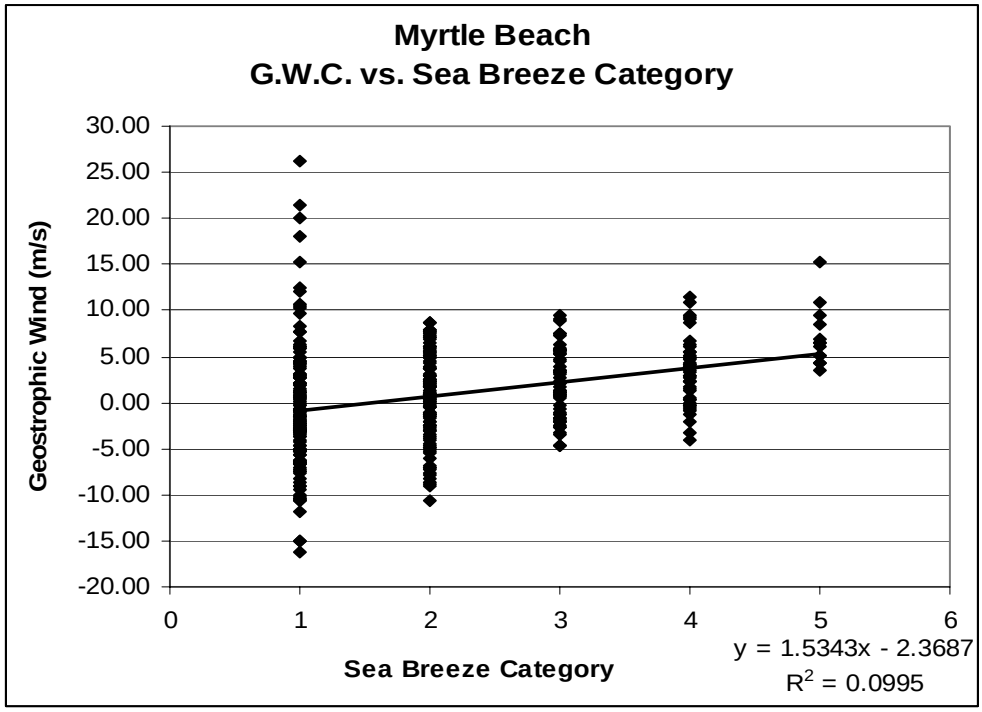

Figure 4.9 ***Variation of the geostrophic wind component with sea breeze category for Myrtle Beach data.***

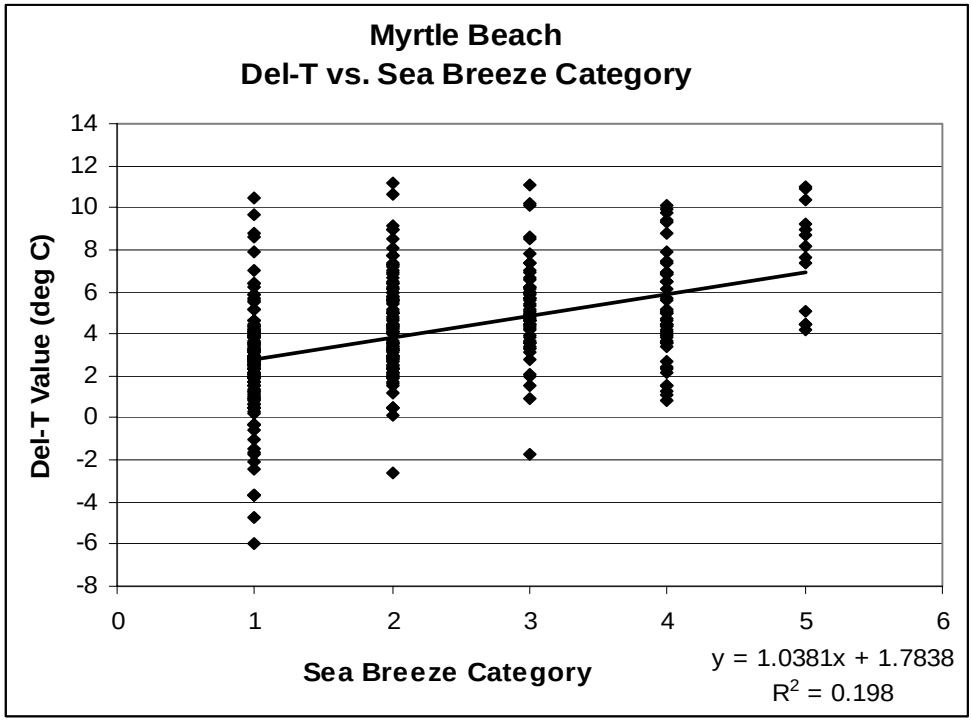

Figure 4.10 ***Variation of the del-T value (based on CO-OPS water temperature data) with sea breeze category for Myrtle Beach data.***

Although there does seem to be a positive relationship between both variables (G.W.C. and del-T) and the sea breeze category as indicated by the trendline, the low R^2 score for both diagrams indicates a wide dispersion of values.

The multiple regression equation for both variables against the sea breeze categories is calculated as:

$$Y = 0.038(X_1) + 0.16(X_2) + 1.45 \qquad (4.1)$$

where Y is the sea breeze category, X_1 is the del-T value, and X_2 is the value for the G.W.C. The multiple regression equation represents the best linear combination of the independent variables (del-T and the G.W.C.) that is maximally correlated with the dependent variable, in this case the sea breeze category. The R^2 value associated with equation (4.1) is 0.23, modestly higher than the R^2 values for the individual regressions equations of the G.W.C. and del-T versus sea breeze category but low enough to question the equation's reliability as a predictor.

Analysis of the data in Figure 4.10 indicates that the del-T value of 2.0 ° C seems to be a threshold value for sea breeze development. Of the 117 sea breeze events at the MYR site during the research period, only eight (or 6.8%) were characterized by del-T values below 2.0 ° C. On a similar note, all but four of the sea breeze events fell within a range of the G.W.C. from -5.0 m/s to 10.0 m/s.

The correlation between del-T values and the sea breeze category, the del-T values this time based on satellite-derived water temperatures, produces Figure 4.11. Again we see a positive relationship as with Figure 4.10, as expected. However, a lower R^2 value and higher incidence of negative del-T values associated with sea breeze events (an illogical association considering that positive values of the del-T produce the

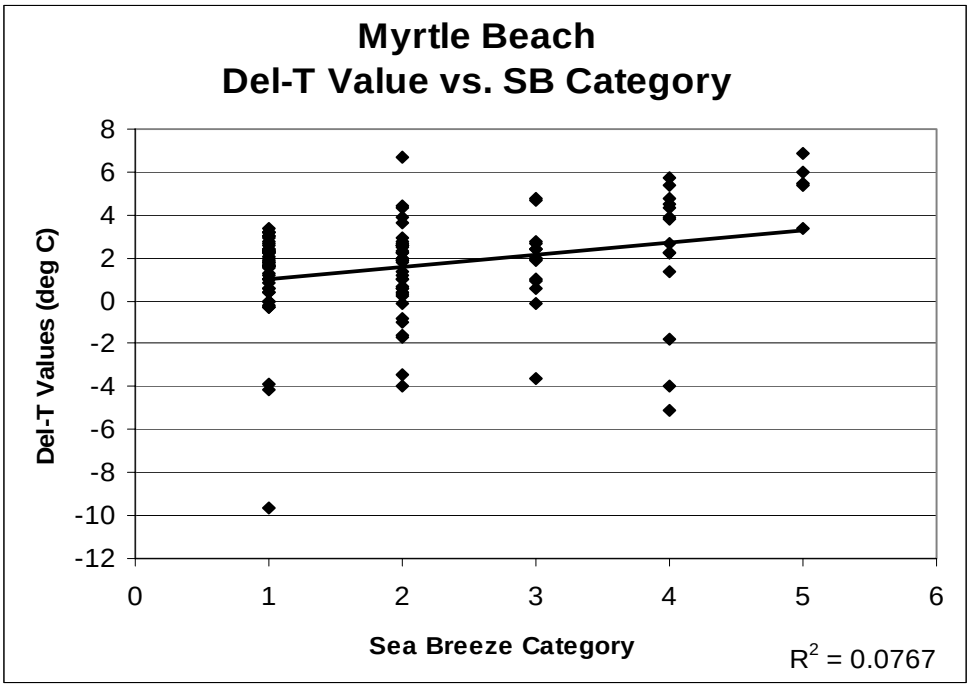

Figure 4.11 ***Variation of the Del-T Value (based on SEACOOS water temperature data) with sea breeze category using Myrtle Beach data from 2004***

sea breeze circulation) indicates that for the Myrtle Beach site, the CO-OPS water temperature data probably reflects the desired values of the del-T more accurately.

It is important to acknowledge the circumstances under which the variables work against each other, for example, when a high del-T (which would support sea breeze development) coincides with a high positive value for the G.W.C., the sea breeze would likely be pinned to the coast. To analyze the effects of del-T alone on sea breeze development, those days with values of the G.W.C. above/below ± 4.0 m/s were disregarded for the moment, effectively creating a "calm" environment with a reduced chance of the two variables working against each other. Figure 4.12 shows a diagram of such an analysis. In this figure it seems again as if the value of 2.0 ° C represents a good threshold value for sea breeze development, with only 12.1 % falling below the theshold value. Note also that the R^2 value for this regression relationship is actually lower than

that of Figure 4.10, the same analysis for the entire dataset. It is difficult to characterize this set of del-T values as a reliable predictor given the R^2 values associated with the analysis. Certainly a positive del-T value is a necessary condition for sea breeze development, and a threshold value of around +2.0 ° C appears to be generally required.

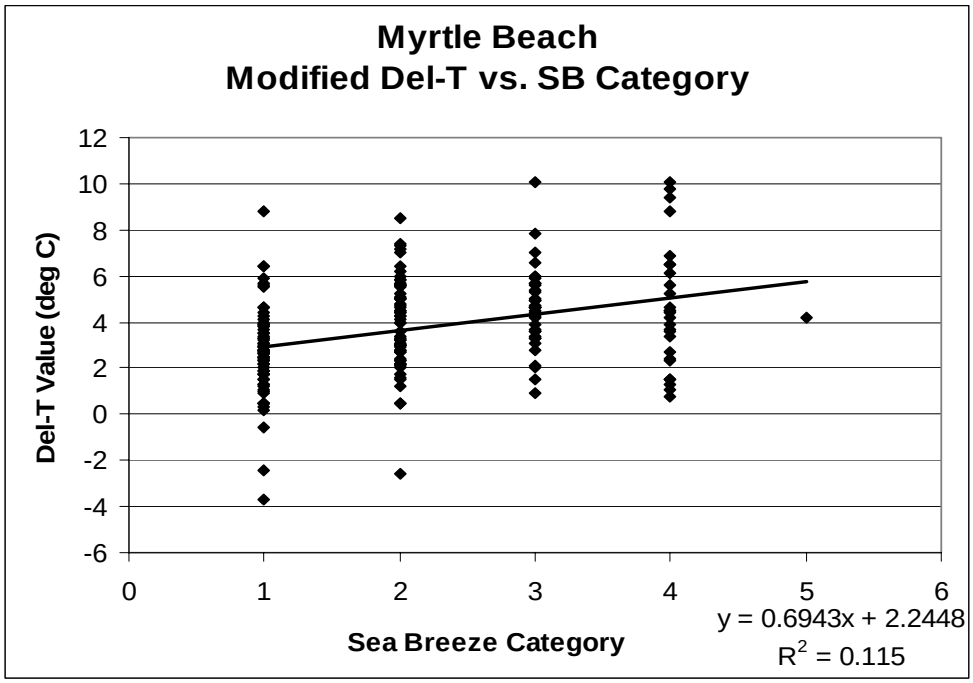

Figure 4.12 ***Variation of del-T value (based on CO-OPS data) with sea breeze category, modified by refining the range of G.W.C. values (btwn. -4.0 m/s and +4.0 m/s) for Myrtle Beach data.***

If we examine again the relationship of the G.W.C. to the sea breeze categories, this time filtering out the days with del-T values below the +2.0 ° C threshold, the result is Figure 4.13. The filtering process results in a modest improvement in the R^2 score. Let us further refine this analysis by disregarding values of the G.W.C. above 10.0 m/s and -10.0 m/s (Figure 4.14). These values would be associated with strong winds perpendicular to the coast that would presumably either pin the front to the coast, if it

forms at all (in the case of a strong offshore component), or disrupt the circulation and perhaps wash out the signals of frontal passage in the observational data (in the case of a strong onshore element). Indeed, there are only four sea breeze events in the research period for the Myrtle Beach site that are characterized by these strong G.W.C. values.

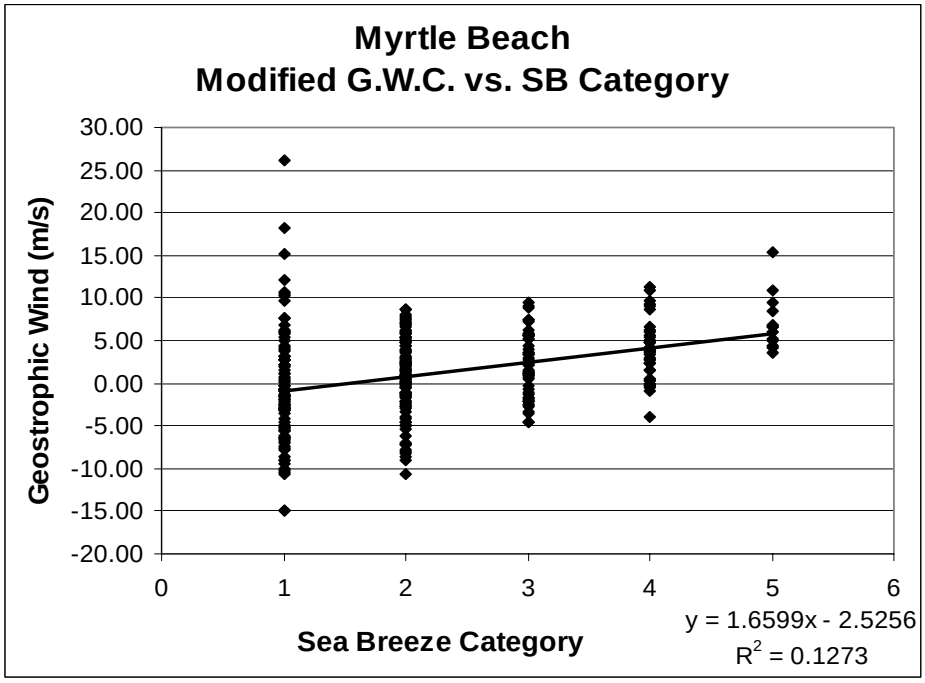

Figure 4.13 ***Variation of G.W.C. values vs. sea breeze category for Myrtle Beach data, filtering out sub-threshold del-T values (CO-OPS data)***

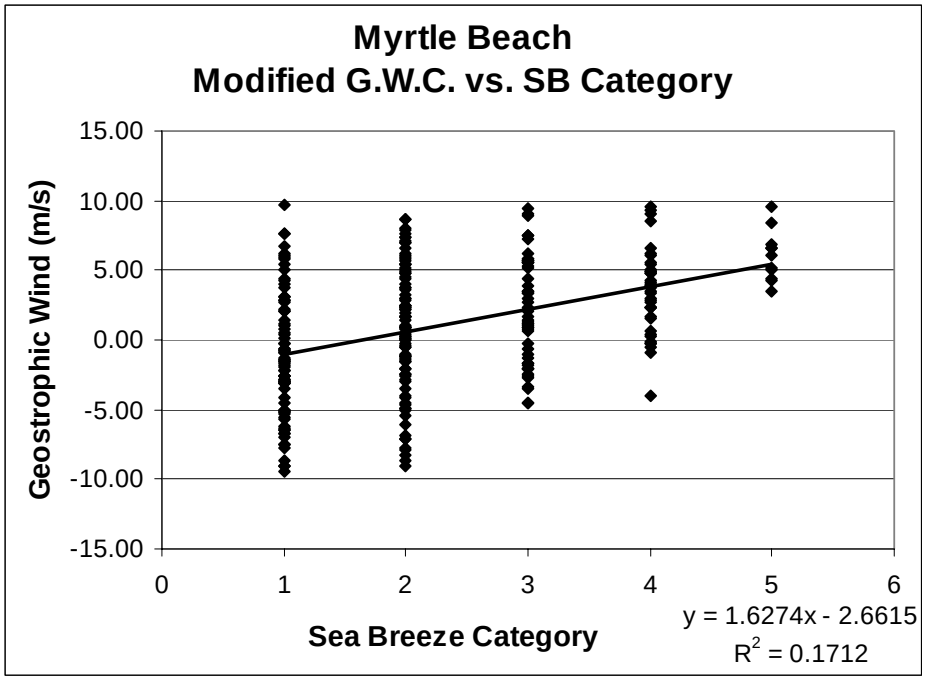

Figure 4.14 ***Variation of G.W.C. values with sea breeze category for Myrtle Beach data, filtering out sub-threshold del-T values (CO-OPS data) below +2.0 ° C and strong G.W.C. values (above 10.0 m/s and below -10.0 m/s).***

The multiple regression equation fitted for this modified dataset (super-threshold del-T values, strong G.W.C. values filtered out) is calculated as the following:

$$Y = 0.072(x1) + 0.163(x2) + 1.44 \qquad (4.2)$$

Where Y is the sea breeze category, x1 is the value for del-T, and x2 is the value for the G.W.C. The R^2 value for this equation is 0.24, slightly higher than the score associated with equation (4.1), the multiple regression fitted for the entire dataset, but it is clear there is still a high degree of dispersion in the data.

After the filtering processes described above, the total Myrtle Beach dataset of 366 days had been reduced to 285 days. Of these 285 days, 113 were characterized by a negative G.W.C. (onshore flow), 170 were characterized by a positive G.W.C. (offshore flow), and two were near zero (neutral flow). This proportion of onshore to offshore

flows makes sense when we consider the distribution frequency of geostrophic winds shown in Figure 4.5, along with the angle of the coastline at the MYR site, illustrated in table 1.1 and Figure 1.5 as being around 44 degrees from the north.

Sea breeze events (observational classes three, four, or five) composed 47.7 % of the offshore events. However, sea breeze events made up only 20.5 % of the days characterized by onshore flows, and all of these occurred with relatively light onshore winds (below -5.0 m/s). If we examine those days with relatively light onshore G.W.C. values (above -5.0 m/s) the percentage of sea breeze events increases to 28.8 %. Logically, development of the sea breeze should be just as likely to occur with onshore flow as offshore flow, if not more so. One possible explanation is that sea breeze events coinciding with onshore flow are under-represented in the dataset.

Previous studies have observed the difficulties in detection for sea breeze events coinciding with onshore synoptic flow (Atkins and Wakimoto, 1997). In fact in some studies the definition of the sea breeze circulation in observational data was merely the presence of onshore winds. Recall that the set of criteria of sea breeze detection for this study, the classification system explained in the *Methodology* section, was more complex, accounting for changes in air temperature and dewpoint as well as wind vector. The wind direction shift associated with sea breeze frontal passage becomes much harder to detect when the direction before and after frontal passage is almost the same. Moreover, if the synoptic-scale flow is already coming off the ocean even before the sea breeze circulation develops, the maritime air mass may already be more or less in place over inland areas, mitigating the expected changes in temperature and dewpoint. Sea breeze events

associated with offshore synoptic-scale flows are much easier to detect because the wind shift and the change in air mass are more drastic.

If we assume that the classification system introduced in the *Climatology* section is too strict a definition for the detection of sea breeze frontal passage, examination of the data with a less rigid definition for frontal passage might be warranted. Geostrophic wind has been established as the wind caused by the balance between the pressure gradient and Coriolis forces. For the purposes of this study, ageostrophic wind is defined as the vector difference between the total wind and the geostrophic wind. Differences between the total and geostrophic wind vectors are associated with surface friction and acceleration, as well as with local phenomenon such as the sea breeze circulation. Values for the ageostrophic wind component perpendicular to the coast were calculated by subtracting the component of the geostrophic wind vector perpendicular to the coastline from the total wind vector (from surface observations at the airport sites) perpendicular to the coastline. If we recall that negative values of the wind components equate to onshore winds (and positive to offshore), sea breeze events, wherein offshore ambient winds turn to offshore or lighter onshore ambient winds become stronger, should usually be associated with negative values of the ageostrophic wind component.

Figure 4.15 shows the correlation between values for del-T and the ageostrophic wind component. As expected, the majority of ageostrophic wind values are negative. The negative relationship between the two variables, where stronger values of the ageostrophic wind coincide with higher del-T values, also agrees with expectations. However the low R^2 value again indicates a high degree of unexplained variance.

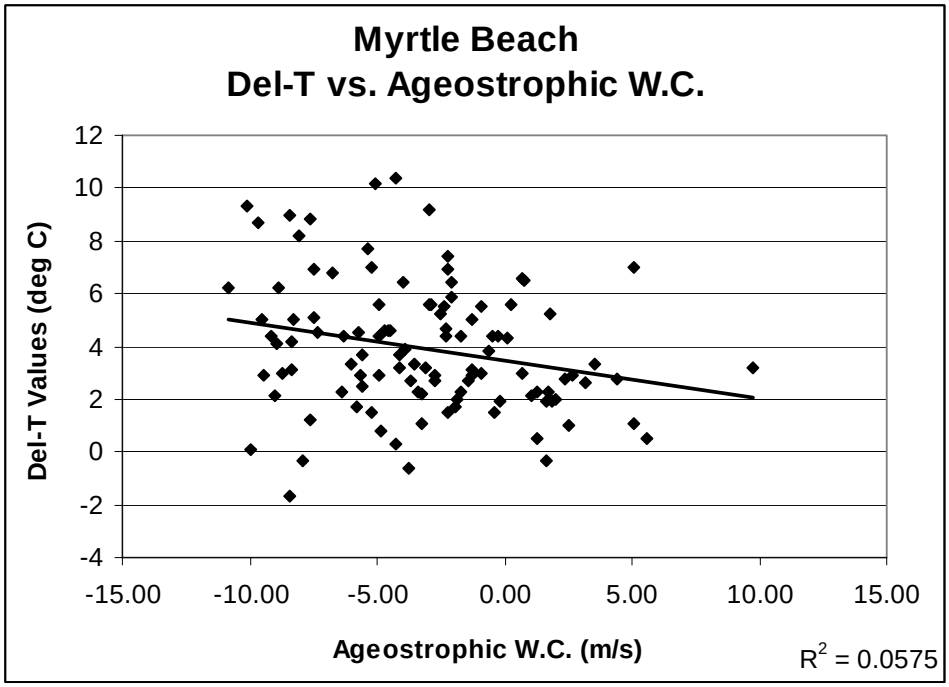

Figure 4.15 ***Variation of ageostrophic wind component values with del-T values (based on CO-OPS water temperature data) for the Myrtle Beach data for 2004***

Previous studies have also discussed the intuitive relationship between the synoptic-scale wind flow and frontal passage at a given station. Obviously, a positive (offshore) G.W.C. might be expected to delay the passage of the sea breeze front through inland sites. Figure 4.16 shows the scatterplot relationship between the geostrophic wind component (G.W.C.) and frontal passage times recorded from observational data. As expected there is a positive relationship in the data, although the spread is relatively high (low R^2 value).

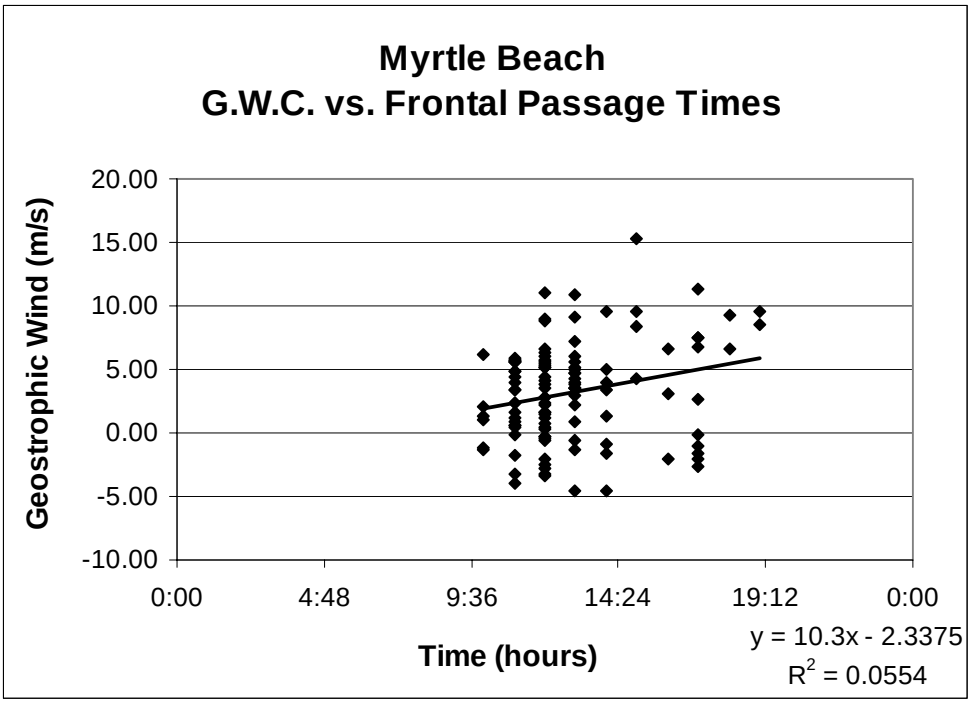

Figure 4.16 ***Variation of values of the geostrophic wind component (G.W.C.) with frontal passage times noted from surface observations at the Myrtle Beach airport site.***

There were 337 days in the database of satellite imagery for the Myrtle Beach site. The discrepancy between this number and the size of the observational dataset (366 days) is explained by a month-long technical difficulty with the SCO's archive of *GOES* satellite data in the summer of 2004. There were 89 sea breeze events detected by satellite imagery. Fifty-five of these events (61.8 %) coincided with offshore synoptic-scale flows (positive G.W.C.). Incidentally, 91.0 % of these events were associated with del-T values above our established threshold value of 2.0 ° C.

Figure 4.17 illustrates the relationship between values for the G.W.C. and sea breeze front inland penetration distances. As expected, there is a negative relationship between the two variables, indicating that while positive values of the G.W.C. (offshore synoptic-scale flow) hold the sea breeze front closer to the coast, near zero or negative

values of the G.W.C. tend to allow for further inland penetration. Again, a high degree of unexplained variance (low R^2 value) casts doubt on the analysis of this graphic. Analysis of observational data earlier in this section led to the hypothesis that data for sea breeze events coinciding with onshore synoptic scale regimes was under-represented due to detection difficulties. By the same token, these events might well be under-represented in the analysis of satellite imagery as well. Recall that a degree of surface convergence is necessary for the development of the cumulus clouds along the sea breeze front. An onshore ambient flow would tend to discourage such convergence. If we assume that onshore-regime sea breeze development is under-represented, then a better representation of the events in the analysis of Figure 4.17 might be assumed to result in an ever higher degree of negative correlation.

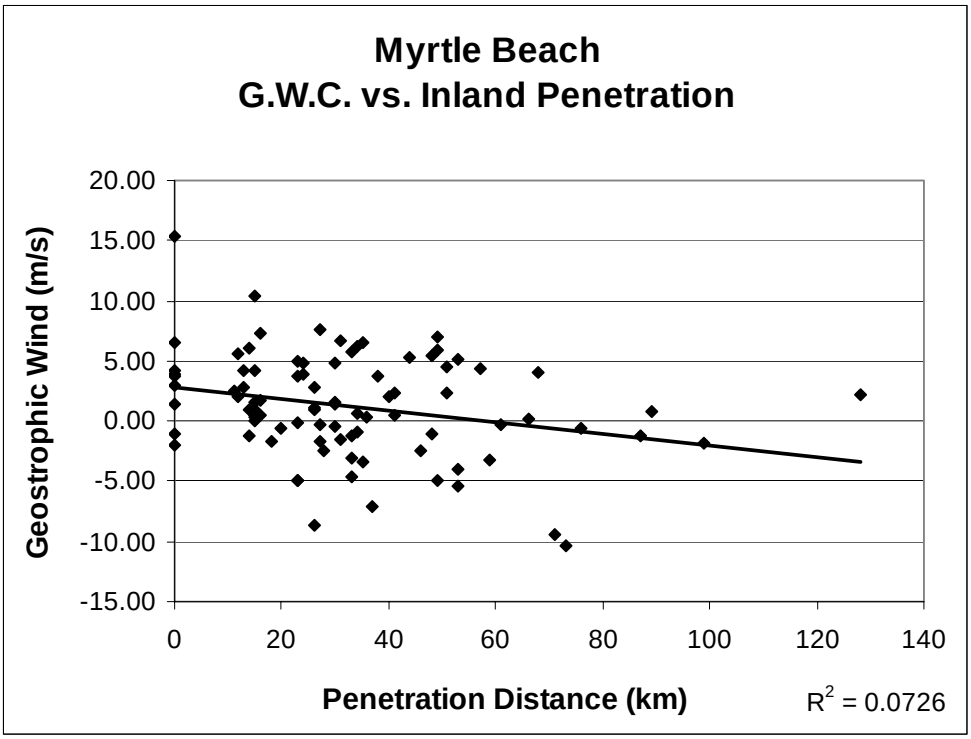

Figure 4.17 ***Variation of the G.W.C. with inland penetration distances measured on satellite imagery for Myrtle Beach data.***

Note again that the vast majority of sea breeze events tend to take place within the G.W.C. range of -10.0 m/s to 10.0 m/s and in fact all but five occur in the -8.0 m/s to 8.0 m/s range. Just as we observed with the analysis of observational data, it seems that the sea breeze forms (or is more detectable) preferentially with lighter synoptic-scale winds.

4.3 Wilmington

Recall from the *Climatology* section that the unique shape of the coastline near Wilmington (illustrated in Figure 2.5) creates a higher degree of ambiguity in the detection of the sea breeze front on satellite imagery than at the other stations. To account for some of the ambiguity, the analysis in that section was conducted for data from both coasts separately.

By the same token, consider the effects of the geostrophic wind vector on sea breeze evolution around the Wilmington site. A given vector (both magnitude and direction) would affect sea breezes originating from the south and east coasts very differently. For example, a geostrophic wind direction of 257 ° and magnitude 9.9 m/s was recorded for the Wilmington site at noon on April 5th, 2003. The component of this vector perpendicular to the east coast near the Wilmington site is offshore at about 5.7 m/s. However, the component perpendicular to the south coast is onshore at about -4.7 m/s. Figure 4.18 shows the frequency distribution of wind direction values associated with the geostrophic wind vector, along with a rough approximation of the coastlines that form the Cape Feare peninsula for reference. To account for the differences caused by these coastlines, analyses of the two sets of geostrophic wind component data were conducted separately.

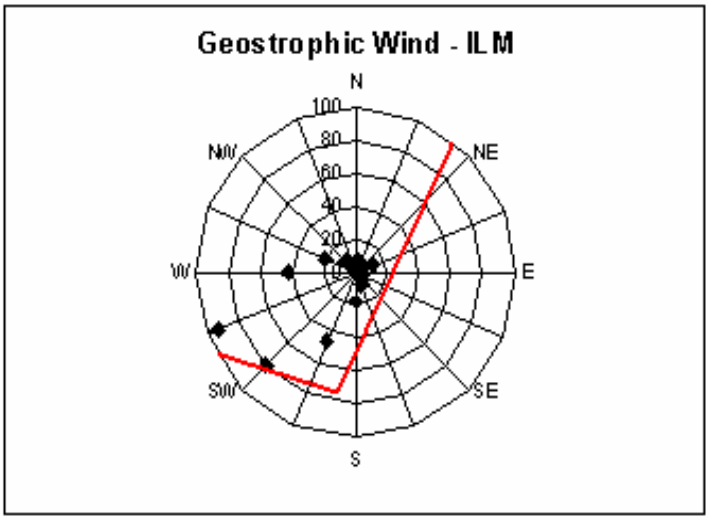

Figure 4.18 ***Frequency of wind directions noted from analysis of geostrophic wind calculated from NARR data for Wilmington. Red lines approximate the orientation of the Cape Feare Peninsula.***

Examination of the data for del-T values and sea breeze categories reveals a threshold value of about 2.0 ° C for sea breeze development – only 7.7 % of sea breeze development takes place with del-T values below 2.0 °, so days with sub-threshold del-T values are disregarded. Similar analysis using del-T values based on the SEACOOS satellite-derived water temperature data also indicates a sea breeze detection threshold of about two or three degrees C.

Figures 4.19 and 4.20 show the relationship between the G.W.C. and sea breeze categories for the south-facing and east-facing coasts, respectively, along with the trendline, regression equation and R^2 values for each. Interestingly trendlines associated with each diagram indicate a positive relationship between the G.W.C. and sea breeze category for both datasets. This means that for the east-facing coast, sea breeze events are correlated with stronger values of the G.W.C., somewhat contrary to previous results. However, the majority of values for both diagrams fall in a range covering about 20 m/s (from -15.0 m/s to 5.0 m/s for the south-facing coast, and from -5.0 m/s to 15.0 m/s for

the east-facing coast). If we consider the orientation of the coasts relative to each other and the distribution of the geostrophic winds shown in Figure 4.18, the analysis of Figures 4.19 and 4.20 makes more sense. Since both diagrams share the same sea breeze category data and (prior to the calculation of the wind components perpendicular to the coast) the same geographic wind data, the correlation should be similar.

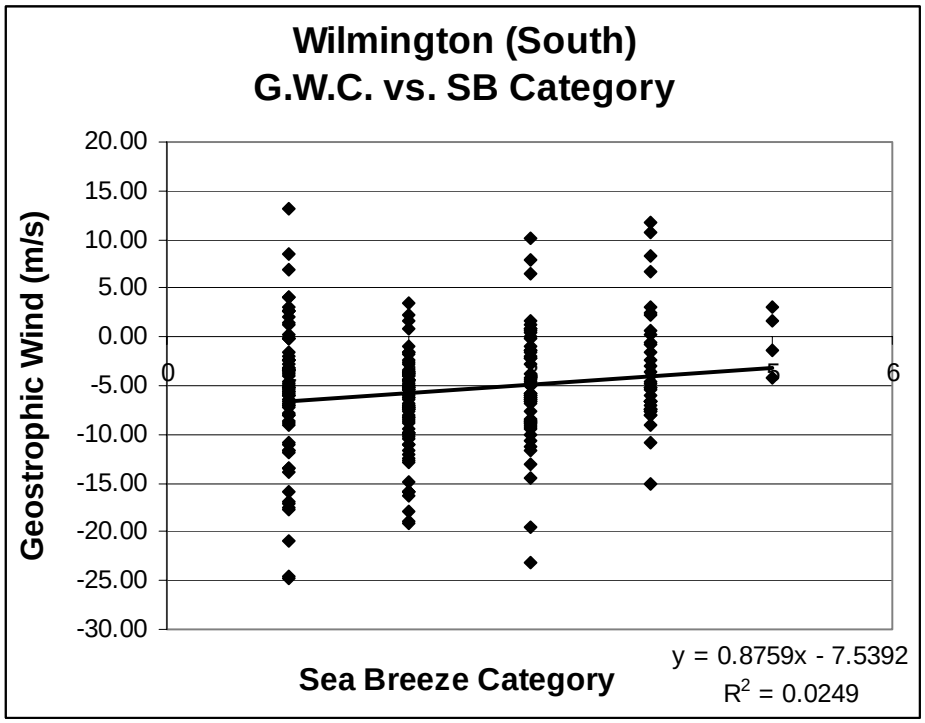

Figure 4.19 ***Variation of the geostrophic wind component with sea breeze category for Wilmington (south coast) data.***

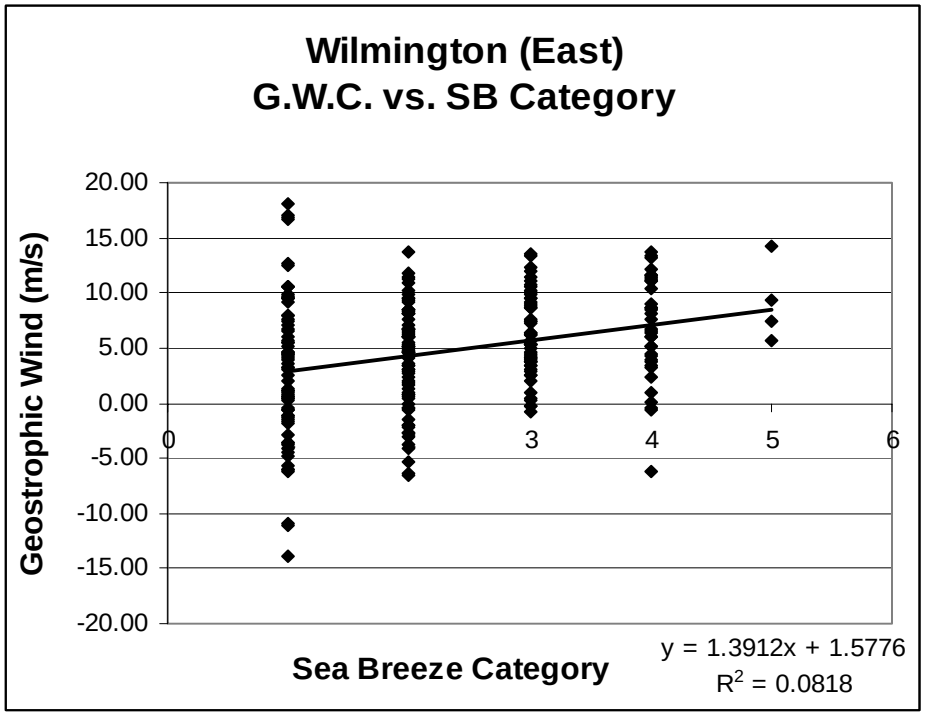

Figure 4.20 ***Variation of the geostrophic wind component with sea breeze category for Wilmington (east coast) data.***

Figures 4.21 and 4.22 show the correlation between the geostrophic wind component and frontal passage times recorded from observational data, again with the regression equations and associated R^2 values included. The relationship is similar for both coasts, a positive relationship similar to Figures 4.19 and 4.20, and both characterized by a high degree of variance.

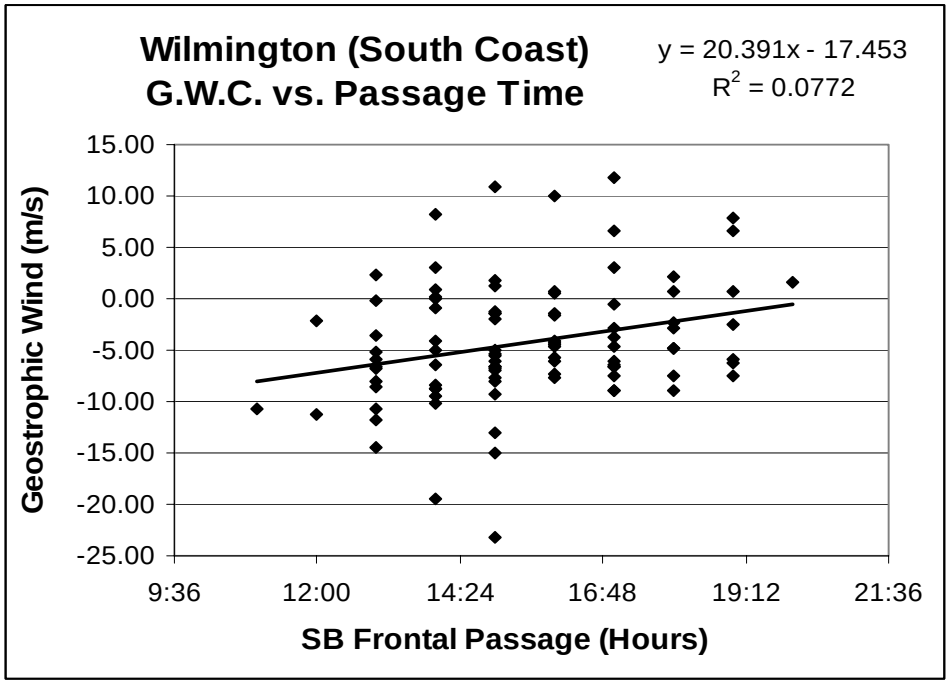

Figure 4.21 ***Variation of values of the geostrophic wind component (G.W.C.), calculated for the coast south of Wilmington, with frontal passage times noted from surface observations at the Wilmington airport site.***

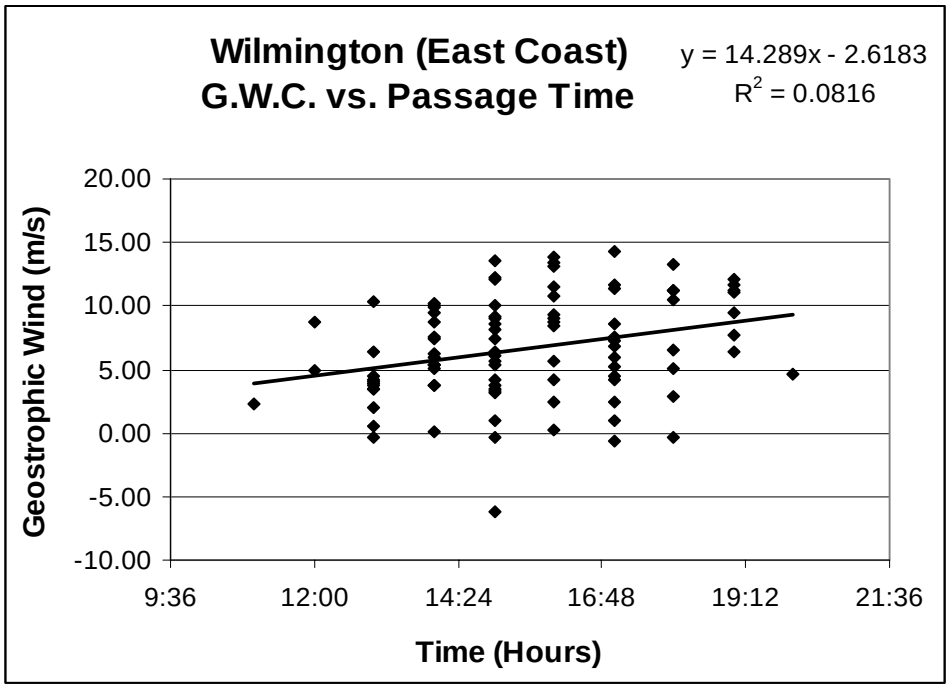

Figure 4.22 ***Variation of values of the geostrophic wind component (G.W.C.), calculated for the coast east of Wilmington, with frontal passage times noted from surface observations at the Wilmington airport site.***

Figures 4.23 and 4.24 represent the relationships between the G.W.C. and inland penetration distances measured from satellite imagery. As expected, both show a negative correlation between the variables, however, the R^2 value for the south-coast relationship is stronger, and the slope of the trend line is more negative. A shift of the mass of data points to the left is also noticeable when we compare Figure 4.23 to Figure 4.24, another indication of the southeast North Carolina "pocket" that was identified in the *Climatology* section.

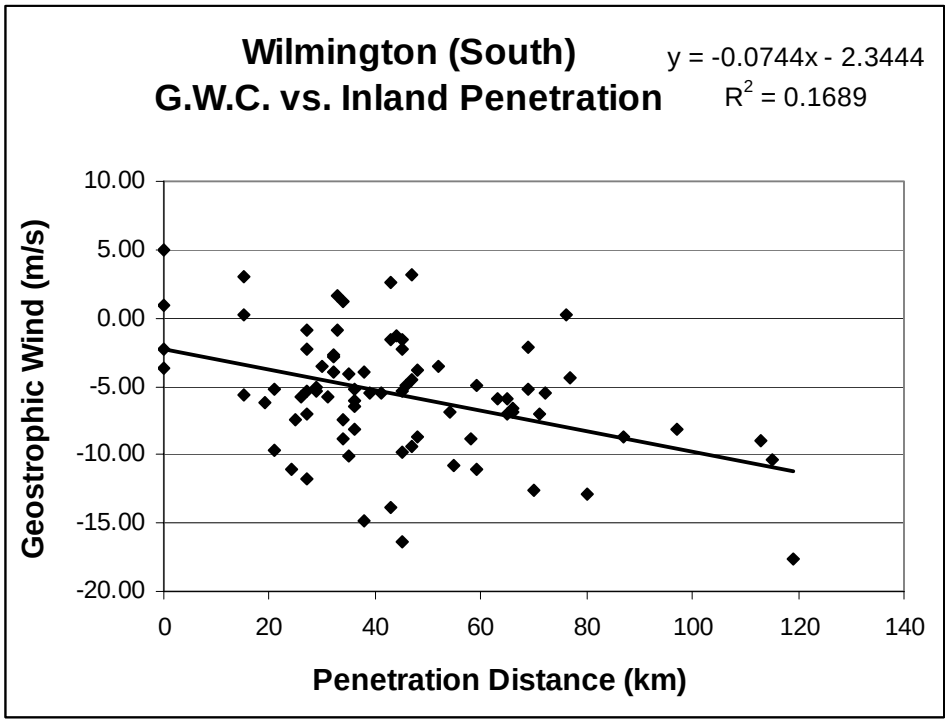

Figure 4.23 ***Variation of the G.W.C. with inland penetration distances measured on satellite imagery from the coast south of Wilmington.***

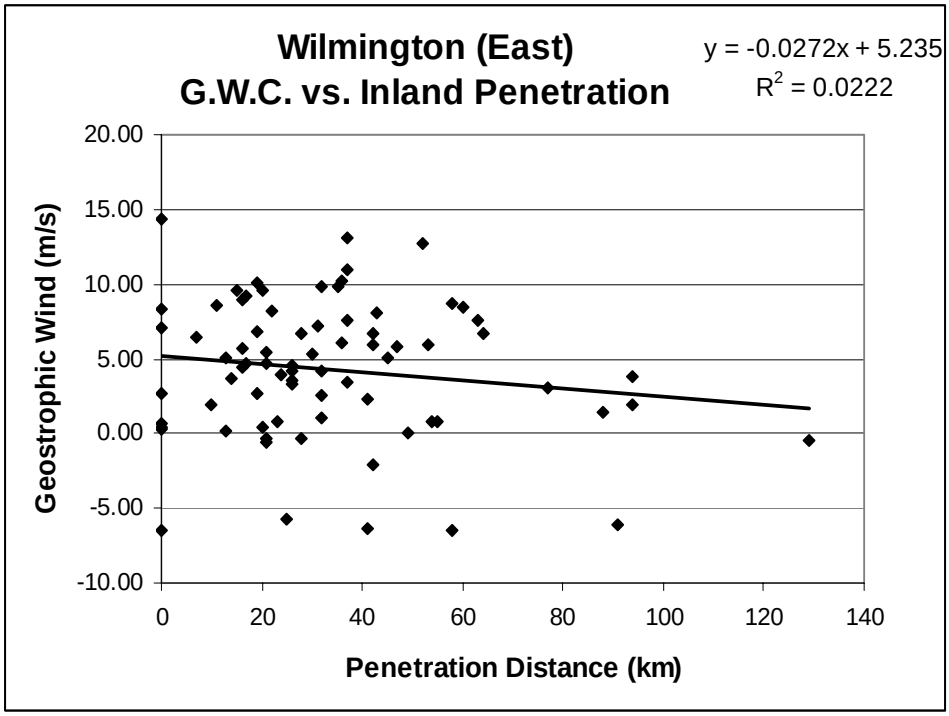

Figure 4.24 ***Variation of the G.W.C. with inland penetration distances measured on satellite imagery from the coast east of Wilmington.***

4.4 Savannah

Recall from Figures 4.1 through 4.4 that, compared with the other sites, there seems to be a larger difference between air temperatures and water temperatures for the Savannah dataset, at least based on the CO-OPS water temperature data. Table 4.1 shows a table of the average temperature differentials and the "threshold" values of del-T for each of the four coastal sites based on the CO-OPS water temperatures, while Table 4.2 shows the same table based on SEACOOS satellite-derived water temperatures. Figure 4.25 also shows that the distribution of del-T values (from CO-OPS data) is generally higher than that of the other coastal sites.

Table 4.1 ***Values for average del-T and del-T threshold (both ° C) for each coastal site based on CO-OPS water temperatures***

	SAV	CHS	MYR	ILM
Average	6.3 ° C	2.0	4.0	3.7
Threshold	3.5 ° C	1.0	2.0	2.0

Table 4.2 ***Values for average del-T and del-T threshold (both ° C) for each coastal site based on SEACOOS water temperatures***

	SAV	CHS	MYR	ILM
Average	2.8 ° C	3.6	1.6	3.8
Threshold	0.0 ° C	2.0	0.0	3.0

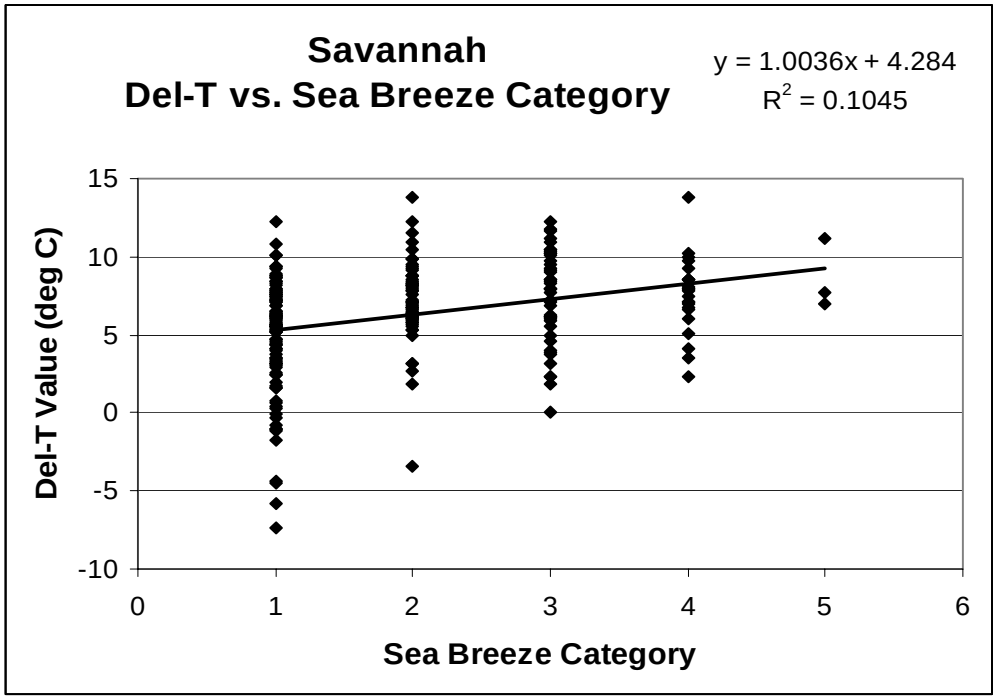

Figure 4.25 ***Variation of the del-T value (based on CO-OPS water temperature data) with sea breeze category for Savannah data.***

Interestingly the correlation between the G.W.C. and the sea breeze categories (illustrated in Figure 4.26) is near neutral, with a wide dispersion reflected in the small R^2 value, especially in the first two categories. The fact that the range narrows as the certainty in sea breeze development increases suggests again that the sea breeze tends to form (or is easier to detect) with lighter synoptic-scale winds. We can further illustrate this by breaking the data analyzed in Figure 4.26 down between offshore (positive geostrophic) and onshore (negative geostrophic) ambient wind flow, in Figures 4.27 and 4.28. Note that the regression lines both move towards the neutral geostrophic wind flow as the certainty in sea breeze detection increases. Figure 4.30 represents the relationship between the G.W.C. and sea breeze penetration distance, and generally follows the trends established in the same analysis for the Myrtle Beach and Wilmington sites.

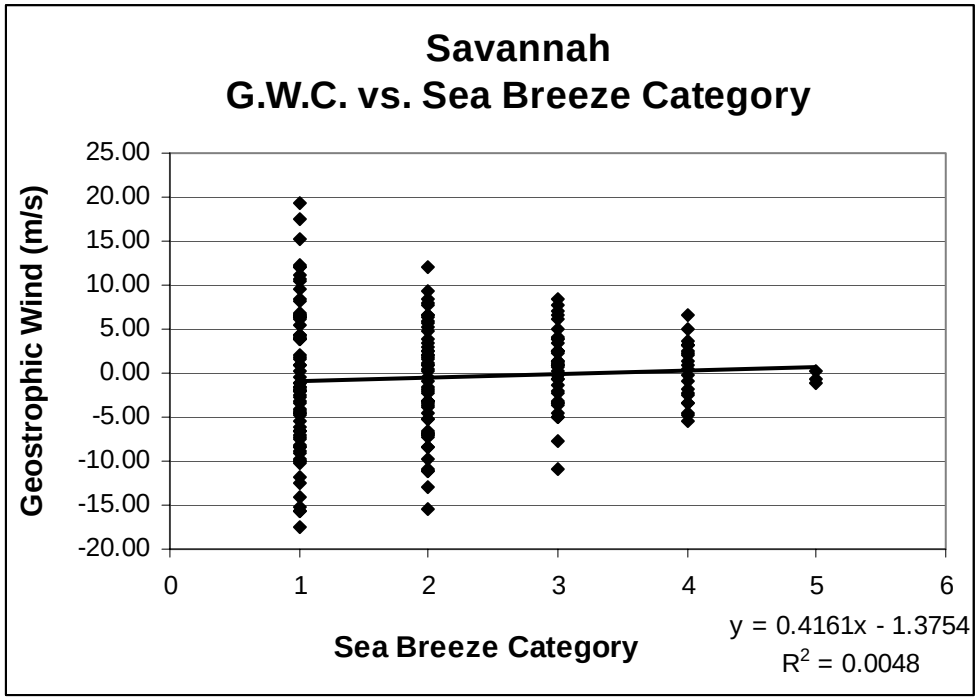

Figure 4.26 ***Variation of the geostrophic wind component with sea breeze category for Savannah data.***

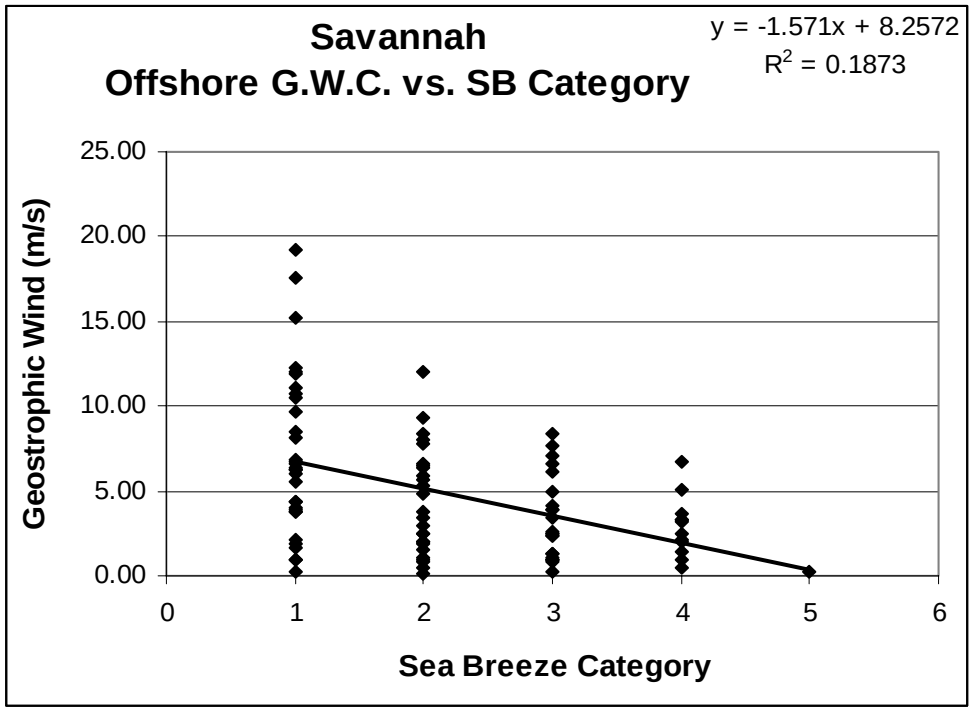

Figure 4.27 ***Variation of the geostrophic wind component (offshore values only) with sea breeze category for Savannah data.***

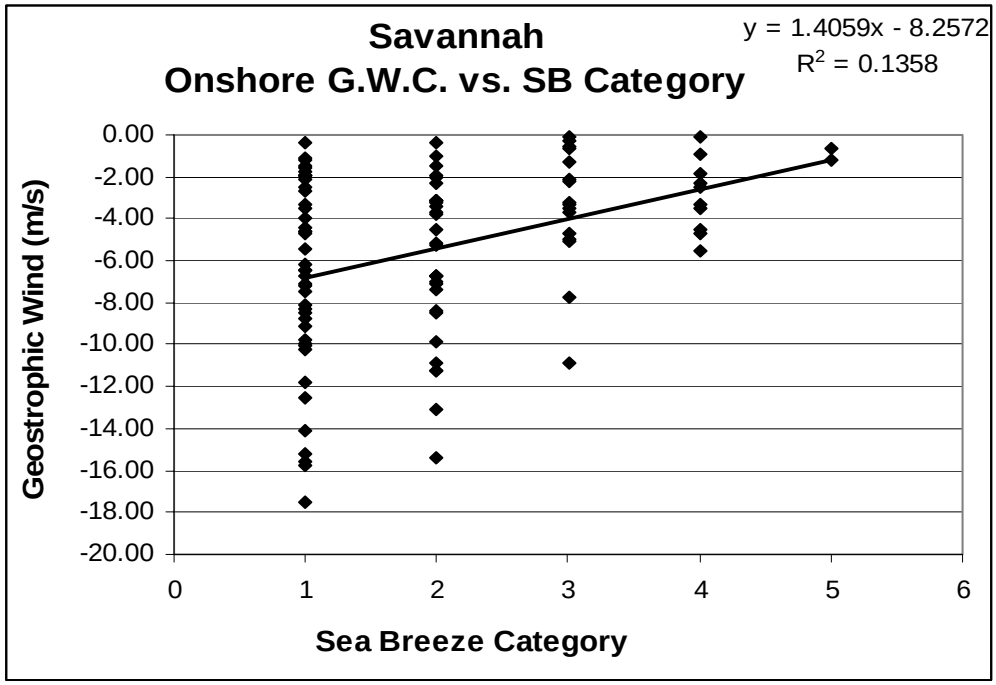

Figure 4.28 ***Variation of the geostrophic wind component (onshore values only) with sea breeze category for Savannah data.***

Figure 4.29 shows the correlation in Savannah area data between values for the component of the ageostrophic wind vector perpendicular to the coast and del-T values. Since water temperatures for 2004 from the CO-OPS network site near Savannah proved unavailable, del-T values in this analysis were based on the satellite-derived water temperatures taken from the SEACOOS system. Recall that negative values of the ageostrophic wind component are typically associated with the sea breeze front, and characterized the large majority of the Myrtle Beach dataset (see Figure 4.15). Interestingly, positive values of the ageostrophic wind component occur as frequently as negative values, indicating that passage of the sea breeze front is less frequent at the Savannah site compared with the Myrtle Beach site. This supposition makes sense when the relative proximity of each site to the coast is considered – sea breeze events would be expected to occur more frequently and be easier to detect closer to the coast, a la the Myrtle Beach site. However the miniscule R2 value indicates an almost total lack of correlation between the two variables in question. It is hard to conclude one way or the other from the analysis of the data in this study whether the ageostrophic wind value is an accurate representation of sea breeze frontal passage at the given coastal stations.

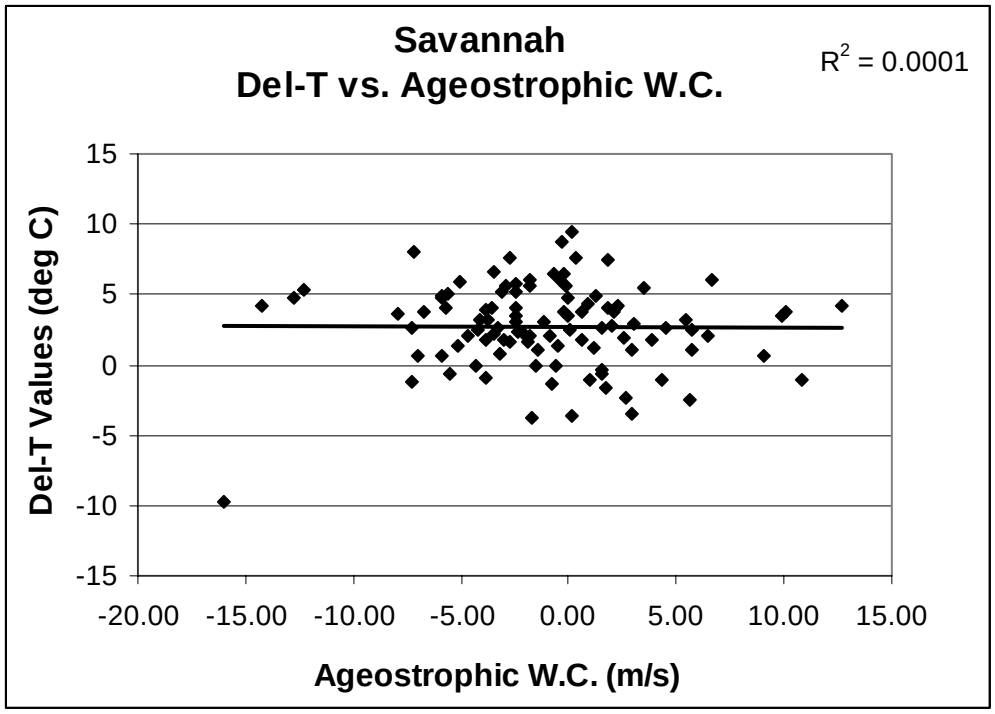

Figure 4.29 ***Variation of ageostrophic wind component values with del-T values (based on SEACOOS satellite-derived water temperatures) for the Savannah data for 2004.***

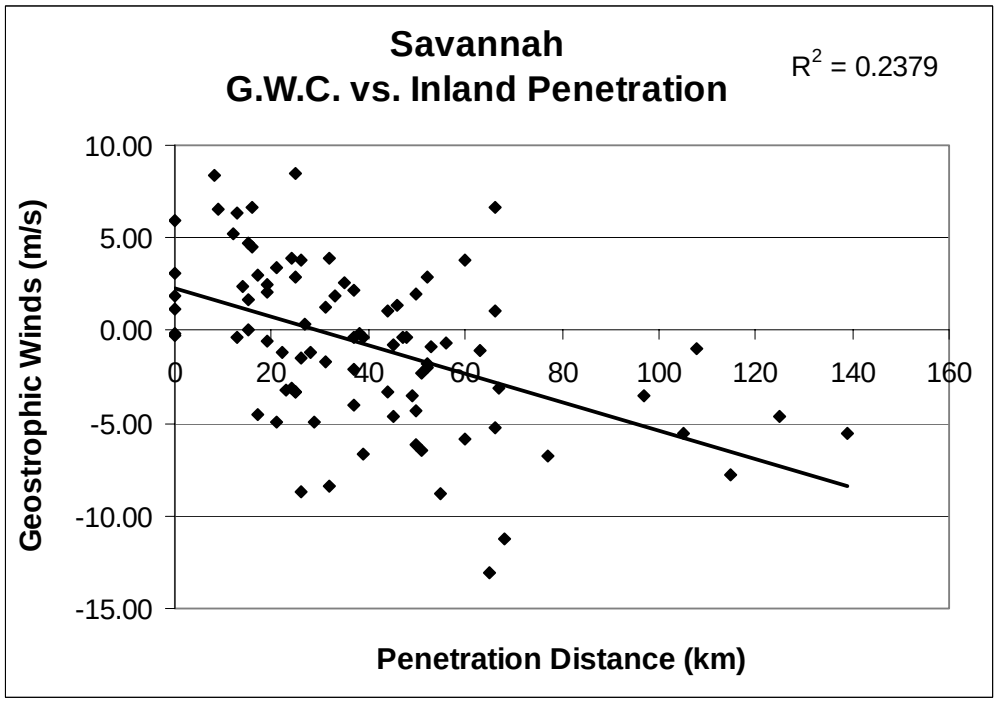

Figure 4.30 ***Variation of the geostrophic wind component with inland penetration distances of the sea breeze front measured on satellite imagery from the coast near Savannah.***

4.5 Charleston

Figure 4.31 shows the correlation between geostrophic wind component values and the sea breeze categories for the Charleston dataset. The relationship, like the one between the two variables in the Savannah data, is nearly zero (neither positive or negative). The Charleston and Savannah sites are the farthest stations from the coast relative to the other sites, and this distance might explain why there is less positive relationship between sea breeze detection and the geostrophic wind component. Presumably the farther from the coast a station is, the higher the probability of missed detection – sea breezes coinciding with offshore geostrophic winds would be more likely to be held up between the coast and the station, while sea breezes coinciding with onshore winds would be weaker after traversing a farther distance over land. Passage of the sea breeze front again appears to be most likely with lighter synoptic-scale winds, with only two events coinciding with geostrophic winds outside of the range between -10.0 m/s and 10.0 m/s.

Figure 4.32 shows the relationship between the G.W.C. and inland penetration distances of the sea breeze front for the Charleston dataset. Analyses of the other stations have indicated that further inland penetration is typically associated with light onshore winds, and that trend continues with the Charleston analysis.

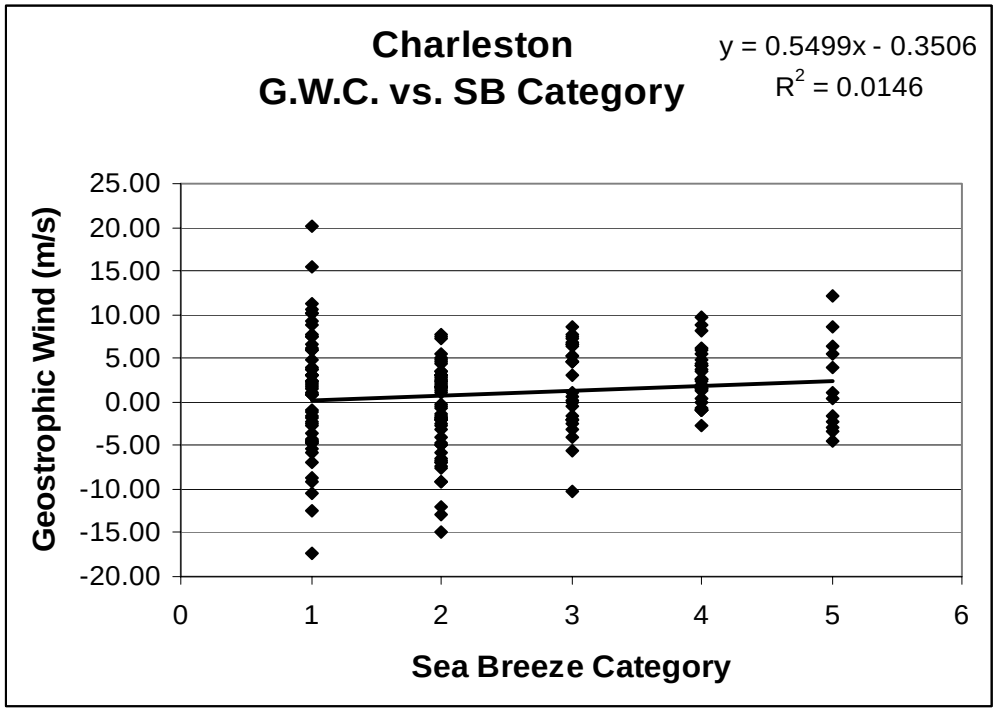

Figure 4.31 ***Variation of the geostrophic wind component sea breeze category for Charleston data.***

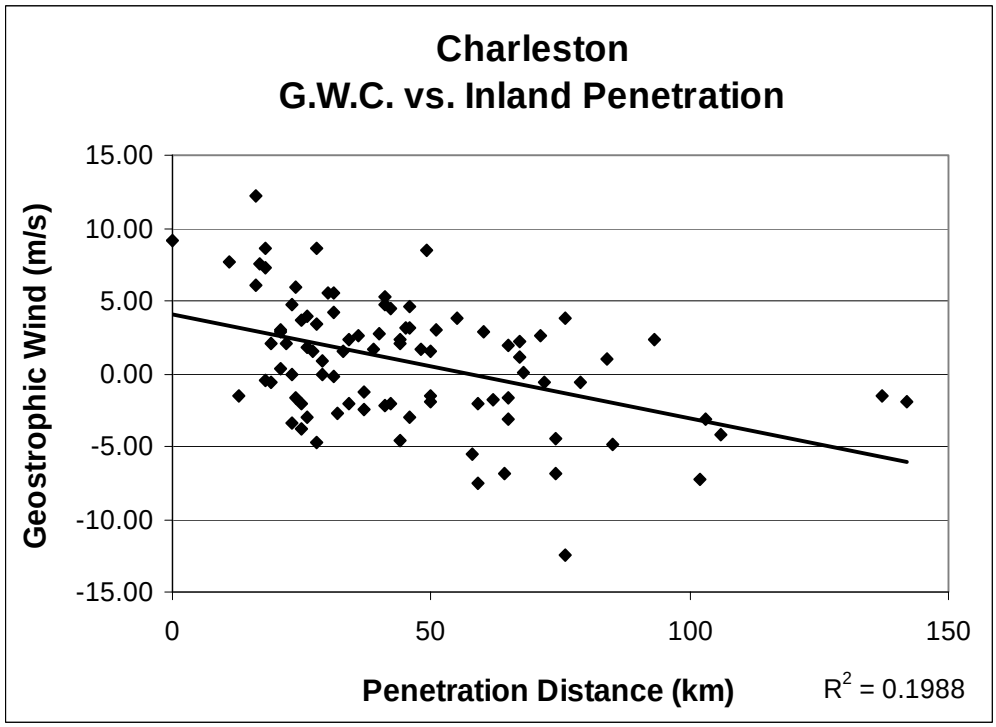

Figure 4.32 ***Variation of the geostrophic wind component with inland penetration distances of the sea breeze front measured on satellite imagery from the coast near Charleston.***

4.6 General Analysis

The differences from station-to-station in the measurement of water temperatures have been explained before, but a few generalized statements can be made about the situation overall. Of the sea breeze events recorded for all four stations, only 10.2 % coincided with del-T values below 2.0 ° C. Sea breeze events comprised 36.4 % of the days encompassing the entire research period with del-T values based on the CO-OPS water temperature data at and above 2.0 ° C, compared with just 12.4 % of those days with a del-T below 2.0 ° C. Similarly, sea breeze events make up 37.9 % of days with del-T values (based on SEACOOS data) at and above 2.0 ° C, and only 16.3 % of days with del-T values below 2.0 ° C.

We also noted in the individual analyses of the coastal sites that passage of the sea breeze front was more frequent with lighter synoptic scale winds. Just 5.5 % of sea breeze events for all four coastal sites occurred with geostrophic winds above 10.0 m/s (offshore winds) and below -10.0 m/s (onshore), while in contrast, 67.3 % of sea breeze events occurred with geostrophic winds between -6.0 m/s and 6.0 m/s.

As noted both in this study and in previous research, poor signal detection of sea breeze events associated with onshore ambient flow regimes seems to provide a major hindrance to comprehensive representation of the sea breeze. Of the sea breeze events recorded in this study, 63.0 % coincided with positive values of the geostrophic wind component, despite the fact that the research period was split almost evenly between days with onshore and offshore synoptic-scale wind regimes.

Table 4.3 shows the relative percentage likelihood of sea breeze detection associated with combinations of the values for del-T (based on the CO-OPS water

temperatures) and the G.W.C. Obviously the percentage in the upper left cell corresponds with the "best-case" scenario, while the value in the lower right cell is associated with the poorest situation for sea breeze detection. The percentages do not sum to 100 because they are proportions of separate datasets (i.e., the dataset encompassing days with super-threshold del-T values and offshore ambient winds (positive values of the G.W.C.) rather than one dataset. If we assume an under-representation of sea breeze events associated with onshore synoptic-scale flow, then the percentages on the bottom row are probably lower than reality. If we disregard "strong" values of the G.W.C. (above 10 m/s and below -10 m/s), Table 4.4 is the result.

Table 4.3 ***Percentage likelihood of sea breeze detection associated with certain combinations of values for del-T and the geostrophic wind component.***

	Super-Threshold Del-T Values (2.0 ° C and above)	Sub-Threshold Del-Values (below 2.0 ° C)
Offshore Ambient Winds (positive values of G.W.C.)	45.3 %	13.1 %
Onshore Ambient Winds (negative values of G.W.C.)	27.6 %	9.6 %

Table 4.4 ***Percentage likelihood of sea breeze detection associated with certain combinations of values for del-T and the geostrophic wind component, filtering out strong values of the G.W.C. below -10.0 m/s and above 10.0 m/s.***

	Super-Threshold Del-T Values	Sub-Threshold Del-T Values
Offshore Ambient Winds (+ G.W.C.)	45.2 %	14.8 %
Onshore Ambient Winds (- G.W.C.)	30.0 %	10.6 %

Recall the values of the del-T threshold for each station, summarized in Table 4.1. Table 4.5 shows the likelihood of sea breeze detection for the best- and worst-case scenarios at each coastal station, based on combinations of the threshold del-T values and onshore/offshore synoptic-scale flows. In general, it appears that the frequency of sea breeze detection improves with proximity to the coast – likelihood of detection is higher for the closest stations to the coast (Myrtle Beach and the Wilmington east-coast site) than for the two farthest sites (Savannah and the south-coast Wilmington dataset).

Table 4.5 ***Percentage likelihood of sea breeze detection for "best" and "worst"-case combinations of values for del-T and the geostrophic wind component.***

	SAV	CHS	MYR	ILM-S	ILM-E
Best Case (super-threshold Del-T, offshore G.W.C.)	38.3 %	45.9 %	47.0 %	32.0 %	43.8 %
Worst Case (sub-threshold Del-T, onshore G.W.C.)	20.0 %	7.5 %	14.3 %	7.5 %	3.9 %

4.7 Testing the Sea Breeze Index

Recall the Sea Breeze Index (SBI) introduced in the *Introduction/Literature Review* section of this document from the study by Frysinger, et. al. (2003) in the form:

$$SBI = \pm U^2 / \Delta T \qquad (2.1)$$

where U was the cross-coast component of the synoptic winds (onshore = positive) and ΔT was the temperature difference between land and water surfaces ($\Delta T = T_{land} - T_{ocean}$). It is an index that by its derivation can only be used on days characterized by an offshore synoptic-scale wind flow and positive values of ΔT ($T_{land} > T_{ocean}$). An equilibrium level

was defined for the KCHS (Charleston International Airport) data of SBI = 3.23 $m^2s^{-2}K^{-1}$ that represented the slope of a line emanating from the origin on a graph of U^2 plotted against ΔT. Hourly records affected by the sea breeze generally fell to the right and below this line, while records unaffected by the sea breeze generally fell to the left and above. Theoretically any sea breeze that might have affected hourly records to the left of and above this line is blocked by a strong offshore synoptic flow.

Recall also that there were fundamental differences between that study and this one. The researchers in the previous study used hourly meteorological data from surface observation stations at KCHS and Folly Beach in SC similarly to this researcher's method, but used inland surface observations as a surrogate approximation of the synoptic-scale wind regime, while this study used geostrophic wind values calculated from model analyses. Also, the previous study and the SBI developed from it analyzed and forecasted for hourly data, while predictions in this study dealt with sea breeze development on a day-to-day basis.

Still, a brief comparison seems warranted considering the similar intentions and geographic location of the two projects. Figure 4.32 reflects an analysis of the reliability of the SBI as a predictor using geostrophic wind and del-T values from this study. U^2 and ΔT data (or in the parlance of this document, the square of the geostrophic wind component and del-T values) comes from the Myrtle Beach site. This site was chosen (rather than the KCHS site that corresponded with the Frysinger study) because of the completeness of the del-T dataset.

The arrow to the right and below represents the equation $y = 3.2(x) + 0$, or the critical SBI value of 3.2 $m^2s^{-2}K^{-1}$ calculated by Frysinger et. al. (2003) for their KCHS

data set. Of the 164 data points below and to the right of the Frysinger critical SBI value, there were 60 points associated with observational sea breeze days, 51.7 % of all sea breeze days and 36.6 % of below-critical days. Of the 184 super-critical days, 55 were classified as sea breeze days, or 29.9 % of the data points above the critical SBI line. Using the Frysinger sub-critical value for these data returns only a slight increase in the proportion of sea breeze days to non-sea breeze days than super-critical values.

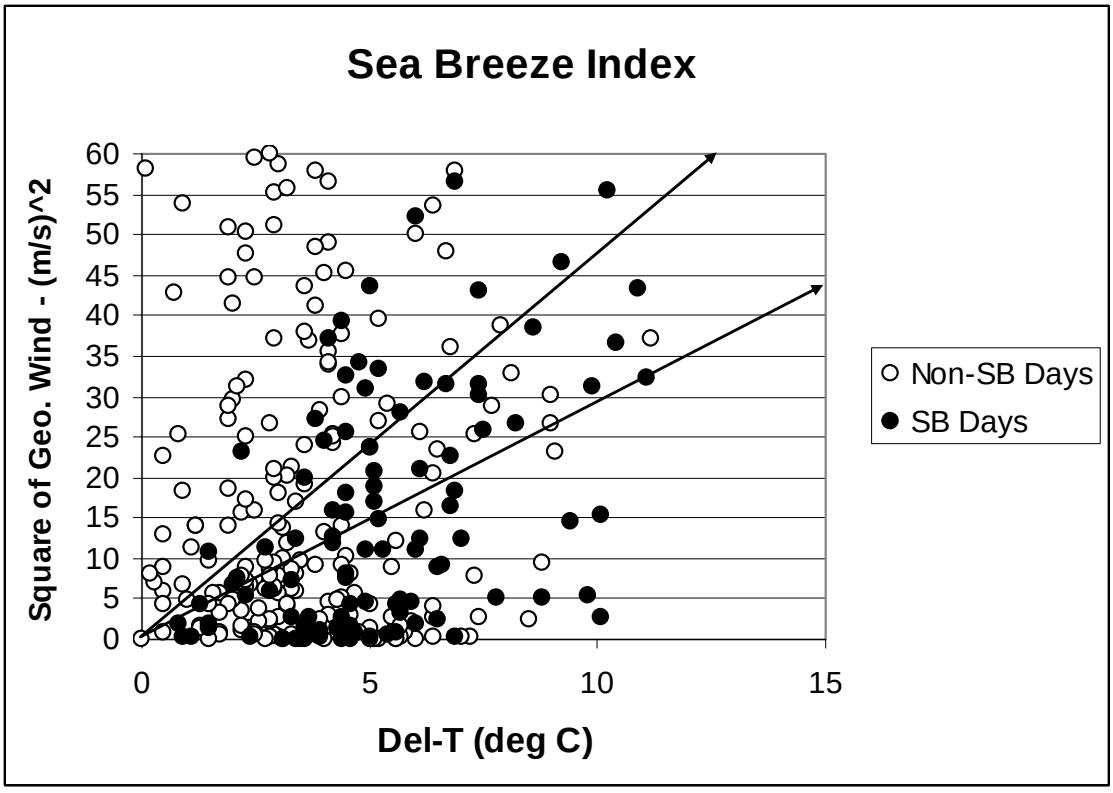

Figure 4.33 ***Test Run of the SBI on Myrtle Beach data. White dots represent non-sea breeze days and black dots represent sea breeze days, based on the classification system introduced in the*** **Climatology** ***section of this document.***
Upper Left Arrow: SBI = 6.0 $m^2s^{-2}K^{-1}$, Lower Right Arrow: SBI = 3.2 $m^2s^{-2}K^{-1}$

After some tests with other critical values, an SBI value closer to 6.0 $m^2s^{-2}K^{-1}$ (the line to the left and above) was found to be a better critical value for the Myrtle Beach data used in this study. Of the 125 points above and to the left of this critical line, only 26 points, or 20.8 % of the dataset, were classified as sea breeze days. However, 89 of the 223 points below and to the left of the critical line, or 39.9 % of the sub-critical values, were associated with sea breeze days.

SECTION FIVE: Conclusions and Future Work

5.1 Climatology

Detection of the sea breeze frontal passage through any particular site is a function of the changes induced by the front in the hourly records of the site for the variables air temperature, dewpoint, wind speed, and wind direction. The hourly observational data needed for this study were obtained from the CRONOS database, a catalog of records from the network of measurement stations across the Southeast, through the NC State Climate Office.

The classification system developed for this study was somewhat subjective but could be easily quantified for use in other projects and contexts. Those changes included a drop in temperature, a corresponding rise in dewpoint, and a shift in the wind vector (both direction and magnitude). A class "five" day was characterized as having changes in all four variables at the same hour, all consistent with changes expected from sea breeze frontal passage. On a class "four" day, all four changes occurred and were spread out over a period of an hour or two, or three of the changes occurred with one neutral or unchanged variable, and so on and so forth. Further analysis of data for the four coastal sites (Savannah, GA, Charleston and Myrtle Beach, SC, and Wilmington, NC) throughout the document was often based on this classification system. Classes three through five were generally acknowledged as "sea breeze days", while classes one and two were not.

At all sites, specific changes in the hourly readings attributed to the sea breeze were on the order of a 1-2 degrees (C) decrease in air temperature coupled with a 2-3

degrees (C) rise in dewpoint. Station-to-station variation in these changes may once again have been a function of proximity to the coast, although statistical significance tests (specifically a Chi-square test) run on the data were inconclusive, most arguing for significance but some against.

The average time that frontal passage took place at the sites was found to be linked to relative distance to the coast – where the Myrtle Beach airport site (MYR), at a distance of about 2 km from the coast, was first influenced by the sea breeze front around 1300 LDT, it took another three to four hours on average for the front to penetrate to the Savannah site (SAV) some 35 km inland. The effect on the daily evolution of air temperature, dewpoint, and wind vector readings was also a function of proximity to the coast. The MYR curve of air temperature versus time reached an early peak and often plateaued for the afternoon hours, whereas the same curve for SAV achieved a higher peak later in the afternoon, although it was found to be not as late as a curve for measurement sites well inland, such as CAE (Columbia, SC).

Certain changes in the wind vector were observed and identified as having been caused by sea breeze frontal passage. Again the timing of such changes was heavily dependent on the location of each station relative to the coast, but the changes were consistent from station to station. Passage of the front caused a shift in direction to around just south of directly onshore (depending on the orientation of the near-site coastline) regardless of what ambient wind flow was in place, and an increase in wind speed was observed as well. The effects of the Coriolis force working to turn the wind vector clockwise were observed as well. The shape of the coastline around Wilmington, with two almost perpendicular coastlines meeting to form the Cape Fear Peninsula just

south of the city (Figure 1.6), caused a pattern in some of the wind direction data such that a sea breeze forming on the closer, east-facing coast appeared to affect the station for a time before the sea breeze forming on the south-coast began to dominate the record. This pattern was not universally observed in all the Wilmington data, however. A certain degree of ambiguity characterized much of the analysis of the Wilmington data, and there is room for some refinement in the methodology when it comes to this unique situation.

Visible satellite imagery was assimilated for the purpose of examining the inland extent of the circulation, again through a catalog of imagery collected by the Climate Office from NCAR archives. Recall that the sea breeze front is denoted on visible satellite imagery by a linear formation of cumulus clouds of varying discernability, usually parallel to the coast (although the orientation depended on the synoptic-scale wind regime). This method does not account for all sea breeze fronts and indeed, the correlation between sea breeze development on satellite imagery and in the hourly observations is relatively low. However it has been established in previous studies that the use of satellite imagery in this capacity has some key advantages over other remote sensing techniques, such as radar imagery.

Analysis of this satellite imagery was conducted using ArcGIS software. Penetration distances of 20-40 km were the norm, while distances of 50-80 km were more rare. The unique coastline around Wilmington again forced a modification of the technique applied in this study, as the significant differences in penetration distances observed from the south- and east-facing coasts forced a division in the data accordingly. Specifically, the sea breeze front penetrated further inland from the south-facing coast

than did the front that developed on the east-facing coast, creating a "pocket"-like phenomenon in that part of southeastern North Carolina below Wilmington.

The complex interaction of surface boundaries including the sea breeze front over inland areas of the Carolinas has been studied and documented previously (Koch and Ray, 1997) and was observed here as well – just under a third of the sea breeze fronts observed and measured by satellite imagery in this study were skewed to some degree by interaction with inland phenomena, such as thunderstorm outflow boundaries. This interaction and the thunderstorm activity that oftens results are important aspects of the climatology of the area that are ripe for more in-depth research.

5.2 Correlation Study

Two factors were determined from a review of relevant literature to be significant to the development and evolution of the sea breeze circulation. The driving mechanism for sea breeze development as explained in the *Introduction/Literature Review* section of this document is the temperature difference across the land/water surface interface. To this end, water temperature data from the CO-OPS network were assimilated and compared with observations of air temperature at the 1200 (noon) LDT hour, producing a value known throughout this document as the "del-T" value. In the post-development stage, the evolution of the sea breeze circulation depends on the synoptic-scale wind flow. As a measure of this regime, geostrophic wind data was accumulated for each coastal site. NARR model analysis data was accessed via the NOAA's NOMADS archive and analyzed using GEMPAK software to obtain the geostrophic wind vector. A

simple calculation produced the component of this vector perpendicular to the coast for the noon hour.

Due to the idiosyncratic variations in the del-T and geostrophic wind component datasets from station-to-station, analysis of the data was conducted first for each site separately. The first and most thoroughly analyzed site was Myrtle Beach, due to the completeness of the del-T data (relative to the Charleston and Savannah sites) and the lack of coastline irregularity that confuses analysis of the Wilmington data.

Despite the incongruities in the del-T data and the previously discussed under-representation of sea breeze events associated with onshore synoptic-scale flows, there are a few patterns that were noted. Threshold values for del-T seemed necessary for sea breeze development, ranging from around 1.0 ° C at Charleston to around 3.5 ° C at Savannah. Sea breeze detection was rare below these threshold values. Also, sea breeze events occurred more frequently with lighter synoptic-scale winds, specifically with values for the geostrophic wind component between -10.0 m/s and 10.0 m/s, where negative values coincided with onshore ambient winds and vice versa. Examination of satellite imagery indicated that inland penetration distances depended on values for the geostrophic wind value as well, as all coastal sites displayed a negative relationship between the two variables – increased penetration distances coincided with light onshore synoptic scale winds (small negative G.W.C. values).

5.3 Future Work

There is obvious room for improvement in the methodology of this research, although the methods in this study were chosen for the best combination of availability,

continuity, and reliability of the data involved. Analysis tends to indicate that sea breeze events associated with onshore ambient wind regimes were under-represented, compared with results from prior studies. Some of these prior projects used only the presence of onshore wind flows in the record of hourly observations to define the presence of the sea breeze (Frysinger, et. al. 2003). It appears that the definition of the sea breeze for this study may have been too strict and might not have accounted for all sea breeze events within the research period. Sea breeze events that were not included in this study were presumably characterized by a much weaker-than-average signature in the observational data. However, at the beginning of this research, a simpler definition was considered to be problematic in that it lead to a higher incidence of the erroneous inclusion of non-sea breeze events in the dataset. Analysis in this document conducted with a less rigid definition of sea breeze detection, specifically negative values of the ageostrophic wind (the difference in the observed and geostrophic wind vectors), proved no more conclusive than analysis using the sea breeze classification system. However, there were indications that negative values of the ageostrophic wind occurred more frequently at the Myrtle Beach site than the other sites, a characteristic that would tend to agree with the intuitive idea that sea breeze detection occurs more often closer to the coast.

By the same token, any under-representation of sea breeze development in the satellite imagery is probably likewise due to the weakness of the event's signature. As discussed previously, detection of the sea breeze front on satellite imagery depended on the presence of the line of cumulus clouds along the frontal boundary. Too much cloudiness, or not enough of it, would lead to a misdiagnosis of no sea breeze regardless of whether a sea breeze front were present or not. Horizontal mass convergence at the

surface along the front leads to the development of the tell-tale line of clouds. Of course, this convergence would be more likely with an offshore synoptic-scale wind regime, and it may be that sea breeze events associated with onshore ambient wind flows are under-represented in the satellite dataset as well. The higher sensitivity of radar (especially in clear-air mode) is a prime reason why that sensing instrument has been used in other studies to detect sea breeze fronts (Wakimoto and Atkins, 1994, Gilliam et. al., 2004). However, the limited range and relative paucity of radar imagery in clear-air mode made the satellite imagery a more desirable source of remotely-sensed data.

Del-T values were calculated from hourly records of air temperature from ASOS stations and water temperature data from the CO-OPS network. From Figures 2.2 through 2.5, it is obvious that not all of the water temperature guages were ideally located for recording true ocean water temperatures, particularly for the Wilmington site. However these sites offered data with the best combination of contiguousness and precision. Examination of water temperature data derived from satellite sources, courtesy of the SEACOOS system, largely tended to substantiate the accuracy of the CO-OPS water temperatures, although there were minor differences. Ideally, station-to-station variability in the measurement of water temperature data could be corrected by using a different source, such as the portable recording instruments used in studies such as Frysinger, et. al. (2003). Del-T data with more representativeness and station-to-station continuity might make an analysis of trends in sea breeze evolution more precise.

As noted in the *Climatology* section, the presence of and interaction with other surface boundaries over inland areas results in distortion along the sea breeze front, often to the point that the sea breeze frontal boundary becomes hard to distinguish from the

other boundaries. Koch and Ray (1997) explored the distinctions between the separate boundaries in central North Carolina, but a more substantive study of this interaction, and the effect that the interaction has on precipitation patterns, would be useful.

LIST OF REFERENCES

Arritt, R.W. 1993: "Effects of the Large-Scale Flow on Characteristic Features of the Sea Breeze" J. of Applied Meteorology, Vol. 32, pgs. 116-125

Atkins, N.T., Wakimoto, R.M., Weckwerth, T.M. 1995: "Observations of the Sea-Breeze Front During CaPE. Part II: Dual-Doppler and Aircraft Analysis" Monthly Wx. Review, Vol. 123. pgs. 944-969

Atkins, N.T., Wakimoto, R. M. 1997: "Influence of the Synoptic-Scale Flow on Sea Breezes Observed during CaPE" Monthly Wx. Review, Vol. 125, pgs. 2112-2130

Baker, R.D., Lynn, B.H., Boone, A., Tao A.K., Simpson, J. 2001: "The Influence of Soil Moisture, Coastline Curvature, and Land-Breeze Circulations on Sea-Breeze-Initiated Precipitation" J. of Hydrometeorology, Vol. 2, pgs. 193-21

Barry, R.G., Chorley, R.J. 1992: Atmosphere, Weather, and Climate. Sixth Edition, Routledge Publishing, 392 pgs.

Bechtold, P., Pinty, J-P., Mascart, P. 1991: "A Numerical Investigation of the Influence of Large-Scale Winds on Sea-Breeze- and Inland-Breeze-type Circulations" J. of Applied Meteorology, Vol. 30, pgs. 1268-1279

Boybeyi, Z. and S. Raman 1992: "A Three-Dimensional Numerical Sensitivity Study of Convection over the Florida Peninsula" Boundary-Layer Meteorology, Vol. 60, pgs. 325-359

Connell, B. H., Gould, K. J., Purdom, J. F. W. 2001: "High-Resolution *GOES-8* Visible and Infrared Cloud Frequency Composites over Northern Florida during the Summers of 1996-1999" Weather and Forecasting, Vol. 16, pgs. 713-724

Connor-Linton, J. 2003: "Chi-Square Tutorial" Georgetown Linguistics Dept. URL: http://www.georgetown.edu/faculty/ballc/webtools/web_chi_tut.html

Dailey, P.S., Fovell, R.G. 1999: "Numerical Simulation of the Interaction between the Sea-Breeze Front and Horizontal Convective Rolls. Part I: Offshore Ambient Flow" Monthly Wx. Review, Vol. 127, pgs. 858-878

Darby, L.S., Banta, R.M., Pielke, R.A. 2002: "Comparisons between Mesoscale Model Terrain Sensitivity Studies and Doppler Lidar Measurements of the Sea Breeze at Monterey Bay" Monthly Wx. Review, Vol. 130, pgs. 2813-2838

Frysinger, J. R., Lindner, B. L., Brueske, S. L. 2003: "A Statistical Sea-Breeze Prediction Algorithm for Charleston, South Carolina" Weather and Forecasting, Vol. 18, pgs. 614-625

Gilliam, R.C., Raman, S., Niyogi, D.D.S 2004: "Observational and Numerical Study on the Influence of Large-Scale Flow Direction and Coastline Shape on Sea-Breeze Evolution" Boundary-Layer Meteorology, Vol. 111, Pgs. 275-300

Kingsmill, D.E. 1995: "Convection Initiation Associated with a Sea-Breeze Front, a Gust Front, and their Collision" Monthly Wx. Review, Vol. 123, pgs. 2913-2933

Koch, S. E., Ray, C. A. 1997: "Mesoanalysis of Summertime Convergence Zones in Central and Eastern North Carolina" Weather and Forecasting, Vol. 12, pgs. 56-77

Kuettner, J. P. 1959: "The Band Structure of the Atmosphere" *Tellus*, Vol. 2, pgs. 267-294

Miller, S. T. K., Keim, B. D. 2003: "Synoptic-Scale Controls on the Sea Breeze of the Central New England Coast" Weather and Forecasting, Vol. 18, pgs. 236-248

Nichols, M.E., R.A. Pielke, and W.R. Cotton 1991: "A Two-Dimensional Numerical Investigation of the Interaction between Sea Breezes and Deep Convection over the Florida Peninsula" Monthly Wx. Review, Vol. 119, pgs. 298-323

Ohashi, Y., Kida, H. 2002: "Local Circulations Developed in the Vicinity of both Coastal and Inland Urban Areas: A Numerical Study with a Mesoscale Atmospheric Model" J. of Applied Meteorology, Vol. 41, pgs. 30-45

Simpson, J.E. 1994: Sea Breeze and Local Winds. Cambridge University Press, 234 pgs.

Wakimoto, R. W., Atkins, N. T. 1994: "Observations of the Sea-Breeze Front during CaPE. Part I: Single-Doppler, Satellite, and Cloud Photogrammetry Analysis" Monthly Wx. Review, Vol. 122, pgs 1092-1114

Walsh, J. E. 1974: "Sea Breeze Theory and Applications" J. of Atmospheric Science, Vol. 31, pgs. 2012-2026

Xu, L., Raman, S., Madala, R.V., Hodur, R. 1996: "A Non-Hydrostatic Modeling Study of Surface Moisture Effects on Mesoscale Convection Induced by Sea Breeze Circulation" Meteorology and Atm. Physics, Vol. 58, pgs. 103-122

Zhong, S., Takle, E.S. 1992: "An Observational Study of Sea- and Land-Breeze Circulation in an Area of Complex Coastal Heating" J. of Applied Meteorology, Vol. 31, pgs. 1426-1438